CLAY SURFACE PROPERTIES BY WATER VAPOR SORPTION METHODS

Master of Science Thesis

By

Idil Deniz Akin

Department of Civil and Environmental Engineering
University of Wisconsin-Madison

MASTER OF SCIENCE IN CIVIL ENGINEERING

May 2014

CLAY SURFACE PROPERTIES BY WATER VAPOR SORPTION METHODS

A thesis in partial fulfillment of the requirements for the degree of Master of Science in Civil and Environmental Engineering at the University of Wisconsin-Madison

Approved by:

William J. Likos, PhD

ABSTRACT

Classification of expansive soils is a required component of geotechnical design to improve the long-term performance of structures. The current methods to classify swelling soils are based primarily on indices like the Atterberg limits, which are indirectly related to clay mineralogy and clay structure. The long-term goal of this research is to explore alternative ways to classify clays and to modernize geotechnical soil classification methods using measurement and analysis techniques based on clay surface properties. Clay surface properties such as specific surface area (SSA) and cation exchange capacity (CEC) are indicative of the clay mineralogy. For expansive clays, interactions of the clay surface with water molecules influence behavior. Consequently, water vapor sorption methods may potentially be used to determine clay surface properties.

SSA is the measure of surface area per unit mass (m^2/g). SSA measurement methods can be classified into three main categories: physical methods, positive adsorption methods, and negative adsorption methods. The most common techniques are positive sorption methods, where the sorption of molecules on the surface is measured. The sorbates can be either polar (*e.g.*, N_2) or non-polar (*e.g.*, Ethylene Glycol Monoethyl Ether (EGME), water vapor). CEC is a measure of exchangeable mineral charge. Common measurement techniques include those based on replacing the cations in the natural exchange complex with a known cation species (*e.g.*, ammonium displacement method)

A water vapor sorption isotherm characterizes the relationship between relative humidity (R_H) and the equilibrium moisture content of some material in that environment obtained along an adsorption (wetting) or desorption (drying) path at some temperature. A water vapor sorption isotherm is equivalent to a soil water characteristic curve (SWCC) since R_H and soil suction can

be directly related by Kelvin's equation. A sorption isotherm, therefore, is a direct measurement of how the physical and chemical interactions between water and the soil surface result in water retention, and thus is an indirect measurement of the fundamental compositional and surface properties of the material (mineralogy, SSA, CEC).

In the first chapter of this thesis SSA values obtained by Brunauer-Emmett-Teller (BET) Theory are determined from water vapor sorption isotherms obtained at low relative humidity values, and compared with values obtained using the more conventional EGME retention method. Thirteen samples of natural clayey soils and a suite of mixtures of end member Wyoming bentonite and Georgia kaolinite are tested. Additional comparisons are made for a suite of Mg^{+2}, Ca^{+2}, Na^{+}, K^{+}, and Li^{+}-saturated forms of the bentonite to examine influences of exchangeable cation type and to extend the possible range of water vapor sorption isotherms over a wide range.

The second chapter examines the performance and applicability of six existing isotherm models (Freundlich, Brunauer-Emmett-Teller, Frenkel-Halsey-Hill, Guggenheim-Anderson-de Boer, Double Log Polynomial, and Dubinin-Astakhov) for representing the water vapor sorption behavior of clayey soils. Dry mixtures of Wyoming bentonite and Georgia kaolinite are tested to cover a wide range of possible isotherms. Trends observed in the equation parameters with increasing bentonite content are discussed and analyzed separately for adsorption and desorption processes.

In the third chapter, an original empirical method is proposed to indirectly estimate the CEC of clayey soils based on relatively simple water vapor sorption measurements. A master curve is obtained from measured water vapor sorption isotherms of 24 clayey soil samples. The

validation of the proposed method is independently tested using twelve samples of natural clayey soils and nine water vapor sorption isotherms available in the literature.

To my dear grandpa, Ömer Akçay

ACKNOWLEDGEMENTS

I would like to express my sincere gratitude to my advisor Professor William J. Likos for his guidance and support throughout my master studies and his confidence in me. I wish to thank him for having me in his research group.

I am also grateful to Professor James M. Tinjum and Professor Tuncer B. Edil for accepting to be in my defense committee, and for contributing to the progress of my research with their valuable comments and ideas at our weekly research meetings. I wish to thank Professor Edil also for his advice about non-academic topics.

Special thanks to Professor Sam Kung for caring about my research, encouraging, and helping me. His sincere willingness to help my research greatly motivated me at the time I was struggling. Thank you to Xiadong ‘Buff’ Wang for his time and help to perform conventional geotechnics tests.

I would also like to thank my professors at the Civil Engineering Department of my undergraduate university, Middle East Technical University, for encouraging me seeking a degree at the University of Wisconsin-Madison. Special thanks to my friends in Turkey, particularly Naz and Hazal, for their true friendship and support.

Thank you to the whole Geofamily, and my friends in Madison, particularly Faith, Erin, Missy, Yang, and Emre. With their support, and wonderful company I have enjoyed my life in this beautiful city, and never felt alone.

Finally, special and the greatest thanks to my dear family, particularly my mom Filiz Akın, my dad Mehti Akın, my sister Zeynep Cansu Akın, and my uncle Mehmet Akif Akçay. Feeling their endless love and support always gives me the motivation and power to reach my goals.

Financial support for this study was provided by the National Science Foundation (NSF) under grant CMMI 1304119. Any opinions, findings, and conclusions or recommendations expressed in this material are those of the authors and do not necessarily reflect the views of NSF.

TABLE OF CONTENTS

ABSTRACT ii

ACKNOWLEDGEMENTS vi

TABLE OF CONTENTS viii

LIST OF TABLES xiii

LIST OF FIGURES xiv

CHAPTER 1- SPECIFIC SURFACE AREA OF CLAYS USING WATER VAPOR AND EGME SORPTION METHODS 1

- 1.1 INTRODUCTION 1
- 1.2 BACKGROUND 3
  - 1.2.1 Adsorption Theories 3
    - 1.2.1.1 Langmuir Adsorption Theory 3
    - 1.2.1.2 BET Multimolecular Adsorption Theory 4
  - 1.2.2 Existing Methods to Determine SSA 6
    - 1.2.2.1 Nitrogen Sorption Method 6
    - 1.2.2.2 Ethylene Glycol (EG) Sorption Method 6
    - 1.2.2.3 Ethylene Glycol Monoethyl Ether (EGME) Sorption Method 7
    - 1.2.2.4 Methylene Blue (MB) Sorption 8
    - 1.2.2.5 Water Vapor Sorption Method 9
  - 1.2.3 Water Sorption Isotherms 9

1.3 MATERIALS AND METHODS 11

1.3.1 Clays and Clay Mixtures 11

1.3.2 Ethylene Glycol Monoethyl Ether (EGME) Method 12

1.3.3 Water Vapor Sorption Method 14

1.4 RESULTS AND DISCUSSION 17

1.4.1 Swelling Classification based on Likos (2008) Approach 17

1.4.1 Water Vapor Sorption Isotherms 18

1.4.2 Surface Area Calculations using BET Theory 20

1.4.3 One-Point Surface Area Calculations 23

1.5 SUMMARY AND CONCLUSIONS 25

1.6 REFERENCES 26

1.7 TABLES 33

1.8 FIGURES 34

CHAPTER 2- EVALUATION OF MODELS FOR WATER VAPOR SORPTION ISOTHERMS OF CLAYS 46

2.1 INTRODUCTION 46

2.2 BACKGROUND 48

2.2.1 Water Sorption Isotherms 48

3.1.1 Freundlich (F) Model 49

3.1.2 Brunauer, Emmett, and Teller (BET) Model 50

3.1.3 Frenkel-Halsey-Hill (FHH) Model 52

3.1.4 Guggenheim-Anderson-de Boer (GAB) Model 53

3.1.5 Double Log Polynomial (DLP) Model 54

3.1.6 Dubinin-Astakhov (D-A) Model 56

2.3 MATERIALS AND METHODS 57

2.3.1 Bentonite-Kaolinite Mixtures 57

2.3.2 Water Vapor Sorption Isotherms 57

2.3.3 Fitting Parameters 58

2.3.4 SSA Calculation 59

2.4 RESULTS and DISCUSSION 60

2.4.1 Equation Fitting 60

2.4.2 Equation Parameters 61

2.4.2.1 Freundlich Equation 61

2.4.2.2 BET Equation 62

2.4.2.3 FHH Equation 63

2.4.2.4 GAB Equation 64

2.4.2.5 DLP Equation 66

2.4.2.6 D-A Equation 67

2.4.3 Specific Surface Area (SSA) Comparison 69

2.5 IMPLICATIONS 70

2.5.1 Isotherm Estimation from SSA_{EGME} 70

2.6 SUMMARY AND CONCLUSIONS 71

2.7 REFERENCES 72

2.8 TABLES 79

2.9 FIGURES 81

CHAPTER 3- CATION EXCHANGE CAPACITY OF CLAYS FROM WATER VAPOR SORPTION ISOTHERM 93

3.1 INTRODUCTION 93

3.2 BACKGROUND 94

3.2.1 Ammonium Displacement Method 94

3.2.2 Methylene Blue (MB) Titration Method 95

3.2.3 Surface Tension Methods 96

3.2.4 Relationship between SSA and CEC 96

3.2.5 Normalization of Water Vapor Sorption Isotherms with CEC 98

3.3 MATERIALS 99

3.4 METHODS 100

3.4.1 Water Vapor Sorption Isotherms 100

3.4.2 Specific Surface Area (SSA) 101

3.4.3 Cation Exchange Capacity (CEC) 102

3.4.4 Determination of Freundlich K Parameter 103

3.4.5 Obtaining the Surface Charge-Normalized Sorption Curve 103

3.4.6 Determination of CEC from Water Vapor Sorption Isotherm.............................. 104

3.5 VALIDATION OF THE METHOD AND DISCUSSIONS 105

3.6 SUMMARY AND CONCLUSIONS 106

3.7 REFERENCES 107

3.8 TABLES 112

3.9 FIGURES.. 115

EXECUTIVE SUMMARY 121

LIST OF TABLES

Chapter 1

Table 1. Surface properties and Atterberg limits of the natural soils (** from Benson and Trast (1995), * from Erin L. Hunter, n.d.: not determined).

Chapter 2

Table 1. Summary of the isotherm equations and optimization parameters.

Table 2. Surface properties and Atterberg limits of the natural soils (** from Benson and Trast (1995), * from Erin L. Hunter, n.d.: not determined).

Chapter 3

Table 1. Surface Properties of test soils (* from Erin L. Hunter).

Table 2. Surface Properties of Colorado Soils (water vapor sorption isotherms of the soils 1-4 were obtained from Morteza Khorshidi, Colorado School of Mines, Golden CO).

Table 3. Chemicals used in the ammonium displacement and the proposed water vapor sorption method.

LIST OF FIGURES

Chapter 1

Figure 1. IUPAC classification of sorption isotherms (after Sing *et al*. 1985).

Figure 2. Comparison between SSA_{EGME} using large (76-mm) and small (50-mm) sample sizes.

Figure 3. Comparison between SSA_{BET} from water vapor sorption isotherms for air-dried and oven-dried samples.

Figure 4. Swelling classification based on Likos (2008) approach.

Figure 5. Measured water vapor desorption isotherms for natural clays.

Figure 6. Measured water vapor desorption isotherms for bentonite-kaolinite mixtures.

Figure 7. Measured water vapor desorption isotherms for cation-exchanged bentonite.

Figure 8. Adsorbed water content and heat of hydration for cation-exchanged bentonite.

Figure 9. Comparison of SSA_{BET} obtained from water vapor adsorption (w) and desorption (d) isotherms.

Figure 10. Comparison between EGME-based surface area and H_2O-based surface area: (a) results from current study and the literature for SSA < 100 m^2/g; (b) results from current study over the entire range of SSA.

Figure 11. Comparison between surface area from BET analysis and one-point (w_{20}) method.

Figure 12. Comparison between surface area from BET analysis and one-point (w_{47}) method: (a) $n = 1.0$; (b) $n = 1.7$.

Chapter 2

Figure 1. IUPAC classification of sorption isotherms (after Sing *et al*. 1985).

Figure 2. Measured water vapor sorption isotherms: (a) end-members; (b) mixtures (desorption).

Figure 3. R^2 values of the equations: (a) wetting curve optimization; (b) drying curve optimization.

Figure 4. Trend in parameters of the F Equation with increasing bentonite content: (a) K; (b) m.

Figure 5. Trend in parameters of the BET Equation with increasing bentonite content: (a) X_m; (b) C.

Figure 6. Trend in parameters of the FHH Equation with increasing bentonite content: (a) X_m; (b) K; (c) s.

Figure 7. Trend in parameters of the GAB Equation with increasing bentonite content: (a) X_m; (b) c_1; (c) k_b.

Figure 8. Trend in parameters of the DLP Equation with increasing bentonite content: (a) c_1; (b) c_2; (c) c_3; (d) c_4.

Figure 9. Trend in parameters of the D-A Equation with increasing bentonite content: (a) X_m; (b) E; (c) n.

Figure 10. Comparison of SSA values determined by BET, FHH, GAB, D-A, DLP, and EGME methods.

Figure 11. Relationship between $\mathrm{SSA}_{\mathrm{EGME}}$ and $\mathrm{SSA}_{\mathrm{BET}}$ for medium to low-SSA mixtures (SSA < 450 m^2/g).

Figure 12. Water vapor sorption isotherms estimated from $\mathrm{SSA}_{\mathrm{EGME}}$ and recommended range of the DLP model parameters: (a) best fit among 13 natural clays, Wcs Andrews soil; (b) worst fit among 13 natural clays, New Orleans soil.

Chapter 3

Figure 1. Schematic representation of the soil sample at full MB saturation (after Cokca and Birand 1993).

Figure 2. Relationship between SSA and CEC: (a) results from current study and the literature for SSA_{water}; (b) results from current study and the literature for SSA_{EGME}.

Figure 3. CEC-normalized water vapor desorption isotherms of homoionic bentonites.

Figure 4. CEC-normalized water vapor desorption isotherms of natural soils.

Figure 5. Surface charge-normalized sorption curve.

Figure 6. Relationship between the measured CEC values and the values calculated by the proposed water vapor sorption method.

CHAPTER 1

SPECIFIC SURFACE AREA OF CLAYS USING WATER VAPOR AND EGME SORPTION METHODS

1.1 INTRODUCTION

Specific surface area (SSA) quantifies mineral surface area per unit mass and is expressed in meters squared per gram (m^2/g). SSA for clay minerals varies widely depending on mineralogy, ranging from as much as about 800 m^2/g for expansive clay minerals such as smectite, depending on the extent of exposed interlayer surface, to as little as about 10 m^2/g for non-expansive clay minerals such as kaolinite. Because the surface area of silt-, sand-, and gravel-sized particles is negligible by comparison, the surface area of natural soils containing a distributed mixture of such particles is dominated by SSA of the clay fraction, even if this fraction is very small.

Numerous studies have shown that SSA is a valuable intrinsic property related to the more general properties and engineering behavior of fine-grained soils. Correlations have been made between SSA and plasticity (Atterberg limits), cation exchange capacity (CEC), dispersion behavior, compressibility, biological processes, sorption behavior, and frost heave susceptibility (*e.g.*, Farrar and Coleman 1967, Churchman and Burke 1991, Muhunthan 1991, Anderson and Tice 1972, Santamarina *et al*. 2002). Swelling potential of problematic expansive clays has been directly related to SSA by a number of studies (Ross 1978, Chittoori and Puppala 2011). In many respects, SSA may be a more fundamental and convenient basis than conventional geotechnical analyses such as grain size and plasticity for quantifying the composition and behavior of fine-grained soils (Lutenegger and Cerato 2001).

There are a variety of methods available for estimating SSA of soils, including physical methods such as X-ray diffraction (XRD) to determine crystallographic information, scanning electron microscopy (SEM) to determine shape and dimension of particles, and mercury intrusion porosimetry (MIP) to determine effective pore size distribution from which SSA may be inferred (Likos *et al*. 2010). More common methods include positive adsorption methods, where the accumulation of some substance at the mineral surface is measured, or negative adsorption methods, where the loss of some substance from the surface is measured. Liquid-phase sorption techniques include the use of Ethylene Glycol (EG) (Dyal and Hendricks 1950), Ethylene Glycol Monoethyl Ether (EGME) (Carter *et al*. 1965, Cerato and Lutenegger 2002), p-Nitrophenol (Ristori *et al*. 1989), polyvinylpyrrolidone (PVP) (Blum *et al*. 2011), Methylene Blue (MB) dye (Kahr and Madsen 1995), and the hemoglobin molecule (Paykov and Hawley 2013). Gas-phase techniques include the use of nitrogen (N_2), a non-polar molecule applicable for probing external surface area, or water vapor (H_2O), a polar molecule applicable for probing both internal (interlayer) and external surface area (Quirk 1955, Newman 1983, Środon and McCarty 2008, Likos 2008). Comparisons among these various SSA measurement approaches for clays and clayey soils have been made by a number of researchers (*e.g.*, Newman 1983, deJong 1999, Arnepalli *et al*. 2008, Santamarina *et al*. 2002, Tuller and Or 2005, Yukselen and Kaya 2006, Arthur *et al*. 2012).

Newman (1983) describes potential advantages of using H_2O as a probe molecule for estimating SSA of clays: (*i*) water has access to the whole mineral surface (internal and external) such that, in principle, it should be possible to estimate total SSA of both expansive and non-expansive minerals; (*ii*) water is present in natural soil and so is most likely to represent field behavior; and (*iii*) the relatively high vapor pressure of H_2O at ambient temperature is easy to control. Recent improvements in available technologies for rapidly measuring water vapor sorption of clays and clayey soils (*e.g.*, Likos *et al.* 2011) have made clay characterization using water vapor a potentially attractive alternative in geotechnical testing practice. There are, however, a number of uncertainties associated with H_2O monolayer formation, interlayer swelling, capillary condensation, and the influences of exchangeable cation type (*e.g.,* Quirk 1955, Chiou and Rutherford 1997, Quirk and Murray 1999, Newman 1983).

The EGME method has attained relative prominence as one of the more commonly adopted methods for measuring SSA for soils because it does not require sophisticated equipment and can produce repeatable results if careful test protocols are followed. The objective of this study, therefore, is to compare SSA measurements obtained using the conventional EGME method with those using various water vapor sorption methods. Comparisons are made over a wider range of SSA than previously considered and using both naturally occurring clays and a suite of artificial clay mixtures.

1.2 BACKGROUND

1.2.1 Adsorption Theories

1.2.1.1 Langmuir Adsorption Theory

Langmuir (1918) states that a solid surface adsorbs gas molecules if the surface atoms of the solid attract the gas molecules. The strength of attractive forces is assumed only enough to adsorb a single layer of gas molecules on the solid surface. Energy of adsorption is assumed to be constant, which implies a uniform surface. Thus, the sorption of gases on solid surfaces can be modeled by Equation (1):

$$\frac{P}{X} = \frac{1}{c \cdot X_m} + \frac{P}{X_m} \tag{1}$$

where X is the amount of adsorbate adsorbed (g) per gram of adsorbent at pressure P, X_m is the quantity adsorbed when the adsorbent is covered with a molecular monolayer (g/g), and c is a constant. X_m and c are found from the slope and intercept of the plot P vs P/X or by choosing a constant value for c and solving the equation for X_m. Then, SSA is calculated by the equation

$$SSA = \frac{X_m \cdot N \cdot A}{M} \quad [m^2/g] \tag{2}$$

where N is the Avogadro's number ($6.02 \cdot 10^{23}$ mol^{-1}), A is the area covered by a single adsorbate molecule (m^2), and M is the molecular mass of the adsorbate in grams.

1.2.1.2 BET Multimolecular Adsorption Theory

The Brunauer-Emmett-Teller (BET) Theory (Brunauer *et al*. 1938) has its basis in statistical thermodynamics. Although dependent on many assumptions, it is still a widely accepted theory of physical adsorption (Dutcher *et al*. 2011). Two basic assumptions for the derivation of the equation are: (i) the surface of the adsorbent is homogeneous, and (ii) there is no lateral interaction between the adsorbed molecules.

The rate of condensation of molecules from the gas phase is equated to the rate of molecules evaporated from the second layer of adsorbed molecules. The rate of condensation from the second layer is equated to the rate of evaporation from the third layer, and so on. Below the saturation water pressure, the surface fraction of adsorbed molecules will increase with the increasing partial pressure of the sorbate. This means that the thickness of the adsorbed layer will not be a constant through the sorption process, but will change depending on the values that are specific for each layer. The heat of adsorption of the molecular layers is assumed to be equal to the heat of liquefaction after the formation of first monolayer. Also, the evaporation-condensation conditions are assumed to be identical, except for the first layer. The last assumption is that, at the saturation vapor pressure, the number of adsorbed layers is infinite. The BET equation (Equation 3) is then derived by summing the fractional coverage at each layer. Thus, the theory is also referred as the kinetic theory of multimolecular adsorption.

$$\frac{P}{X(P_0-P)} = \frac{1}{X_m C} + \frac{C-1}{X_m C} \cdot \frac{P}{P_0} \tag{3}$$

where X is the mass of adsorbate at vapor pressure P and temperature T, P_0 is the corresponding saturated vapor pressure, and X_m is the quantity adsorbed (g/g) at monolayer coverage. The BET constant C is an energetic term defined as

$$C = \frac{exp(E_1-E_L)}{RT} \tag{4}$$

where $E_1$is the heat of adsorption of the first molecular layer of adsorbate, E_L is the heat of condensation of the adsorbate, R is the molar gas constant (8.314 J $mol^{-1}K^{-1}$), and T is the absolute temperature (K). The difference (E_1 – E_L) is a measure of the energy of interaction (J/mol) between the first monolayer of adsorbed molecules and the surface. Large values of (E_1 – E_L) indicate large forces of hydration between the surface and the monolayer.

Similar to Langmuir Theory, X_m and C can be calculated by the slope and intercept of the plot P/P_0 vs $P/(X\cdot(P_0-P))X$ or by choosing a constant value for C and solving the equation for X_m. Then, SSA is calculated by using Equation (2).

Due to the assumptions made to derive the equation, BET theory is not expected to give a perfect fit for the whole R_H range. As noted by Ponec *et al.* (1974), the BET equation tends to give lower adsorption values than experimental results when R_H is low. This is because a single heat of adsorption is assumed for the whole surface when calculating the monomolecular coverage with the BET theory. However, in the actual case, the surface is not homogeneous. There might be some more active adsorption sites that have a higher heat of adsorption than the average value. After the degree of surface coverage (w / X_m, where w is the gravimetric water content) reaches 0.5 g/g, the surface becomes more homogeneous having more similar properties that can be assumed as a single value. At higher R_H values the case is the opposite. That is, the value calculated from the BET equation is usually greater than the experimental value (Ponec *et al.* 1974).

1.2.2 Existing Methods to Determine SSA

1.2.2.1 Nitrogen Sorption Method

In the nitrogen sorption method, N_2 gas is adsorbed on the clay surface. Then, BET theory is applied to find the monomolecular coverage, and to calculate the SSA. Since nitrogen is a nonpolar molecule, theoretically it cannot penetrate into the clay mineral interlayers. Therefore, the surface area calculated represents the external surface area. However, as noted by Santamarina *et al*. (2002), a small amount of N_2 can still penetrate into the interlayers if the clay has pores larger than the size of the nitrogen molecule, causing a slightly higher SSA calculation than the actual external surface area. Nitrogen molecules are attracted to the surface by Van der Waals forces, and multilayer adsorption can occur on the external surface.

1.2.2.2 Ethylene Glycol (EG) Sorption Method

In this method proposed by Dyal and Hendricks (1950), soil specimens are saturated with the polar molecule EG and desiccated in a vacuum desiccator. Weight measurements of the soil-EG mixture are obtained to determine the weight of EG retained on the soil sample. When the weight reaches a constant value (in 24 to 39 hours), it is assumed that there is only one monolayer of EG molecules retained on the soil surface, and the SSA is calculated by the equation:

$$SSA = \frac{X_r}{X_S \cdot 3.10 \cdot 10^{-4}} \tag{5}$$

where X_r is the weight of EG (g) retained by the specimen, X_s is the initial weight of the soil, and $3.10 \cdot 10^{-4}$ is the amount of EG (g) necessary to form a monolayer on a 1-m^2-clay surface. To obtain this value, first the surface area (SA) of montmorillonite is calculated from unit cell dimensions of a = 5.25 Å and b = 9.20 Å by Equation 6.

$$SA = 5.25 \cdot 9.20 \cdot 10^{-20} \cdot 6.02 \cdot 10^{23} = 2.91 \cdot 10^{5}\ m^{2} \text{ in one mole (360 g)} \tag{6}$$

where $6.02 \cdot 10^{23}$ is Avogadro's number. Then, SSA is calculated as $2.91 \cdot 10^{5}/360 = 810\ m^{2}/g$, which is accepted as the theoretical SSA of Na-montmorillonite. The amount of EG required to form monomolecular layer is 0.25 g, so $3.10 \cdot 10^{-4}$ is obtained by dividing 0.25 g by 810 m^2.

If clay specimens are heated (to 600 °C) prior to testing, the clay structure is destroyed. Interlayer swelling is prevented, so only external surface area is obtained. If the specimens are not heated, the total surface area is obtained (Dyal and Hendricks 1950).

The EG Method had been widely used for SSA calculations (*e.g.* Bower and Gschwend 1952, Bower and Goertzen 1959, Puri and Murari 1963) until Carter *et al*. (1965) developed the EGME Method, where the only major difference is the type of the polar molecule adsorbed.

1.2.2.3 Ethylene Glycol Monoethyl Ether (EGME) Sorption Method

As mentioned above, the EGME Method follows the same basic protocol as the EG Method. Surface area is calculated by using the mass of a polar molecule, EGME, retained on the clay surface after desiccating the EGME-saturated clay. One monomolecular layer of EGME is assumed to be retained on the clay specimen when the weight of the mixture becomes constant. The weight of EGME required to form a monomolecular layer on a square meter of surface was calculated as 286 μg by using the value of 810 m^2/g calculated by Dyal and Hendricks (1950) as the surface area of montmorillonite and the measured value of 231.7 mg/g as the EGME retained by montmorillonite.

The EG and EGME methods give very similar results (Carter *et al*. 1965), but using the EGME Method has some advantages over the EG Method. The main advantage is that since the EGME molecule has a higher vapor pressure at room temperature than the EG molecule, the evaporation rate is higher. Thus, the time required for desiccation of the EGME molecules until a monomolecular layer is retained on the clay surface is less than the time required for desiccation of the EG molecules. Another advantage of the EGME Method over the EG Method reported by Carter *et al*. (1986) is that there is less specimen handling in the EGME Method, so the probable discrepancies due to the user effect is less. Cerato and Lutenegger (2002) developed the EGME Method and recommended a procedure which was mainly followed in this research with some alterations that will further be discussed.

1.2.2.4 Methylene Blue (MB) Sorption

The MB Method also has the same basic idea as the previously discussed methods that use polar molecules to calculate SSA. That is, the amount of MB forming a monomolecular layer on the clay surface is used together with the known surface area of the molecule itself. Since MB is a colored dye, the monolayer coverage is determined by measuring the amount remained in the solution with a colorimeter or a spectrometer. The monomolecular layer of MB is assumed to be formed when the flocculation is optimum. The surface area of MB was calculated as 1.30 nm^2

(Kalousek and Blahnik 1955). By using this value, Hang and Brindley (1970) proposed an equation (7) to calculate the SSA.

$$SSA = M_f \cdot 130 \cdot 6.02 \cdot 10^{-2}\ m^2/g \tag{7}$$

where M_f is the meq of methylene blue adsorbed per 100 g clay. This method can be used both for determining the CEC and SSA of clayey soils.

1.2.2.5 Water Vapor Sorption Method

In the water vapor sorption method, either a single point is assumed as the monolayer coverage, or BET Theory can be applied on the water vapor sorption data to calculate the SSA. Mooney *et al*. (1952), Cases *et al.* (1992), and Likos and Lu (2002) used a range of R_H values and the corresponding water contents to calculate the SSA from BET theory. Newman (1983), Puri and Murari (1964), and Tuller and Or (2005) used a single value of R_H and the corresponding water content. Although the obtained results will be different, it is possible to use both the desorption and the adsorption curve to determine monolayer coverage or to apply the BET Theory.

1.2.3 Water Sorption Isotherms

A sorption isotherm of a soil is a plot of the amount of gas that the soil sorbs on the surface with changing vapor pressure of that gas at a constant temperature. For water vapor sorption isotherms, the gas is water vapor and the changing pressure is represented by the changing relative humidity (R_H) of the environment. The International Union of Pure and Applied Chemistry (IUPAC) (1985) classified physisorption isotherms into six types after the studies of Brunauer at al. (1938), Brunauer *et al*. (1940), and Brunauer (1945). The isotherms are shown in

Figure 1. In the IUAPC classification, Sing *et al.* (1985) also explains the solid properties that the different isotherm types represent.

Type I isotherms are formed by solids with small external surfaces. The sorption is limited and determined by the accessible micropore volume as these solids are generally microporous and have relatively small external surfaces. Type II isotherms are obtained if the solid is nonporous or macroporous. Monolayer-multilayer sorption can occur unrestrictedly. Point B in Figure 1 represents the stage where monolayer adsorption is completed and multilayer adsorption starts. The interaction between the solid surface and the adsorbate is strong (Montes-H *et al.* 2003). Type III isotherms are formed when there is no strong attraction between the solid surface and the adsorbate. The Type I, Type II and Type III isotherms are all reversible, which means the drying curve follows the same path as the wetting curve. Type IV isotherms show hysteresis, which means the paths of the drying and the wetting curves are different. This is mainly because of capillary condensation. The solid holds more water while drying than while wetting. Type IV isotherms are obtained if the solid is mesoporous. The initial part of the Type IV isotherm is very similar to the Type II isotherm, which represents monolayer-multilayer adsorption. Type V isotherms are not very common. They also show hysteresis, and the initial part of the isotherm can be attributed to the Type III isotherm, which represents weak interaction between the solid surface and the adsorbate. Type VI isotherms show stepwise multilayer adsorption on a uniform, non-porous solid surface. Each step represents a monolayer adsorption. After one layer of adsorbate is adsorbed, the second layer starts to form.

1.3 MATERIALS AND METHODS

1.3.1 Clays and Clay Mixtures

Tests described herein were conducted using 13 samples of natural clayey soils, a suite of artificially prepared bentonite-kaolinite (B-K) mixtures, and various cation-exchanged forms of a natural Na^+/Ca^{2+} bentonite. Natural clays were selected from the University of Wisconsin-Madison (UW) soil bank, which contains clayey soil samples having a wide range of properties and geological histories, including glacial tills and glacio-fluvial clays from the midwest and northeastern regions of the United States, residual soils from the southeast, marine clays from the gulf coast, alluvial clays from the intermountain range and west coast, and eolian clayey soils from the northwest (Benson 2014). Samples range from non-plastic to highly plastic and have both narrow and broad particle-size distributions. Bentonite-kaolinite mixtures were prepared in seven mass-controlled ratios denoted by their respective bentonite (B) and kaolinite (K) content (100K, 20B/80K, 50B/50K, 70B/30K, 80B/20K, 90B/10K, 100B). End member bentonite and kaolinite for these mixtures was obtained from the Source Clay Repository of the Clay Minerals Society (Bain *et al.* 2001). This included SWy-2, which is a Na^+-rich montmorillonite from Crook County, Wyoming, and KGa-1b, which is a low-defect kaolinite from Washington County, Georgia. An additional series of sorption experiments was conducted using cation-saturated forms of a natural Na^+/Ca^{2+} bentonite to produce homoionic Na^+, K^+, Li^+, Ca^{+2}, and Mg^{+2} forms. Cation exchange was accomplished by treating the clay two times with a 1.0 M solution of the chloride of monovalent cations or a 0.1 M solution of the chloride of divalent cations, followed by repeated washing with deionized water and a check for excess chloride using $AgNO_3$. Combined, the suite of test soils represents a wide range of natural and artificial clays having a broad spectrum of mineralogy, surface area, cation exchange capacity, and corresponding H_2O and EGME sorption behavior. Table 1 shows the surface properties and Atterberg limits of the test soils

1.3.2 Ethylene Glycol Monoethyl Ether (EGME) Method

Carter *et al*. (1965) first suggested the use of the EGME method as an alternative to earlier use of EG for SSA determination. Cerato and Lutenegger (2002) adapted EGME testing procedures described by Carter *et al*. (1986) and investigated the effects of several variations in testing protocol, including the amount of EGME used, the mass and size fraction of soil used, the age of EGME-$CaCl_2$ solvate used for vapor pressure control, and the size of the equilibration chamber. Repeatability analyses for two clays indicated a standard deviation (σ) of 21.7 m^2/g for clay having a mean (μ) SSA of 167 m^2/g and σ of 16.3 m^2/g for clay having a mean SSA of 49 m^2/g. These results suggest a coefficient of variation ($COV = \sigma/\mu$) for typical EGME-based SSA measurements on the order of about 10% to 30%.

The EGME test apparatus and procedures adopted for this study were based on the general recommendations of Cerato and Lutenegger (2002) with minor modifications as noted. Samples were initially air-dried and pulverized, if necessary, to pass a #40 (0.425 mm) sieve and then oven dried at 105° C for 24 h. Approximately one gram of cooled material was mixed with three cm^3 of laboratory grade EGME in a 50-mm-diameter (23-mm height) aluminum tare, and gently mixed to form slurry using a swirling hand motion. The EGME-clay slurry was then sealed in an equilibration chamber (cylindrical glass desiccator) having an inside diameter of 250 mm and connected to a vacuum pump capable of providing approximately 70 kPa vacuum. EGME-$CaCl_2$ solvate was prepared by mixing 100 g of anhydrous $CaCl_2$ with 20 cm^3 of EGME and placed in the headspace along with the samples. The purpose of the solvate is to maintain a constant EGME vapor pressure and minimize loss of EGME from the monolayer formed on mineral surfaces (Carter *et al*. 1965). Specimens were kept in the sealed desiccator for 20 min, after which vacuum was applied to promote evaporation of excess EGME from the specimens. Specimens were removed after eight hours and weighed to 0.0001 g using an analytical balance. If any specimen remained visibly wet with EGME after eight hours, no measurement was taken to minimize excessive specimen handling and disturbance of the vapor pressure. Subsequent weight measurements were then taken approximately every four hours until the change between two measurements became less than 0.001 g. The amount of time required for equilibration depended to some extent on SSA, but was generally obtained within 48 to 72 hours, slightly higher than the time recorded by Cerato and Lutenegger (2002). This difference is attributed to the use of lower vacuum and to the fact that more specimens were tested concurrently in a single desiccator.

The mass of EGME retained by a sample at equilibrium was assumed to correspond to monolayer coverage on the mineral surface, such that SSA could be determined from:

$$SSA_{EGME} = \frac{M_a}{2.86 \cdot 10^{-4}\left(M_s\right)} \tag{8}$$

where M_a (g) is the mass of EGME retained at equilibrium and M_s (g) is the initial dry mass of the clay sample. The constant $2.86 \cdot 10^{-4}$ has units of g/m^2 and quantifies the mass of EGME required to cover 1.0 m^2 of mineral surface, as estimated by Dyal and Hendricks (1950).

It should be noted that the 50-mm sample tare adopted in the test protocol is smaller than the 76-mm × 25-mm tare suggested by Cerato and Lutenegger (2002). The smaller tare was selected so that a larger number of samples (~12) could be placed in a single desiccator for concurrent testing. Also, the smaller container found to prevent soil from being pulled out of the tare during vacuum evacuation and thus precluded the requirement for porous lids to retain the soil. Comparisons among several samples equilibrated in 76-mm tares and 50-mm tares indicated only minor (< 5.3%) differences in SSA values obtained (Figure 2), and thus the smaller tare size was adopted for all subsequent tests.

1.3.3 Water Vapor Sorption Method

When a hydrophilic material such as clay is placed in a closed atmosphere containing water vapor, water condenses on its surface under physical and chemical bonding mechanisms that decrease the energy of the adsorbed water. Sorption on clay surfaces is governed by several competing mineral-water interaction mechanisms, including hydrogen bonding between water and oxygen or hydroxyl comprising the mineral surfaces, dipole polarization effects arising from mineral surface charge, van der Waals forces, and hydration of exchangeable cations residing at or near the mineral surfaces (*e.g.*, Mitchell 1993). A water vapor sorption isotherm quantifies the relationship between vapor pressure and the moisture content of the material obtained along an adsorption (wetting) or desorption (drying) path at some specific temperature. Water vapor pressure (u_v or P) is typically normalized by saturated vapor pressure (u_{v0} or P_0) such that isotherms may be plotted as gravimetric water content (w) versus relative humidity (R_H), where $R_H = u_v/u_{v0} = P/P_0$. Water vapor sorption isotherms for clays and clayey soils have been studied by a number of researchers using a variety of experimental and computational approaches (Mooney *et al.* 1952, Collis-George 1955, Van Olphen 1965, Cases *et al.* 1992, Berend *et al.* 1995, Likos and Lu 2002, 2003). Because water vapor sorption isotherms are a direct measurement of how interactions between water and clay surfaces result in adsorption, water vapor sorption isotherms provide an indirect measurement of fundamental clay compositional and surface properties such as SSA and CEC that control these interactions.

Water vapor sorption isotherms for soils are most commonly determined following one of two basic approaches: by determining equilibrium R_H in a closed environment containing a sample at known water content (*e.g.*, Tuller and Or 2005), or conversely, by measuring equilibrium water content of a sample placed into a controlled R_H environment (Likos and Lu 2003). Sorption isotherms for the current study were obtained using a commercially available vapor sorption analyzer (VSA) operating in dynamic dewpoint isotherm (DDI) mode (Decagon Devices, Pullman WA). Unlike similar systems for measuring water vapor sorption isotherms from the equilibrium mass of adsorbed water, the DDI approach involves concurrent measurement of sample water content and R_H in a dynamically changing vapor pressure environment. As described by Likos *et al*. (2011), samples are placed into an environmental chamber and continuously wetted or dried by circulating either a vapor-saturated or desiccated air stream through the chamber. Changing R_H is periodically measured using a chilled-mirror dew point sensor (Leong *et al*. 2003, Campbell *et al*. 2007) while concurrently tracking changes in sample mass. Because there is no dependency on complete equilibration at discrete R_H increments, sorption isotherms containing a large number of measurement points may be obtained along hysteretic wetting and drying paths in less than about 24 hours. Likos *et al*. (2011) compared results obtained using the DDI approach and a conventional equilibrium method (Likos and Lu 2003). Agreement between the two measurement approaches was within about 10% to 15% of the full-scale range. Reproducibility was within 6% of the full-scale range.

A preliminary series of tests was conducted to compare sorption isotherms and corresponding SSA estimates for samples that were initially air-dried and oven-dried to 105 ˚C. SSA of air-dried samples was found to be about 10% greater on average than the SSA of oven-dried samples (Figure 3). When the soil is oven-dried prior to the test, the sorption isotherm shifts downwards, meaning the amount of water adsorbed at a given R_H becomes less than for air-dried samples. The shift is more significant for soils having low clay content and small SSA

(Arthur *et al*. 2013). Although the shift can be significant, the slope of the curve does not change significantly and thus SSA determined from the slope, as described subsequently, shows only a minor difference. Based on this observation, air-dried samples were decided to be used for all subsequent tests to minimize potential effects of heating (*e.g.*, for organic-rich natural clays) and to best represent field conditions.

Hysteretic sorption isotherms were obtained along an initial drying path from ambient conditions down to 3% R_H to dry the sample from its initial air-dry water content, immediately followed by a wetting cycle up to 95% R_H and then a second drying cycle back down to 3% R_H. All isotherms were obtained at a set point temperature of 25 ± 0.2 ˚C automatically maintained by the VSA system. Initial air-dry mass of the samples passing #40 sieve was 1.90 ± 0.08 g. Complete adsorption-desorption loops typically contained as many as 170 to 225 discrete measurements and were obtained in 24 to 72 hours.

The mass of water required to form a monomolecular layer, heat of adsorption, and SSA were estimated from the measured H_2O sorption isotherms using BET theory (Brunauer *et al.* 1938). Numerous studies have shown that BET theory may be successfully applied for analyzing water vapor sorption on natural and treated clay surfaces (Keren and Shainberg 1979, Likos and Lu 2002). Application to expansive clays, however, should be done with caution because the sorption mechanisms are complex and depend upon the layer charge of the mineral; valence, amount, and size of exchangeable cations; the extent of interlayer swelling; and the extent of capillary condensation occurring on particle surfaces and interfaces (Chiou and Rutherford 1997, Quirk and Murray 1999). The concept of monolayer coverage forming the basis of BET theory is in fact tenuous because H_2O molecules tend to cluster at the cation and charge sites (Quirk 1955) because capillary condensation may be non-negligible, and because surface area may evolve as the clay adjusts to the adsorption of water (*e.g.,* Salles *et al*. 2009). According to BET theory, physical sorption involves the formation of many molecular layers of adsorbate on the adsorbent surface. Sorption is modeled by Equation 3.

If the cross-sectional area of the adsorbate molecule is known, $\mathrm{SSA_{BET}}$ may be approximated from monolayer coverage X_m according to:

$$SSA_{BET} = \frac{X_m}{M_w} \cdot N \cdot A \tag{9}$$

where, for H_2O sorption on clay, M_w is the molecular mass of water ($M_w = 0.018$ kg mol^{-1}), N is Avogadro's number ($6.02 \cdot 10^{23}$mol^{-1}), and A is the area covered by one H_2O molecule ($A = 10.8 \cdot 10^{-20}$ m^2). According to Equation (3), a plot of $P/X(P_0\text{-}P)$ versus P/P_0 gives a straight line over some range of P/P_0 with slope $(C\text{-}1)/(X_mC)$ and intercept $1/(X_mC)$. Values of X_m and C can thus be obtained from a plot of experimental sorption data to back-calculate the mass of H_2O at monolayer coverage, heat of adsorption, and SSA. The linear range of applicability for water vapor sorption on clay surfaces is generally less than about P/P_0 from 0.4. In this study, BET theory was applied between P/P_0 ranging from 0.1 to 0.3.

1.4 RESULTS AND DISCUSSION

1.4.1 Swelling Classification based on Likos (2008) Approach

The natural soils were classified based on the approach suggested by Likos (2008). Water content at 75% R_H (w_{75}) is plotted against the plasticity index (PI) (Figure 4). Soils having a w_{75} value lower than 0.04 are considered to be non-expansive or low expansive, w_{75} between 0.04 and 0.06 are moderately expansive, w_{75} between 0.06 and 0.08 are highly expansive, and w_{75} greater than 0.08 are classified as very highly expansive. Based on this classification Atlanta-Georgia, Alb 1, Albany red, Alb 2, Mon 2, and New Orleans soils are non or low expansive;

Houston brown, Wcs Andrews, Kamm clay, KF 2, and Denver soils are moderately expansive; Sacramento soil is highly expansive; and KF 1 soil is very highly expansive. Figure 4 also shows that, although the results of KF 1 show a little difference, soils of the current study are in a good agreement with the Likos (2008) results.

1.4.1 Water Vapor Sorption Isotherms

Figures 5 through 7 are plots of water vapor sorption isotherms for each of the test clays obtained along desorption paths. Figure 5 includes results for the series of natural clays; Figure 6 includes results for the bentonite-kaolinite mixtures; and Figure 7 includes results for the cation-exchanged bentonites. Hysteresis between wetting and drying loops was observed for all the clays in a manner consistent with previous studies, but only desorption loops, which were used for SSA calculations, are included here for clarity. Differences in SSA values estimated using BET analysis of the measured wetting loops and drying loops are described subsequently.

The measured sorption isotherms clearly illustrate the positive relationship between R_H and the mass of adsorbed water at equilibrium. The amount of water adsorbed at ~95% R_H ranges from as much as 35% for the high-plasticity and expansive clays to as little as about 2% for the non-expansive clays. The amount of water adsorbed by the kaolinite-bentonite mixtures (Figure 6) over the complete range of R_H increases approximately linearly with increasing bentonite content, a direct reflection of the greater surface area, interlayer swelling, and surface charge of the smectite component. Most of the natural clays and the kaolinite-rich B-K mixtures display characteristics of a standard type II isotherm, indicating that sorption occurs incrementally as monomolecular layers until the adsorbed film grows to a thickness such that it is no longer strongly influenced by the particle surface. Isotherms for the smectite-rich clays, on the other hand, more closely represent type IV isotherms, indicating successive adsorption or desorption of molecular water layers from within expansive interlayers. Similar “wavy” or “step-wise” isotherm characteristics have been noted by numerous researchers for H_2O sorption by expansive clay minerals (*e.g.*, Mooney *et al.* 1952, Collis-George 1955, Van Olphen 1965, Cases *et al.* 1992, Berend *et al.* 1995) and have been described and analyzed in detail by Likos and Lu (2006) and Likos and Wayllace (2010).

The isotherms for the cation-exchanged bentonites (Figure 7) indicate that cation type has an appreciable effect on short-ranged water sorption. Cations of higher valance and smaller size generally tend to have higher energy of interaction with water. Ion heat of hydration (ΔH) for the cations considered here increases in the order K^+ (-314 kJ/mole) < Na^+ (-397 kJ/mole) < Li^+ (-506 kJ/mole) < Ca^{2+} (-1,580 kJ/mole) < Mg^{2+} (-1,910 kJ/mole) (Bohn *et al*. 1985). Figure 8, which is a plot of adsorbed water content at R_H of 20%, 40%, and 60% as a function of ΔH, indicates that water sorption generally scales with cation heat of hydration. This is clearly evident for the bentonites exchanged with monovalent cations (K^+, Na^+, and Li^+), where adsorbed water content sharply and systematically increases with ΔH, but is not evident for the clays exchanged with divalent cations (Ca^{2+}, Mg^{2+}), which do not absorb significantly more water than the bentonites with high-energy monovalent cations. It is also interesting to note that the effect of cation type becomes less evident for R_H values greater than about 60%. Isotherms for the Na^+, Ca^{2+}, and Mg^{2+} bentonites and the un-exchanged (Na^+/Ca^{2+}) bentonite, for example, appear to converge at R_H of about 70%, and remain almost identical for R_H up to ~95%. This is interpreted to reflect the notion that water sorption at lower R_H is dominated by short-ranged hydration mechanisms dependent on cation type and mineral surfaces, but at higher R_H, is dominated by longer-ranged capillary mechanisms dependent on pore structure (Likos and Lu 2012).

1.4.2 Surface Area Calculations using BET Theory

Figure 9 shows results from analyses conducted to compare SSA estimated using BET theory and H_2O sorption isotherms obtained along wetting (adsorption) paths and along drying (desorption) paths. Drying-based and wetting-based SSA values are very similar (within 8.3%) for SSA less than about 100 m^2/g, but deviate significantly for higher surface area materials containing an appreciable component of expansive clay minerals. This is most evident for the B-K mixtures, where it may be observed that even a small percentage of bentonite (*e.g.*, 20B/80K) results in an appreciably higher drying-based surface area ($SSA_{BET,d}$) than wetting-based surface area ($SSA_{BET,w}$). Drying-based surface area for the bentonite-kaolinite mixtures is consistently about two times the wetting-based SSA. The ratio ($SSA_{BET,d}$) / ($SSA_{BET,w}$) ranges from 1.93 to 2.15 and averages 2.06 for the five mixtures. Water-based SSA values for subsequent comparison with EGME-based values are those corresponding to the drying path because BET plots of Equation (3) were consistently linear for decreasing R_H values less than 40% and because the EGME method is also based on an evaporative drying process. One reason why BET plots are not linear for the wetting path might be the effect of surface heterogeneities. When the soil starts to adsorb water from an initially completely dry surface, adsorption is affected by the surface heterogeneities (Mooney *et al*. 1952), causing nonlinearity in the BET plot. For the desorption path, the sorption process is not influenced by surface heterogeneities until the soil surface becomes close to a completely dry state (less than about 10% R_H).

Figure 10 is a direct comparison of SSA estimated from BET analysis of measured H_2O desorption isotherms (SSA_{BET}) and SSA estimated using the EGME method (SSA_{EGME}). Figure 10a includes the current clays along with results from the literature for SSA limited to less than 100 m^2/g, Figure 10b includes results for the clays in the present study over a wide range of SSA.

The EGME and H_2O results are comparable for SSA less than about 100 m^2/g but again deviate for higher SSA. For SSA < 100 m^2/g, the relation between the EGME and H_2O results is captured by the following equation ($R^2 = 0.76$).

$$SSA_{BET}\,(m^2/g) = 0.98 \cdot SSA_{EGME} \tag{10a}$$

At higher SSA, the water-based values are consistently about one half the EGME-based values. The relation between SSA_{BET} and SSA_{EGME} over the entire measured range is best fit ($R^2 = 0.90$) by the linear equation:

$$SSA_{BET}\,(m^2/g) = 0.58 \cdot SSA_{EGME} + 8.96 \tag{10b}$$

There are several possible reasons for the discrepancy observed between SSA_{BET} and SSA_{EGME}. Quirk and Murray (1999), for example, compare values of surface tension (γ) and partial molar volume (v_m) for EGME and H_2O and point out that the product of these two values (γv_m) for EGME is about twice the values for H_2O. Capillary theory and Kelvin's equation (11) dictate that, for a given vapor pressure (u_v), capillary radius (r) is directly proportional to the product (γv_m). Capillary condensation of EGME vapor is thus expected to occur in larger capillaries than at the same partial pressure of H_2O vapor. Excess surface retention by capillary condensation, which would result in an elevated SSA estimate, is thus more likely to occur for EGME sorption than for H_2O sorption. Kelvin's equation supporting this interpretation is as follows:

$$-RTln\left(\frac{u_v}{u_{v0}}\right) = \frac{2\gamma v_w cos\alpha}{r} \tag{11}$$

where R is the universal gas constant, T is temperature, u_{v0} is saturated vapor pressure, and α is interfacial contact angle.

A second possible reason for obtaining almost twice the SSA_{BET} values with the EGME method is related to interlayer swelling in expansive clay minerals, as described by Mooney *et* *al.* (1952). Numerous studies have shown that expansive clay minerals equilibrated with water vapor at R_H values less than about 80% successively adsorb molecular layers of water in the interlayer space, a process referred to as crystalline swelling (Norrish 1954). Interlayer water within this regime is adsorbed or desorbed in a step-wise fashion generally associated with one, two, or three layers of H_2O molecules depending on the prevailing R_H and predominant exchange cation. Interlayer crystalline swelling is manifest in sorption water vapor isotherms by the "wavy" shape pointed out previously for the bentonite-rich materials examined here. If at some prevailing R_H the mineral interlayer favors adsorption of only one water layer (*e.g.*, for Na^+-bentonite at R_H less than about 60%), then two interlayer surfaces will share the same water layer. Neglecting any contribution from external surfaces and particle edges, the corresponding SSA would thus be underestimated by a factor of about two.

Mooney *et al.* (1952) recognized this complication and proposed the following correction for calculating SSA of expansive clay minerals using H_2O sorption:

$$SSA^{*} = \left(2 \cdot SSA_{BET}\right) - SSA_{N_2} \tag{12}$$

where SSA* is corrected specific surface area, SSA_{BET} is surface area estimated from BET analysis of a measured H_2O isotherm, and SSA_{N2} is surface area estimated from nitrogen adsorption (*i.e.*, that corresponding only to external particle surfaces). External surface area SSA_{N2} is subtracted from the first term so as not to take the external surface area into account twice. Thus, while this correction procedure may be practical in cases where a clay sample is known to contain only Na^+-montmorillonite, it will not be practical in cases where the mineralogy of a natural sample is unknown.

Another possible reason for obtaining almost twice the SSA_{BET} values with the EGME method is related to the assumptions of the BET theory. BET theory assumes that, after the first monolayer of water molecules are adsorbed on the clay surface, energy of the second and higher layers of water molecules (E_2) will be equal to the energy of liquefaction (E_L). However, E_2 is actually higher than E_L because the adsorbed layers beyond the monolayer are still affected by the surface charge up to about three adsorbed layers (Gregg and Sing 1982). Assuming that E_2 is equal to E_L causes overestimated C values, underestimated X_m values and, consequently, underestimated SSA values.

1.4.3 One-Point Surface Area Calculations

A number of alternative approaches to BET analysis of full water vapor isotherms have been proposed for estimating SSA and clay surface properties from relatively simple measurements obtained under controlled humidity conditions. Quirk (1955), for example, suggested that a single-point SSA determination could be made by equilibrating samples in a vacuum desiccator with a saturated solution of $CaBr_2$, which yields water vapor pressure corresponding to 19% R_H at 20˚C. Rationale for equilibration at 19% R_H was based on BET observations for a range of clays showing completion of an H_2O monolayer at an average R_H of 21%. Arthur *et al.* (2012) explored this approach by assuming monolayer H_2O coverage occurs at 20% R_H. Surface area was estimated according to:

$$SSA_{w20} = \frac{w_{20}}{M_w} \cdot N \cdot A \tag{13}$$

where w_{20} is gravimetric water content measured at 20% R_H. That study demonstrated good correspondence between water-based SSA values and EGME-based values for 21 Arizona soils. The maximum value of SSA for the suite of soils considered, however, was less than about 150 m^2/g and thus likely did not include clays having an appreciable component of expansive minerals.

Newman (1983) proposed tests involving equilibration with water vapor using a saturated $Ca(NO_3)_2$ solution, which yields an R_H of 47%. Corresponding SSA is calculated according to:

$$SSA_{w47} = \frac{w_{47}}{n \cdot M_w} \cdot N \cdot A \tag{14}$$

where w_{47} is gravimetric water content corresponding to 47% R_H and n is a correction factor set equal to 1.7 for non-expansive soils and equal to 1.0 for expansive soils. Rationale for equilibration at R_H of 47% was based on empirical observation of a close relation between EG and H_2O retention, and the notion that 47% R_H corresponds to one H_2O layer on external surfaces and two H_2O layers on interlayer surfaces of expandable clay minerals having predominantly divalent exchange cations. For non-expansive minerals, Newman (1983) suggested setting the correction factor n = 1.7 based on an estimation that average water layer thickness at 47% R_H is 1.7 times greater than the monolayer thickness.

Figure 11 is a comparison between SSA calculated for all the test clays, including the mixtures and homoionic bentonites, using BET analysis of the measured desorption isotherms and the one-point approach based on w_{20}. Gravimetric water content at 20% R_H for these calculations was obtained directly from the drying loop of the isotherms. The relation between $SSA_{BET,d}$ and SSA_{w20} is best fit (R^2 = 0.85) by the linear equation:

$$SSA_{w20}(m^2/g) = 0.63 \cdot SSA_{BET} + 30.62 \tag{15}$$

Figure 12 is a comparison between SSA_{BET} and SSA_{w47} calculated using w_{47} obtained directly from the drying loop of measured sorption isotherms. Figure 12a shows results with the correction factor n = 1, whereas Figure 12b shows results for n = 1.7. The relation between SSA_{BET} and uncorrected (n = 1.0) SSA_{w47} is best fit (R^2 = 0.91) by,

$$SSA_{w47}(m^2/g) = 1.11 \cdot SSA_{BET} + 40.27 \tag{16}$$

whereas, using n = 1.7 (R^2 = 0.91):

$$SSA_{w47}(m^2/g) = 0.65 \cdot SSA_{BET} + 23.69 \tag{17}$$

SSA values calculated from w_{47} without applying the correction factor exceed the BET-based values by about 2.4% to 95.4% over the entire measured range. The BET-based and w_{47}-based values using $n = 1.7$ are very close for surface area less than about 150 m^2/g (within 5%), suggesting that the corrected w_{47} method for predominantly non-expansive clays is potentially applicable.

1.5 SUMMARY AND CONCLUSIONS

Specific surface area (SSA) values determined using a conventional EGME method and various methods based on water vapor sorption have been obtained and compared. Soils selected for testing included 13 samples of natural clayey soils, a suite of artificially prepared bentonite-kaolinite mixtures, and various cation-exchanged forms of a natural Na^+/Ca^{2+}-bentonite. Oven drying at 105 ˚C was found to have a negligible effect on water vapor sorption for the suite of clays examined and does not significantly affect SSA calculations based on BET analysis. Measured sorption isotherms clearly illustrate the positive relationship between R_H and adsorbed water content. Isotherms for cation-exchanged bentonite indicate that cation type has an appreciable effect on water sorption for R_H less than about 60%. The amount of water adsorbed by clays exchanged with monovalent cations systematically scales with heat of hydration in the order $Li^+ > Na^+ > K^+$. Clays exchanged with divalent cations (Ca^{2+} and Mg^{2+}) adsorb an amount of water comparable to Li^+-exchanged clay, but the amount of adsorbed water no longer scales with cation heat of hydration. SSA calculated using BET theory for adsorption (wetting) isotherms and desorption (drying) isotherms are comparable for predominantly non-expansive materials having SSA less than about 100 m^2/g, but are appreciably different for soils containing expansive clay. Drying-based surface area for the bentonite-kaolinite mixtures is consistently about two times the wetting-based SSA. Surface area estimated from BET analysis of H_2O desorption isotherms and using the EGME method are comparable for SSA less than about 100 m^2/g. Water-based SSA values are consistently about one-half the EGME-based values at higher surface areas. This observation is potentially attributable to excess capillary condensation of EGME at relatively low vapor pressure, the sharing of interlayer water by multiple surfaces for clays containing Na^+-montmorillonite, and underestimating BET X_m parameter due to the assumptions made to derive the equation. Simplified one-point methods for estimating SSA using water vapor sorption compare well with BET-based methods for surface area less than about 150 m^2/g. For expansive clay minerals having higher surface area, however, the relation between H_2O-based SSA and the EGME and one-point methods remain essentially linear, but deviate from one-to-one correspondence. Empirical relations obtained here are recommended for future correlations applied to high-surface-area clays.

1.6 REFERENCES

Anderson, D.M. and Tice, A.R., 1972, “Predicting unfrozen water contents in frozen soils from surface area measurements,” *Highway Research Record No. 393*, pp. 12-18.

Arnepalli, D.N., Shanthakumar, S., Hanumantha Rao, B., and Singh, D.N., 2008, “Comparison of methods for determining specific-surface surface area of fine-grained soils,” *Geotech. Geol. Eng.*, 26: 121-132.

Arthur, E., Tuller, M., Moldrup, P., Resurreccion, A. C., Meding, M. S., Kawamoto, K. and de Jonge, L. W., 2013, “Soil specific surface area and non-singularity of soil-water retention at low saturations,” *Soil Science Society of America Journal*, 77(1), 43-53.

Bain, D., Costanzo, P.M., and Guggenheim, S., (eds.), 2001, *Clays and Clay Minerals*, 49:371-453.

Benson, C.H. and Trast, J.M., 1995, "Hydraulic conductivity of thirteen compacted clays," *Clays and Clay Minerals*, 43: 669-681.

Benson, C.H., 2014, personal communication.

Berend, I., Cases, J., Francois, M., Uriot, J., Michot, L., Maison, A. and Thomas, F. 1995, "Mechanism of adsorption and desorption of water vapor by homoionic montmorillonites," *Clays and Clay Minerals* 43(3): 324-336.

Blum, A., Lopaka, L., and Eberl, D., 2011, "Measurement of clay surface areas by polyvinylpyrrolidone (PVP) sorption: a new method for quantifying illite and smectite abundance," *Clays and Clay Minerals*, 59(2): 212-213.

Bohn, H.L., McNeal, B.L., and O'Connor, G.A., 1985, *Soil Chemistry*, 2^{nd} Edition, John Wiley, New York.

Brunauer, S., Emmett, P.H., and Teller, E., 1938, "Adsorption of gases in multi-molecular layers," *Journal of the American Chemical Society*, 60, 309-319.

Campbell, G.S., Smith, D.M., and Teare, B.L., 2007, "Application of a dew point method to obtain the soil water characteristic," *Experimental Unsaturated Soil Mechanics*, T. Schanz (Ed.), Springer, pp. 71-77.

Carter, D.L., Heilman, M.D., and Gonzalez, C.L., 1965, "Ethylene glycol monoethyl ether for determining surface area of silicate minerals," *Soil Science*, 100(5): 356-360.

Carter, D.L., Mortland, M.M., and Kemper, W.D., 1986, Specific Surface, In *Methods of Soil Analysis, Part 1, Physical and Mineralogical Methods*, Soil Science Society of Americal, Agronomy Mongraph No. 9, Madison, WI.

Cases, J.M., Berend, I., Besson, G., Francois, M., Uriot, J.P., Thomas, F., and Poirier, J.E., 1992, "Mechanism of adsorption and desorption of water vapor by homoionic montmorillonite. I. The sodium exchanged form." *Langmuir*, 8, 2730-2739.

Cerato, A.B. and Lutenegger, A.J., 2002, "Determination of surface area of fine-grained soils by the Ethylene Glycol Monoethyl Ether (EGME) method," *Geotechnical Testing Journal*, 25(3): 314-320.

Chiou, C.T., and Rutherford, D.W., 1997, "Effects of exchanged cation and layer charge on the sorption of water and EGME on montmorillonite clays," *Clays and Clay Minerals*, 45: 867-880.

Chittoori, B., and Puppala, A.J., 2011, "Quantitative estimation of clay mineralogy in fine-grained soils," *Journal of Geotechnical and Geoenvironmental Engineering*, 137(11): 997-1008.

Churchman, G.J. and Burke, C.M., 1991, "Properties of subsoils in relation to various measures of surface area and water content," *Journal of Soil Science*, 42: 463-478.

Collis-George, N., 1955, "The hydration and dehydration of Na-montmorillonite (Belle Fourche)," *Journal of Soil Science* 6(1), 99-110.

deJong, E., 1999, "Comparison of three methods of measuring surface area of soils," *Canadian J. Soil Science*, 79, 345-351.

Dutcher, C.S., Ge, X., Wexler, A.S. and Clegg, S.L., 2011, "Statistical Mechanics of Multilayer Sorption: Extension of the Brunauer-Emmett-Teller (BET) and Guggenheim-Anderson-de Boer (GAB) Adsorption Isotherms," *The Journal of Physical Chemistry*, 115, 16474-16487.

Dyal, R.S. and Hendricks, S.B., 1950, “Total surface of clays in polar liquids as a characteristic index,” *Soil Science*, 69: 421-432.

Farrar, D. and Coleman, J., 1967, “The correlation of surface area with other properties of nineteen British clay soils,” *Journal of Soil Science*, Vol. 18, pp. 118-124.

Gregg, S.J. and Sing, K.S.W, 1982, *Adsorption, Surface Area and Porosity,* 2nd Edition, Academic Press Inc., New York.

Kahr, G., and Madsen, F.T., 1995, “Determination of the cation exchange capacity and the surface area of bentonite, illite and kaolinite by methylene blue adsorption,” *Applied Clay Science,* 9(5): 327-336.

Keren, R., and Shainberg, I., 1979, “Water vapor isotherms and heat of immersion of Na/Ca-montmorillonite systems-II: mixed systems,” *Clays and Clay Minerals*, 27(2): 145-151.

Leong, E.C., Tripathy, S., and Rahardjo, H., 2003, “Total suction measurement of unsaturated soils with a device using the chilled-mirror dew-point technique,” *Géotechnique*, 53(2): 173-182.

Likos, W.J., 2008, “Vapor adsorption index for expansive soil classification,” *Journal of Geotechnical and Geoenvironmental Engineering*, ASCE, 134(7): 1005-1009.

Likos, W.J. and Lu, N., 2002, “Water-vapor sorption behavior of smectite-kaolinite mixtures,” *Clays and Clay Minerals*, 50(5): 553-561.

Likos, W.J. and Lu, N., 2003, “Automated humidity system for measuring total suction characteristics of clay,” *Geotechnical Testing Journal*, 26(2): 178-189.

Likos, W.J. and Lu, N., 2006, “Pore scale analysis of bulk volume change from crystalline swelling in Na^+- and Ca^{2+}-smectite,” *Clays and Clay Minerals*, 54(4): 516 – 529.

Likos, W.J. and Wayllace, A., 2010, "Porosity evolution of free and confined bentonites during interlayer hydration," *Clays and Clay Minerals*, 58(3): 399-414.

Likos, W.J., Bowders, J.J., and Gates, W.P., 2010, "Mineralogy and engineering properties of bentonite," In *Geosynthetic Clay Liners for Waste Containment Facilities*, Bouazza A. and Bowders J.J., Eds., CRC Press, Taylor and Francis, pp. 31-53.

Likos, W.J., Lu, N., and Wenszel, W., 2011, "Performance of a dynamic dew point method for moisture isotherms of clays," *Geotechnical Testing Journal*, 34(4), DOI: 10.1520/GTJ102901.

Likos, W. and Lu, N., 2012, "Characterizing Physical Properties of Clay by Water Vapor Sorption," GeoCongress 2012: pp. 1175-1184, doi: 10.1061/9780784412121.121.

Lutenegger, A.J. and Cerato, A.B., 2001, "Surface area and engineering properties of fine-grained soils," *Proc. 15th Int. Conf. Soil Mech. and Geotechnical Engrg.*, ICSMGE, 1, 603-606.

Mitchell, J.K., 1993, *Fundamentals of Soil Behavior*, John Wiley.

Mooney, R.W, Keenan, A.G., and Wood, L.A., 1952, "Adsorption of water vapor by montmorillonite. II. Effect of exchangeable ions and lattice swelling as measured by X-ray diffraction," *Journal of American Chemical Society*, 74, 1371-1374.

Morgenstern, N.R. and Balasubramanian, B.I., 1980, "Effects of pore fluid on the swelling of clay-shale," *Proc. of the 4th Int. Conference on Expansive Soils*, Vol. 1, pp. 190-205.

Muhunthan, B., 1991, "Liquid limit and surface area of clays," *Géotechnique*, 41(1): 135-138.

Newman, A.C.D., 1983, "The specific surface area of soils determined by water sorption," *J. Soil Science*, 34:23-32.

Paykov, O. and Hawley, H., 2013, “A protein retention method for specific surface area determination in swelling clays,” *Geotechnical Testing Journal*, 36(4): DOI: 10.1520/GTJ20120197

Quirk, J.P. 1955, “Significance of surface areas calculated from water vapour sorption isotherms by use of the B.E.T. equation,” *Soil Science,* 80: 423-30.

Quirk, J.P. and Murray, R.S., 1999, “Appraisal of the ethylene glycol monoethyl ether method for measuring hydratable surface area of clays and soils,” *Soil Sci. Soc. Amer. J.*, 63: 839-849.

Ristori, G.G., Sparvoli, E., Landi, L., and Martelloni, C., 1989, “Measurement of specific surface area of soils by p-nitrophenol adsorption,” *Applied Clay Science*, 4: 521-532.

Ross, G.J., 1978, “Relationships of specific surface area and clay content to shrink-swell potential of soils having different clay mineralogic compositions,” *Canadian Journal of Soil Science*, Vol. 58, pp. 159-166.

Salles, F., Douillard, J-M., Denoyel, R., Bildstein, O., Jullien, M., Beurroies, I., and van Damme, H., 2009, “Hydration sequence of swelling clays: evolutions of specific surface area and hydration energy,” *Journal of Colloid and Interface Science*, 333:510-522.

Santamarina, J.C., Klein, K.A., Wang, Y.H., and Prencke, E., 2002, “Specific surface: determination and relevance,” *Canadian Geotechnical Journal*, 39: 233-241.

Środoń, J., and McCarty, D.K., 2008, “Surface area and layer charge of smectite from CEC and EGME/H_2O-retention measurements,” *Clays and Clay Minerals*, 56(2): 155–174.

Tuller, M. and Or, D., 2005, “Water films and scaling of soil characteristic curves at low water contents,” *Water Resources Research*, 41, W009403, doi:10.1029/2005WR004142.

van Olphen, K., 1965, "Thermodynamics of interlayer adsorption of water in clays," *Journal of Colloid Science* 20: 822-837.

Yukselen, Y. and Kaya, A., 2006, "Comparison of methods for determining specific surface area of soils," *Journal of Geotechnical and Geoenvironmental Engineering*, 132(7): 931-936

1.7 TABLES

Table 1.

		Atterberg limits			Surface Properties		
soil ID	**USCS**	**LL**	**PL**	**PI**	**CEC (meq/ 100 g)**	**SSA-water (m^2/g)**	**SSA-EGME (m^2/g)**
Denver**	CH	49	23	26	23.0	107	151
New Orleans**	CL sandy	30	12	18	8.0	27	51
Sacramento	n.d.	39	22	17	27.8	138	191
Atlanta, Georgia	MH	50	36	14	13.2	50	72
KF1	CL	42	23	19	35.6	157	258
KF2	n.d.	41	15	26	23.4	102	151
Alb1	CL	28	17	11	8.5	38	51
Alb2	CL	36	14	22	8.1	29	51
Albany red	SC	30	16	14	7.6*	32	43
Houston brown	CH	41*	16*	25*	32.2*	90	145
Mon 2	CL	31	17	14	15.2	69	84
Kamm clay	CL	49	21	28	26.3*	84	145
WCS Andrews	CH	50	18	32	17.6*	71	118

1.8 FIGURES

Figure 1.

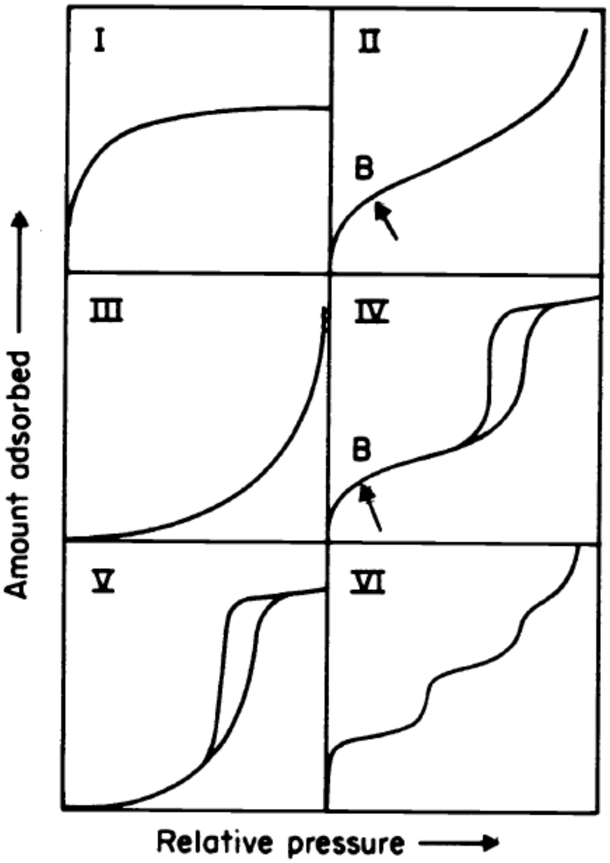

Figure 2.

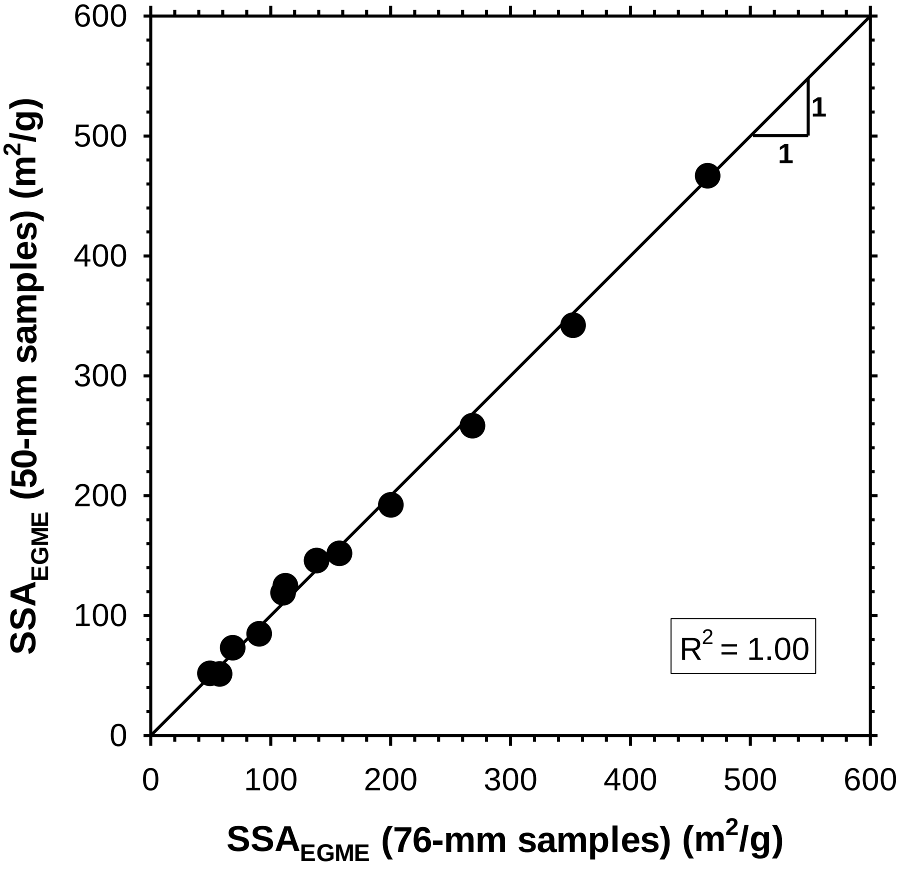
600
500
400
300
200
100
0
0
100
200
300
400
500
600
1
1
R^2 = 1.00
SSA$_{EGME}$ (50-mm samples) (m^2/g)
SSA$_{EGME}$ (76-mm samples) (m^2/g)

Figure 3.

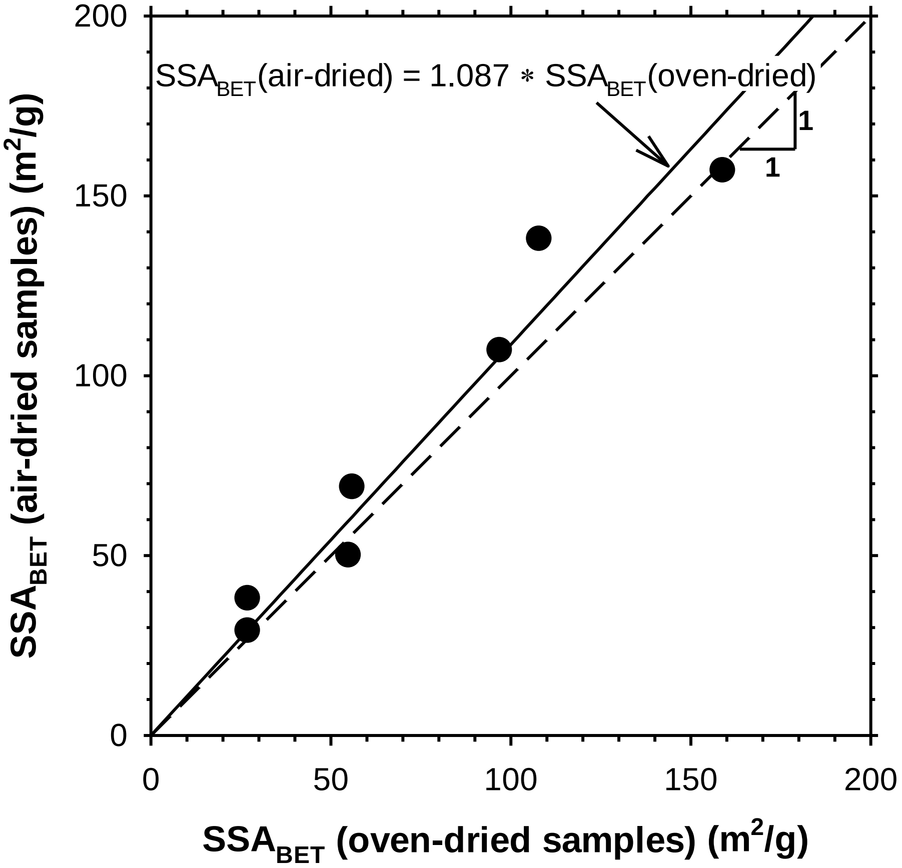

SSA$_{BET}$(air-dried) = 1.087 ∗ SSA$_{BET}$(oven-dried)
1
1
0
50
100
150
200
0
50
100
150
200
SSA$_{BET}$ (oven-dried samples) (m^2/g)
SSA$_{BET}$ (air-dried samples) (m^2/g)

Figure 4.

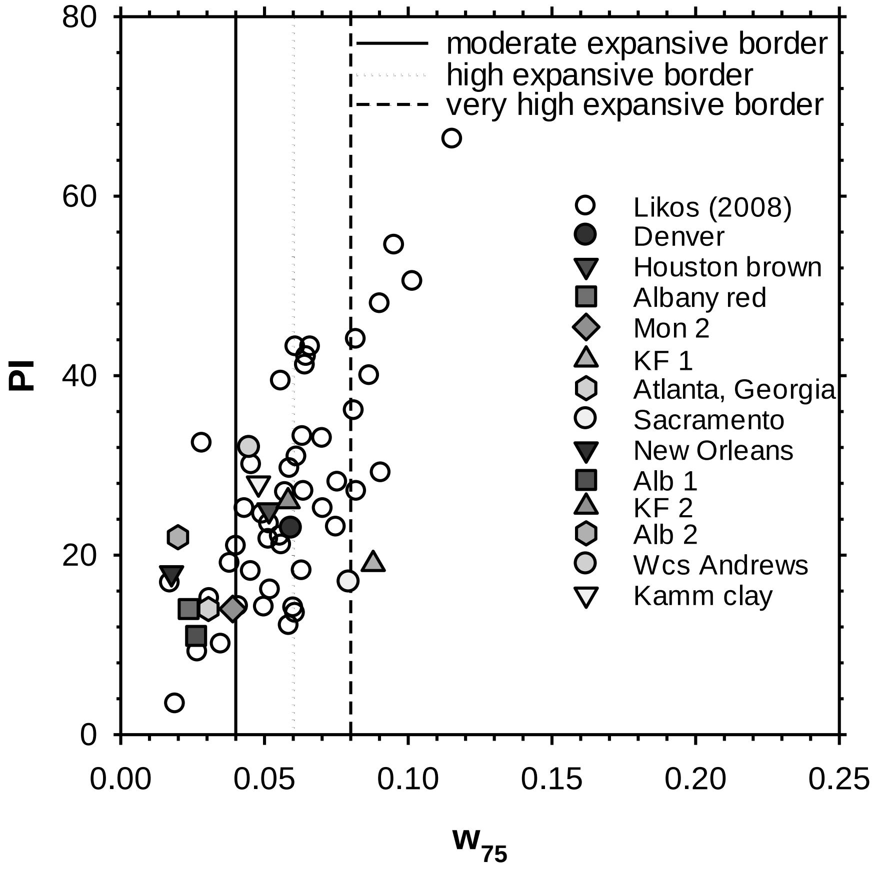

80
60
40
20
0
PI
0.00
0.05
0.10
0.15
0.20
0.25
w_{75}
moderate expansive border
high expansive border
very high expansive border
Likos (2008)
Denver
Houston brown
Albany red
Mon 2
KF 1
Atlanta, Georgia
Sacramento
New Orleans
Alb 1
KF 2
Alb 2
Wcs Andrews
Kamm clay

Figure 5.

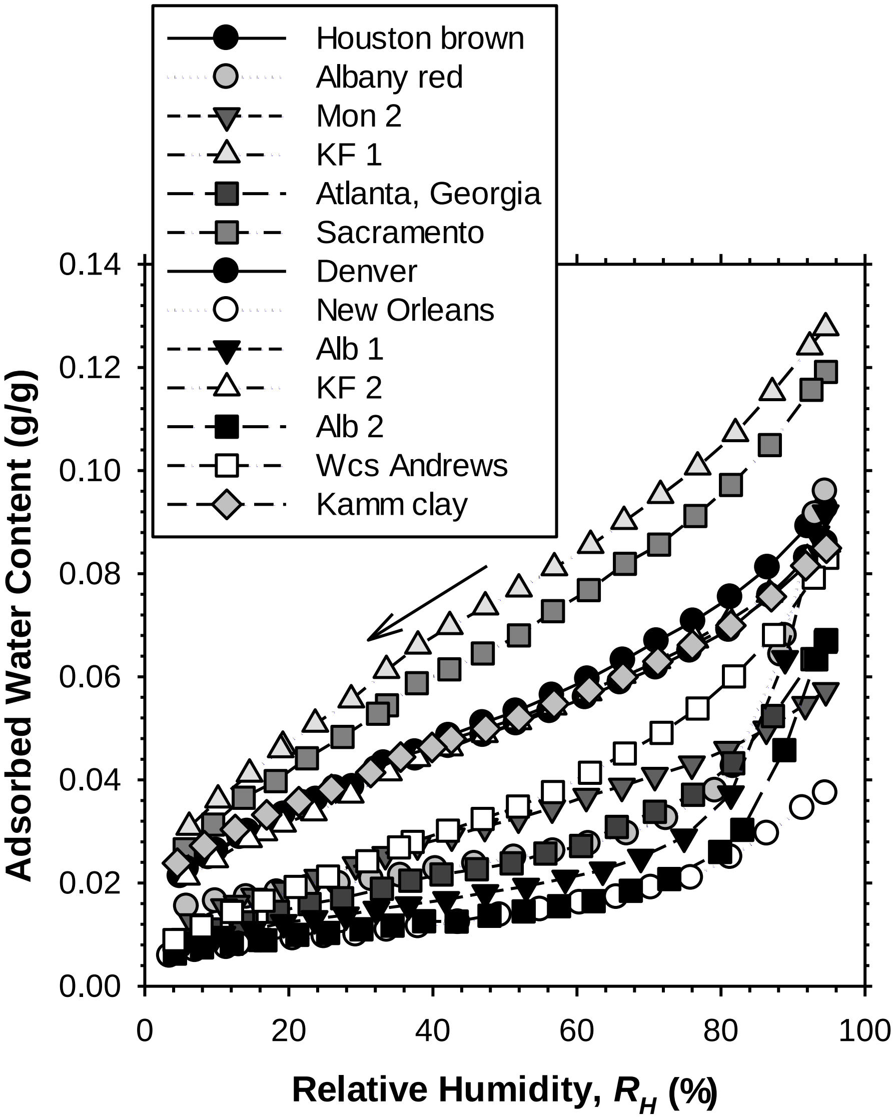
Houston brown
Albany red
Mon 2
KF 1
Atlanta, Georgia
Sacramento
Denver
New Orleans
Alb 1
KF 2
Alb 2
Wcs Andrews
Kamm clay
0.00
0.02
0.04
0.06
0.08
0.10
0.12
0.14
0
20
40
60
80
100
Adsorbed Water Content (g/g)
Relative Humidity, R_H (%)

Figure 6.

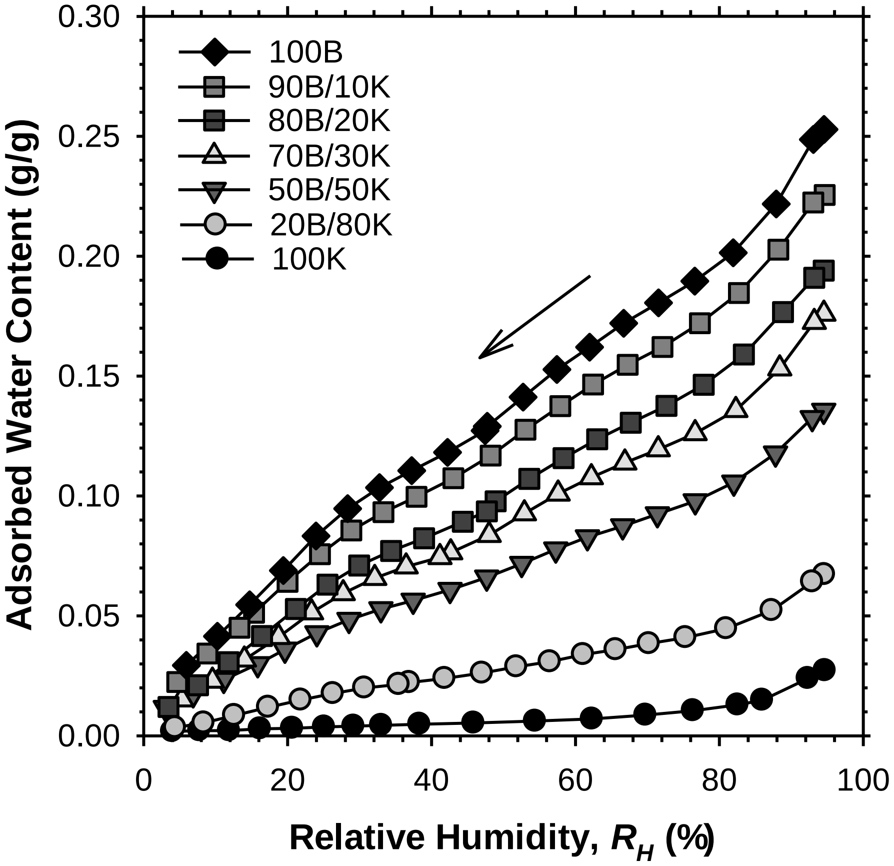
0.30
0.25
0.20
0.15
0.10
0.05
0.00
0
20
40
60
80
100
Adsorbed Water Content (g/g)
Relative Humidity, R_H (%)
100B
90B/10K
80B/20K
70B/30K
50B/50K
20B/80K
100K

Figure 7.

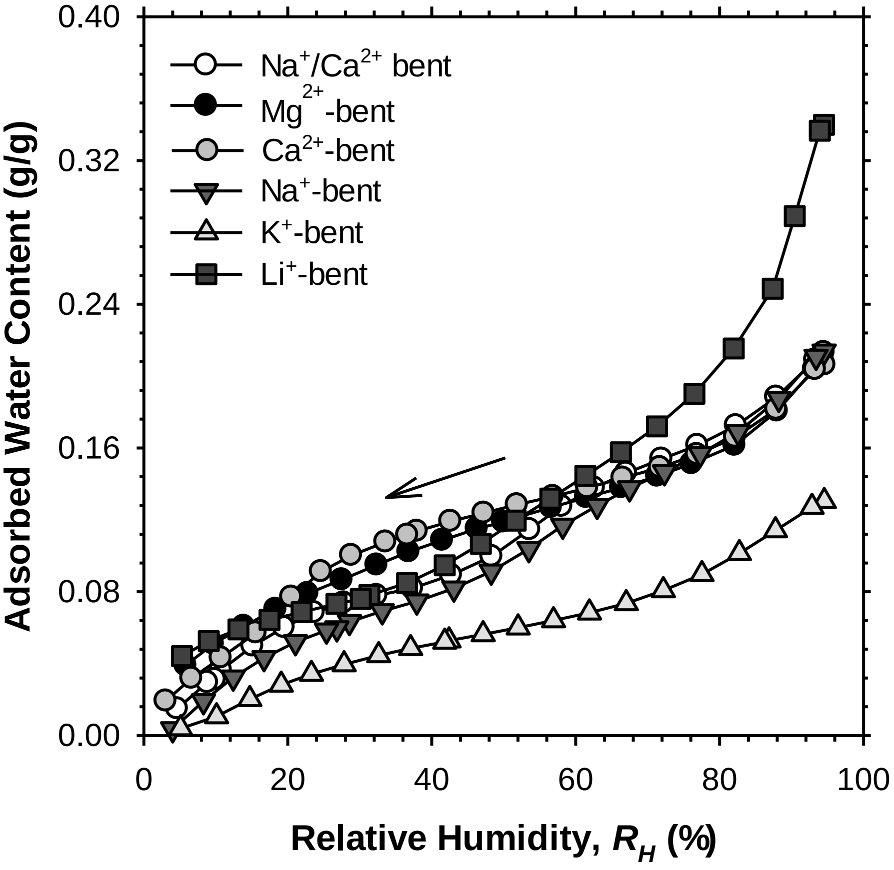
0.40
0.32
0.24
0.16
0.08
0.00
0
20
40
60
80
100
Adsorbed Water Content (g/g)
Relative Humidity, R_H (%)
Na$^+$/Ca^{2+} bent
Mg^{2+}-bent
Ca^{2+}-bent
Na$^+$-bent
K$^+$-bent
Li$^+$-bent

Figure 8.

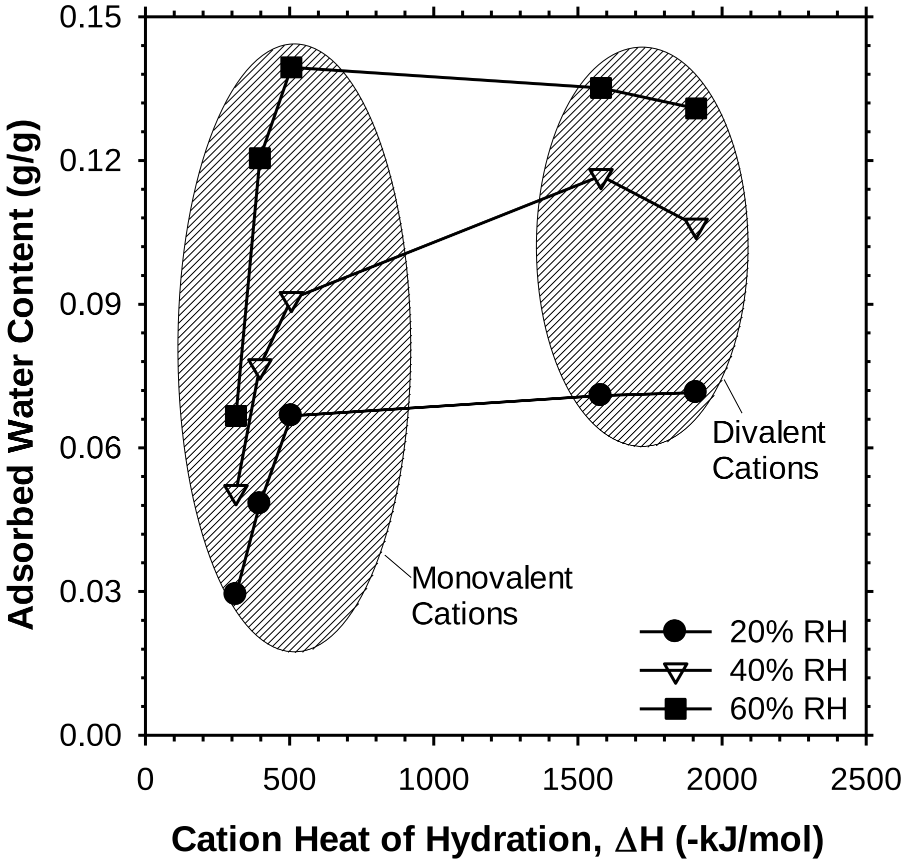
0.15
0.12
0.09
0.06
0.03
0.00
Adsorbed Water Content (g/g)
0
500
1000
1500
2000
2500
Cation Heat of Hydration, ΔH (-kJ/mol)
Monovalent Cations
Divalent Cations
20% RH
40% RH
60% RH

Figure 9.

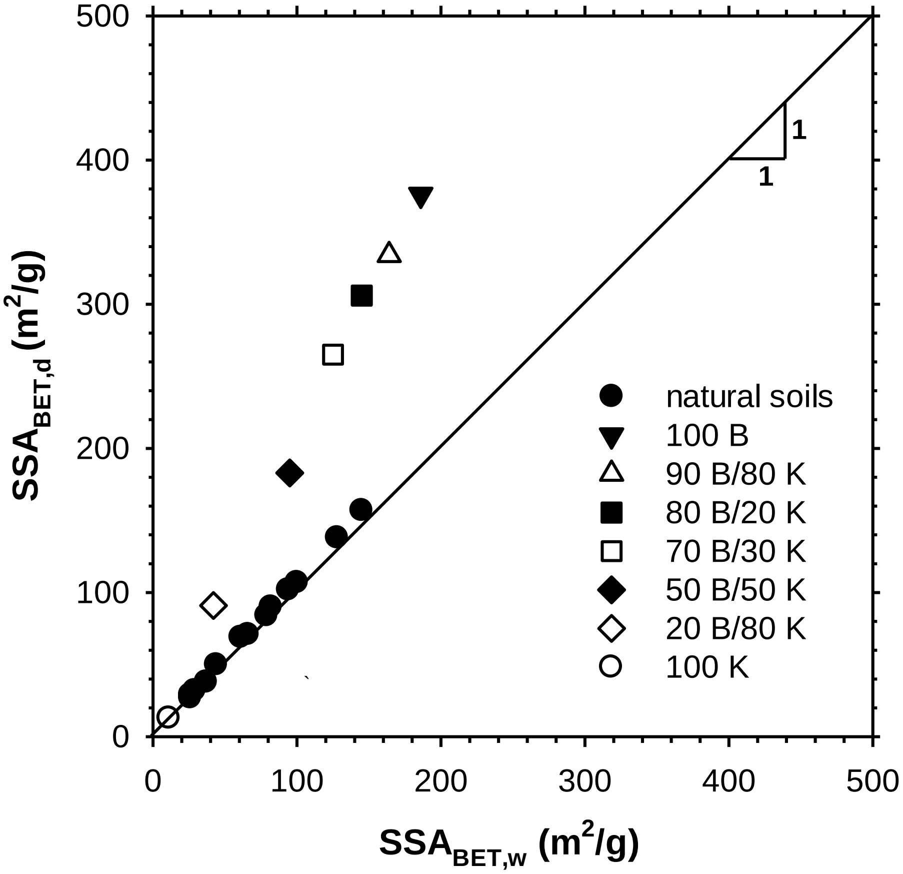
SSA$_{BET,d}$ (m^2/g)
SSA$_{BET,w}$ (m^2/g)
0
100
200
300
400
500
0
100
200
300
400
500
1
1
● natural soils
▼ 100 B
△ 90 B/80 K
■ 80 B/20 K
□ 70 B/30 K
◆ 50 B/50 K
◇ 20 B/80 K
○ 100 K

.

Figure 10.

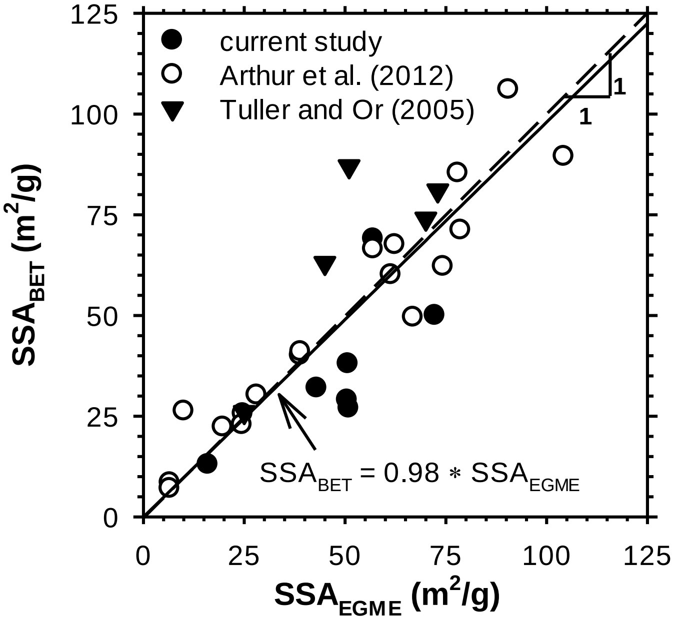

125
100
75
50
25
0
current study
Arthur et al. (2012)
Tuller and Or (2005)
1
1
SSA$_{BET}$ = 0.98 * SSA$_{EGME}$
0
25
50
75
100
125
SSA$_{BET}$ (m^2/g)
SSA$_{EGME}$ (m^2/g)

(a)

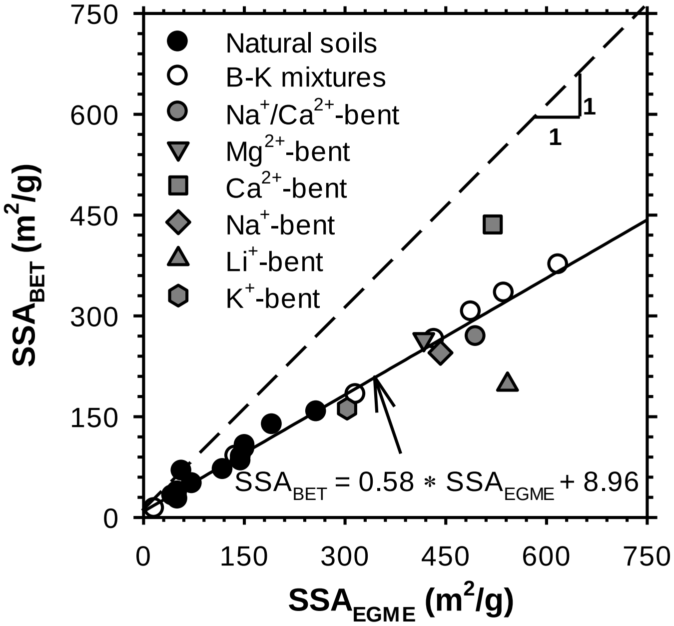

750
600
450
300
150
0
Natural soils
B-K mixtures
Na$^+$/Ca^{2+}-bent
Mg^{2+}-bent
Ca^{2+}-bent
Na$^+$-bent
Li$^+$-bent
K$^+$-bent
1
1
SSA$_{BET}$ = 0.58 * SSA$_{EGME}$ + 8.96
0
150
300
450
600
750
SSA$_{BET}$ (m^2/g)
SSA$_{EGME}$ (m^2/g)

(b)

Figure 11.

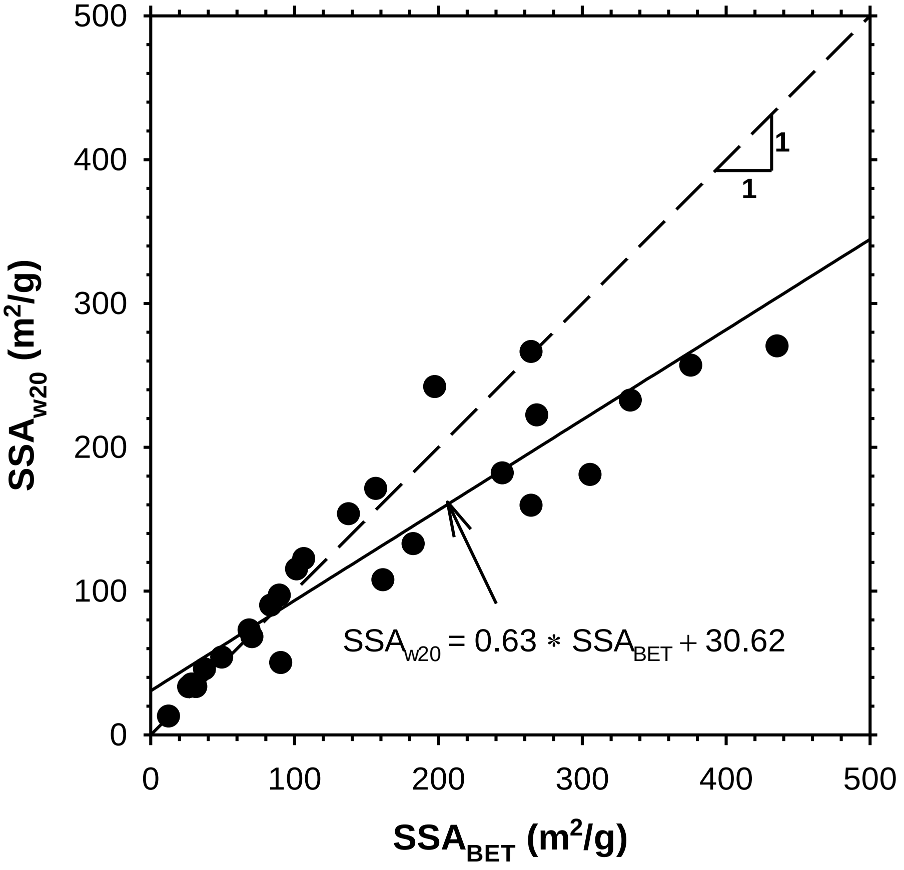

0
100
200
300
400
500
SSA_BET (m²/g)
SSA_w20 (m²/g)
1
1
SSA_w20 = 0.63 * SSA_BET + 30.62

Figure 12.

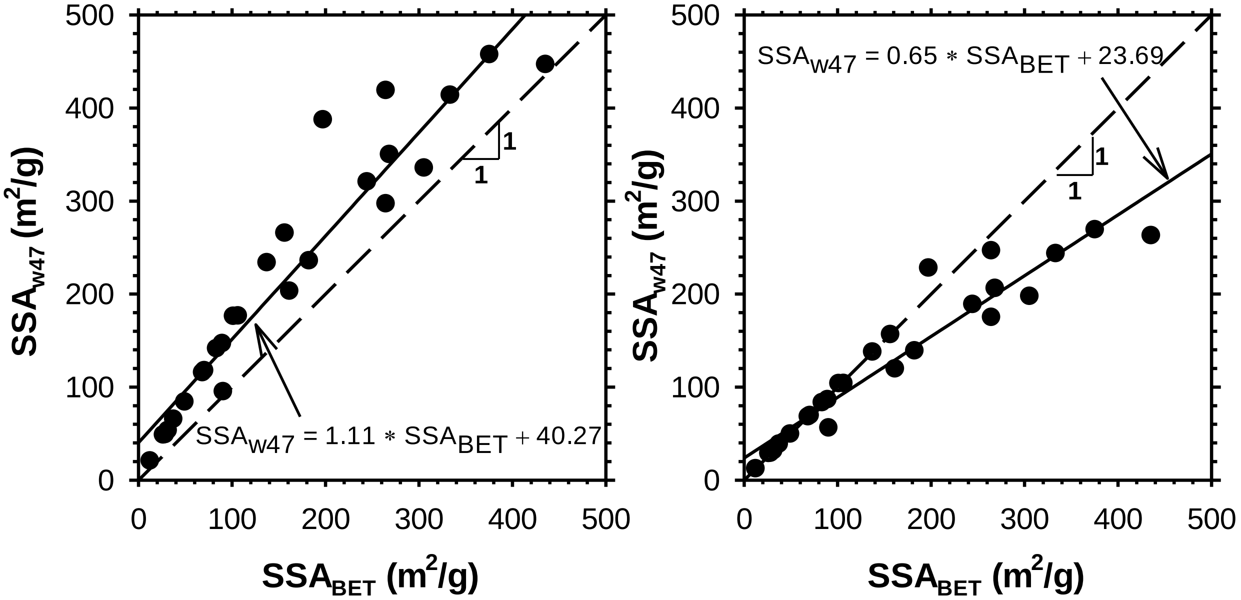

500
400
300
200
100
0
0
100
200
300
400
500
SSA_{w47} (m^2/g)
SSA_{BET} (m^2/g)
1
1
$SSA_{w47} = 1.11 * SSA_{BET} + 40.27$
$SSA_{w47} = 0.65 * SSA_{BET} + 23.69$

(a) (b)

CHAPTER 2

EVALUATION OF MODELS FOR WATER VAPOR SORPTION ISOTHERMS OF CLAYS

2.1 INTRODUCTION

Measuring and modeling the water vapor sorption behavior of soil at high suction has emerged as potentially important for improving the general understanding of saturated and unsaturated soil behavior. Reliable characterization of water vapor sorption is particularly important for clayey soils, since surface forces active in the sorption process can dominate bulk engineering behavior. Swelling and shrinkage, collapse, compressibility, and hydraulic conductivity are all influenced by soil-water interactions occurring at the mineral surfaces (*e.g.*, Petersen 1996, Cerato and Lutenegger 2004). Measurement and analysis of water sorption isotherms could provide a direct or indirect means to clarify mechanisms for interlayer swelling behavior, to classify expansive soils, and to estimate fundamental soil properties including specific surface area (SSA), cation exchange capacity (CEC), and clay mineralogy (*e.g.*, Orchiston 1953, Likos and Lu 2012). Recent developments in geomechanics have indicated that the “residual” or “bound” water associated with clay mineral surfaces cannot be ignored and should be considered in effective stress formulations for predicting unsaturated soil behavior (*e.g.,* Bishop 1959, Fredlund and Morgenstern 1977, Gallipoli *et al*. 2003, Lu and Likos 2006).

While a variety of experimental methods for measuring water vapor sorption by clays and clayey soils have been developed, corresponding theoretical models have not been fully evaluated. Much of the previous modeling effort has been conducted by researchers in different areas of science (*e.g.,* chemical engineering, colloid science, food science) working to model the sorption of gases on various solids. The first sorption isotherm model was proposed by Langmuir (1918), which has been mostly used in chemical engineering practice. Freundlich (1926), Brunauer, Emmet, and Teller (1938), Fowler and Guggenheim (1939), Temkin (1941), Hill (1946), Anderson (1946), de Boer (1953), and Guggenheim (1966), Halsey (1948), Kiselev (1958), Dubinin and Astakhov (1971), and Condon (2006) are some of the researchers who have proposed models for sorption isotherms based on theoretical calculations or empirical testing. Such models have been used to represent mainly adsorption of gases on solids such as charcoals, silica gel, catalysts, chromium oxides, microporous carbons, and various substances in foods (*e.g.*, Brunauer *et al*. 1938, Pagano and Mascheroni 2004). Very few generalized isotherm models have been evaluated specifically for modeling water vapor sorption by clays.

This study investigates the performance of six existing isotherm models for application to the water vapor sorption behavior of clays, including those of Freundlich (F), Brunauer-Emmet-Teller (BET), Frenkel-Halsey-Hill (FHH), Guggenheim-Anderson-de Boer (GAB), Dubinin and Astakhov (D-A), and the Double Log Polynomial (DLP) model. These models are evaluated using water vapor sorption isotherms obtained experimentally for a suite of bentonite-kaolinite mixtures selected to represent a wide range of sorption behavior. The models are separately fit to drying and wetting paths of the measured isotherms. Performance of the models is evaluated separately for wetting and drying paths and as a function of bentonite content. SSA values obtained using the models along measured desorption paths, and compared with the values obtained by the conventional EGME (Ethylene Glycol Monoethyl Ether) method. Implications are evaluated by estimating the water vapor sorption isotherm of natural clayey soils by using SSA_{EGME} values and the recommended range of the DLP model parameters.

2.2 BACKGROUND

2.2.1 Water Sorption Isotherms

A sorption isotherm of a soil is a plot of the amount of gas that the soil sorbs on the surface with changing vapor pressure of that gas at a constant temperature. For water vapor sorption isotherms, the gas is water vapor and the changing pressure is represented by the changing relative humidity (R_H) of the environment. The International Union of Pure and Applied Chemistry (IUPAC) (1985) classified physisorption isotherms into six types after the studies of Brunauer at al. (1938), Brunauer *et al*. (1940), and Brunauer (1945). The isotherms are shown in Figure 1. In the IUAPC classification, Sing *et al.* (1985) also explains the solid properties that the different isotherm types represent.

Type I isotherms are formed by solids with small external surfaces. The sorption is limited and determined by the accessible micropore volume as these solids are generally microporous and have relatively small external surfaces. Type II isotherms are obtained if the solid is nonporous or macroporous. Monolayer-multilayer sorption can occur unrestrictedly. Point B in Figure 1 represents the stage where monolayer adsorption is completed and multilayer adsorption starts. The interaction between the solid surface and the adsorbate is strong (Montes-H *et al.* 2003). Type III isotherms are formed when there is no strong attraction between the solid surface and the adsorbate. The Type I, Type II and Type III isotherms are all reversible, which means the drying curve follows the same path as the wetting curve. Type IV isotherms show hysteresis, which means the paths of the drying and the wetting curves are different. This is mainly because of capillary condensation. The solid holds more water while drying than while wetting. Type IV isotherms are obtained if the solid is mesoporous. The initial part of the Type IV isotherm is very similar to the Type II isotherm, which represents monolayer-multilayer adsorption. Type V isotherms are not very common. They also show hysteresis, and the initial part of the isotherm can be attributed to the Type III isotherm, which represents weak interaction between the solid surface and the adsorbate. Type VI isotherms show stepwise multilayer adsorption on a uniform, non-porous solid surface. Each step represents a monolayer adsorption. After one layer of adsorbate is adsorbed, the second layer starts to form.

2.2.2 Freundlich (F) Model

The Freundlich equation (Equation 1) is an empirical equation that does not have a theoretical basis. Nonetheless, good fits to sorption isotherms may be obtained for various sorbents, including soil (Hamaker and Thompson 1972). The Freundlich equation, which should be used only if the sorption takes place on heterogeneous surfaces, implies that as surface coverage increases, heat of adsorption decreases logarithmically due to surface heterogeneities. In heterogeneous surfaces, there exist different adsorption sites having different adsorption energies. Therefore, the decrease in heat of adsorption is logarithmic. Specifically, the Freundlich equation relates the surface concentration of the adsorbent to the equilibrium solution concentration. For adsorption of water vapor on soil, the surface concentration may be quantified by gravimetric water content (w) as a function of relative humidity (R_H), in the form of

$$w = K R_H{}^{\frac{1}{m}} \tag{1}$$

where K is a constant related to the relative sorption capacity of the adsorbent, and m is a constant related to the intensity of sorption. As implied in Equation 1, adsorbed water content does not reach a limiting value as R_H increases. However, in the actual case, after a certain R_H value, capillary forces start to dominate the water uptake mechanism. At this point adsorption at the mineral surface no longer plays a significant role, and an equation describing surface adsorption is no longer applicable. This fact shows the empirical nature of the equation. The term *1/m* was originally proposed to be around 1 (Freundlich 1932, Hamaker and Thompson 1972, Calvet 1989), which implies that the Freundlich isotherm has a linear shape, although the equation implies a Type I isotherm shape according to IUAPC classification (Sing *et al*. 1985).

2.2.3 Brunauer, Emmett, and Teller (BET) Model

The BET model has its basis in statistical thermodynamics. Although the model is dependent on many assumptions, it is still a widely accepted theory for physical adsorption (Dutcher *et al*. 2011). Two basic assumptions to derive the equation are: (i) the surface of the adsorbent is homogeneous, and (ii) the molecules are adsorbed to neighboring sites independently without lateral interaction, which implies there is no surface tension (McMillan and Teller 1951). This assumption was needed to model multilayer adsorption, because when there is surface tension, and when heat of adsorption of the sorbent layers beyond a monolayer is not greater than the heat of liquefaction, which is the heat released when changing into the liquid phase from the gas phase, multilayer adsorption does not occur (Halsey 1952).

To derive the BET isotherm equation, the rate of condensation of molecules from the gas phase is equated to the rate of evaporation from the second layer of adsorbed molecules. The rate of condensation from the second layer is equated to the rate of evaporation from the third layer, and so on. Below the saturation water vapor pressure, surface coverage will increase with increasing partial pressures. This means that the thickness of the adsorbed layer will not be a constant through the sorption process, but will change depending on values that are specific for each layer. After formation of the first monolayer, heat of adsorption of the molecular layers is assumed to be equal to the heat of liquefaction. Also, the evaporation-condensation conditions are assumed to be identical to each other, except for the ones in the first layer. The last assumption is that, at saturation vapor pressure, the number of adsorbed layers is infinite. The BET equation (Equation 2) is then derived by summing the fractional coverage at each layer. Thus, the theory is also referred as the kinetic theory of multimolecular adsorption.

$$w = \frac{X_m C P}{(P_0 - P)[1 + (C - 1) R_H]} \tag{2a}$$

where w is the amount of adsorbate adsorbed per gram of adsorbent (g/g) at pressure P, X_m is the quantity adsorbed when the adsorbent is covered with a molecular monolayer (g/g), P_0 is the saturation pressure of the gas, and C is a constant related to the heat of adsorption.

$$C = \frac{exp(E_1 - E_2)}{RT} \tag{2b}$$

where E_1 is the heat of adsorption of the first molecular layer of the adsorbate, E_2 is the heat of condensation of the adsorbate, R is the molar gas constant (8.314 J mol^{-1} K^{-1}), and T is the temperature (K).

Due to the assumptions made to derive the equation, the BET model is not expected to be applicable for the whole R_H range. As noted by Ponec *et al*. (1974), the BET equation tends to give lower adsorption values than the experimental results when the R_H is low. This is because a single heat of adsorption is assumed for the whole surface to calculate the monomolecular coverage. In the actual case, however, at low R_H values, the surface usually also has some more active sites having a higher heat of adsorption than the average value. After the surface coverage reaches about 0.5 g/g, the surface becomes more homogeneous. In contrast, at higher R_H values, the case is the opposite. That is, the value calculated from the BET equation is usually greater than the experimental value (Ponec *et al.* 1974). The practical implication is that the BET equation is generally applicable for R_H between about 5% and 35% (Mooney *et al.* 1952, Newman 1987, Yamanaka *et al.* 1990).

2.2.4 Frenkel-Halsey-Hill (FHH) Model

The FHH model, which was developed for multilayer sorption, is regarded as semi-empirical. Halsey (1948) states that to assume the adsorption will be stepwise is not realistic when the adsorbent has a heterogeneous surface. One layer of adsorbate, for example, might be sorbed on low-energy sites, whereas at the same time more than one monolayer might be adsorbed on localized sites of the adsorbent surface. Therefore, to derive the sorption equation of the FHH model, energy effects were considered instead of stepwise adsorption. Surface forces were used since adsorbed layers beyond the monolayer are still affected by the surface charge up to three adsorbed layers (Gregg and Sing 1982). The adsorbed layers are of liquid structure, but have a higher heat of adsorption than the normal liquid because of the Van der Waals forces formed with the surface (de Boer *et al.* 1966). Frenkel (1955), Halsey (1948), and Hill (1949) derived Equation 3 independently by assuming that the adsorbed layers have a planar surface that is parallel to the adsorbent. The derivation comes purely from potential energy effects on adsorption. Chemical potential of the adsorbent is equated to the difference of the potential energy of interaction of a liquid molecule at the adsorbed layer with the adsorbent, and the potential energy of the interaction of a molecule at the adsorbed layer with the semi-infinite liquid in the adsorbent (Hill 1952). The equation of the FHH model is

$$R_H = \frac{1}{\exp\left(\frac{K}{\theta^s}\right)} \tag{3}$$

where θ is the fractional coverage ($\theta = w/X_m$); K is in principle a parameter that is function of the energy of adsorption of the first layer, but in practice is regarded as empirical (Gregg and

Sing 1982); and *s* is a parameter that, for water vapor sorption, depends on the surface structure of the adsorbent. *K* is indicative of the difference in the attraction between the adsorbent and adsorbate molecules, and the attraction between the adsorbent molecules (Hill 1952). As *K* gets larger, the former becomes greater than the latter, and the amount of adsorbed water increases.

Many researchers have proposed different physical meanings for the parameter *s*, all of which are actually related to each other. Halsey (1948) states that *s* is indicative of the strength of interaction between the adsorbate and the adsorbent. When *s* is large, the attraction forces are only effective closer to the surface and the isotherm has Type I shape; whereas, when *s* is small, the van der Waals forces are dominant, which are effective to greater distance, and the isotherm has Type III shape. According to Carrot *et al.* (1982), the effects of micropore and mesopore filling are represented by *s*. A low value of *s* is indicative of capillary condensation in mesopores, whereas an increase in *s* represents micropore filling. Rudzinski and Everett (1992) suggest that when the heterogeneity of the surface increases, the effect of surface structure on the multilayer structure will be larger; thus, there will be a decrease in the value of *s*. For the opposite case, increase in homogeneity, the value of *s* will increase.

2.2.5 Guggenheim-Anderson-de Boer (GAB) Model

The GAB Model is a modified form of the BET Model that is applicable to a wider range of R_H values, generally up to about 80% R_H (Anderson 1946). The GAB equation is also based on theory of statistical thermodynamics. The main difference with BET is that, whereas in the BET model the heat of adsorption of second and higher monolayers is assumed to be constant and equal to the heat of liquefaction, in the GAB Model it is again constant, but less than the heat of liquefaction (Anderson 1946). This lower energy indicates an extended or incomplete hydration shell around the adsorbent. This shows that even the adsorbate that does not bind to the surface is affected by the absorbent (Dutcher *et al*. 2011). In other words, the entropy of adsorption in the second and higher layers is more negative than the entropy of liquefaction, and thus the adsorbed molecules in the layers beyond the monolayer are more ordered than the molecules in the liquid phase (Anderson 1946). This brings an additional parameter to the BET equation, such that the GAB equation can be written as

$$w = \frac{X_m k_b c_1 R_H}{(1-k_b R_H)(1-k_b R_H + c_1 k_b R_H)} \tag{4}$$

where c_1 is a constant that measures the binding strength of water to the primary binding surfaces (Sabard *et al*. 2012), and k_b is the additional parameter that accounts for the difference between the standard chemical potential of the adsorbed molecules in the second or higher layers and the potential of the adsorbate in the liquid phase. The value of k_b should be less than 1, indicating that the heats of adsorption of the second and higher layers are less than the heat of liquefaction. Although the GAB Model is applicable for R_H up to 80%, de Boer *et al.* (1966) states that the equation does not have any physical meaning because k_b less than 1 does not represent multimolecular adsorption. Although the GAB model is used extensively in food science (*e.g.*, Pagano and Masheroni 2004, Stoeckli and Jakubov 1994), no application of this model in geotechnical engineering could be found.

2.2.6 Double Log Polynomial (DLP) Model

The DLP Model was derived by applying the Chi theory proposed for homogeneous surfaces (Condon 2006) to heterogeneous surfaces. The Chi theory has its basis in quantum mechanics. Like the previous models discussed, the Chi model also has its own assumptions. The surface of the adsorbent is described as a large potential box with localized areas having high bonding energies existing on the surface. Adsorbed molecules can move freely along the surface and over or under each other. For the molecules that will be adsorbed on the localized sites, the bonding energy will be equal to the liquefaction energy. The remaining bonding energies between the adsorbed molecules are higher than the liquefaction energy. The final assumption is that the adsorbed molecules are indistinguishable from each other (Fuller and Condon 1988).

Derivation of the DLP model could be done for homogeneous surfaces first by writing the energy equation between the molecules assuming that the energy of the adsorbed molecules is higher than the energy of the potential wells, but low enough to keep the adsorbed molecules close to the surface. To take into account the different paths to arrive at the isotherm, the grand canonical ensemble, which is the probability distribution function for the state of the system of particles that is being maintained in thermodynamic equilibrium (Gibbs 1902), is written and the final form of the isotherm equation (Equation 5) is obtained.

$$X = \frac{SSA \cdot X_m}{A_m \cdot f} (\chi - \chi_c) U(\chi - \chi_c) \tag{5}$$

where X is the amount adsorbed, A_m is the area covered by one mol of adsorbate, f is a constant depending on the relative sizes of the adsorbate and the adsorbent ranging between 1.82 and 1.92, χ is the chi-function $\chi = ln[-ln(R_H)]$, U is the Heaviside step function, and $\chi_c = ln(-E_a/kT)$ where E_a is the energy of the adsorbent surface during adsorption, k is the Boltzmann constant ($1.381 \cdot 10^{-23}$ m^2 kg s^{-2} K^{-1}), and T is the temperature of adsorption (K). The Heaviside step function was used in the equation to avoid having negative X values. U is equal to 0 if $\chi < \chi_c$, and equal to 1 if $\chi > \chi_c$.

For heterogeneous surfaces, the total amount of adsorbate adsorbed is the sum of the amounts adsorbed on each surface plane having different energies. Therefore, by taking the integral of Equation (5) and representing all the constants with single parameters, the isotherm equation of the DLP model that is applicable to heterogeneous surfaces could be obtained (Equation 6).

$$w = c_4\chi^3 + c_3\chi^2 + c_2\chi + c_1 \tag{6}$$

where c_1, c_2, c_3, and c_4 are all constants.

2.2.7 Dubinin-Astakhov (D-A) Model

The D-A model (Dubinin and Astakhov 1971) is based on the concept of micropore filling rather than layer-by-layer adsorption. Derivation of the D-A isotherm equation has its basis in thermodynamic equilibrium determined by dispersion forces. To derive the equation independent of temperature, the volume of the adsorption space is assumed to be constant with changing temperature. By equating the differential molar work of adsorption to the Gibbs loss of energy, Equation (7) was proposed.

$$\theta = exp\left[-\left(\frac{RTln\left(\frac{1}{R_H}\right)}{E}\right)^n\right] \tag{7}$$

where *n* and *E* are temperature-invariant parameters that are specific to the system, *E* being the characteristic adsorption energy and *n* being an empirical constant. *E* can be regarded as an indicator of the average micropore width, where larger *E* shows a smaller micropore width (Stoeckli *et al*. 1994). When *E* gets higher, the isotherm starts to take on the shape of a Type I isotherm. For lower *E* values, the isotherm starts to take on the shape of a Type III isotherm. For the value of the empirical constant *n*, Dubinin and Astakhov (1971) worked with microporous carbon adsorbents and activated charcoals, which have an effective radii of micropores between the range of 0.5 nm to 1.3 nm. *n* was proposed to be equal to 2 for most adsorbents and to be equal to 3 for adsorbents having a micropore radius of about 0.5 nm or smaller. The constant *n* was found to be close to a whole number and can be rounded to the closest integer.

2.3 MATERIALS AND METHODS

2.3.1 Bentonite-Kaolinite Mixtures

Bentonite-kaolinite mixtures were prepared in seven mass-controlled ratios denoted by their respective bentonite (B) and kaolinite (K) content (100K, 20B/80K, 50B/50K, 70B/30K, 80B/20K, 90B/10K, 100B). End member bentonite and kaolinite for these mixtures was obtained from the Source Clay Repository of the Clay Minerals Society (Bain *et al.* 2001). This included SWy-2, which is a Na^+-rich montmorillonite from Crook County, Wyoming, and KGa-1b, which is a low-defect kaolinite from Washington County, Georgia.

2.3.2 Water Vapor Sorption Isotherms

Water vapor sorption isotherms were obtained using a commercially available vapor sorption analyzer (VSA) operating in dynamic dewpoint isotherm (DDI) mode (Decagon Devices, Pullman WA). Unlike similar systems for measuring water vapor sorption isotherms from the equilibrium mass of adsorbed water, the DDI approach involves concurrent measurement of sample water content and R_H in a dynamically changing vapor pressure environment. As described by Likos *et al*. (2011), samples are placed into an environmental chamber and continuously wetted or dried by circulating either a vapor saturated or desiccated air stream through the chamber. Changing R_H is periodically measured using a chilled-mirror dew point sensor (Leong *et al*. 2003, Campbell *et al*. 2007) while concurrently tracking changes in sample mass.

Hysteretic sorption isotherms were obtained along an initial drying path from ambient conditions down to 3% R_H to dry the sample from its initial air-dry water content. This was immediately followed by a wetting cycle up to 95% R_H and then a second drying cycle back down to 3% R_H. All isotherms were obtained at a set point temperature of 25 ± 0.2 ˚C automatically maintained by the VSA system. Initial air-dry mass of the samples was 1.94 ± 0.11 g. Complete adsorption-desorption loops typically contained as many as 170 to 225 discrete measurements and were obtained in 24 to 72 hours.

2.3.3 Fitting Parameters

Model equations were fit to the drying and wetting paths of the isotherm data by using least-squares regression. An R^2 value (Equation 8) was calculated for each path and maximized by using the Solver function of MS Excel.

$$R^2 = 1 - \frac{\sum_{i=1}(w_i - \dot{w}_i)^2}{\sum_{i=1}(\bar{w} - w_i)^2} \tag{8}$$

where w_i is the measured water content at each increment, $\dot{w}_i$ is the water content calculated from the isotherm equation, and $\bar{w}$ is the mean of the measured w values. Table 1 summarizes constants and fitting parameters that were optimized to obtain the highest R^2 value. For the Freundlich model, this included K and m; for the BET model, this included X_m and C; for the FHH model, this included θ, K, and s; for the GAB model, this included X_m, c_1, and k_b; for the DLP model, this included c_1, c_2, c_3, and c_4; and for the D-A model, this included X_m, E, and n.

The equations were fit to the original data in the R_H range of 3% to 80%, where surface forces dominate sorption behavior. No constraints were applied, except that the c_4 parameter in the DLP Equation was assigned to be greater than zero since the opposite would be physically impossible. The reason for not assigning any constraining values to the parameters is to determine the ranges of the parameters that could be used for water vapor sorption on clay surfaces. None of the equations analyzed was proposed to represent this specific behavior. Thus, the values proposed for the equation parameters should not be expected to be same as values in literature. The aim here is to determine the appropriate ranges of equation parameters and applicability of each model to represent water vapor sorption behavior of clays.

2.3.4 SSA Calculation

SSA values were calculated by using the drying paths of the isotherms by using Equation 9.

$$SSA = \frac{X_m \cdot N \cdot A}{M}\ m^2/g \tag{9}$$

where X_m is the monolayer adsorption capacity (g/g), N is Avogadro's number ($6.02 \cdot 10^{23}$ mol^{-1}), A is the area covered by one H_2O molecule (0.108 nm^2), and M is the molecular mass of the adsorbate (18 g/mol). X_m values could be obtained directly from the BET, FHH, GAB, and D-A Equations. However, there is an extra calculation step for the DLP Equation. The c_4 parameter is first obtained by equation fitting, where

$$c_4 = \frac{SSA \cdot X_m}{6 \cdot f \cdot A} \tag{10}$$

Then, the X_m value is obtained by combining Equation 9 and Equation 10.

$$X_m = \sqrt{6 \cdot f \cdot c_4} \tag{11}$$

To find the f parameter, SSA of pure bentonite was assumed as 810 m^2/g, which is the theoretical SSA of montmorillonite obtained from lattice calculations (Dyal and Hendricks 1950). A theoretical f value of 1.27 was obtained.

2.4 RESULTS and DISCUSSION

2.4.1 Equation Fitting

Figure 2 shows the sorption isotherms of bentonite and kaolinite (Fig 2a), and desorption isotherms of the mixtures (Fig 2b). Bentonite shows significant hysteresis; whereas, for kaolinite, hysteresis can be considered negligible. The desorption curves of the mixtures clearly show that as bentonite content increases, the isotherms start to show a more significant stepwise shape.

Figure 3 shows the R^2 values of the equations that were fit respectively to the wetting (Fig 3a) and drying (Fig 3b) curves of the clay mixtures. The equations generally give better fit to the adsorption curves than the desorption curves. The reason for this is that the desorption curve of the bentonite has a more significant stepwise shape than the adsorption curve and representing a stepwise curve is mathematically more difficult. For the mixtures, since bentonite is more dominant in the sorption behavior than kaolinite, even at the low kaolinite percentages, the isotherm shape of the mixture is closer to that of the bentonite.

As seen more clearly in the drying curves, two of the most commonly used equations in geotechnical engineering to model the sorption behavior of soils, BET and FHH equations, do not fit the isotherm data as well as the other four models in the R_H range between 3% and 80%. Researchers agree that the BET equation does not fit the sorption data well after about 0.35 R_H (e.g., Mooney *et al*. 1952, Newman 1987, Yamanaka *et al*. 1990). For the FHH equation, no proposed range could be found.

2.4.2 Equation Parameters

2.4.2.1 Freundlich Equation

Figure 4 shows the change in the parameters of the Freundlich Equation, *K* (Fig 4a) and *m* (Fig 4b), obtained from both the drying and wetting curves with increasing bentonite content. *K* represents the adsorption capacity of the adsorbent. Bentonite has 2:1 units, and in between two successive units, it has an interlayer space, where water and other polar molecules can penetrate. Because of its structure, bentonite has a high specific surface area and, consequently, high sorption capacity. In contrast, kaolinite has 1:1 unit structure and there is no interlayer space in between the units. Consequently, it has lower specific surface area and sorption capacity. Therefore, the value of *K* increases with increasing bentonite content.

The difference between the *K* values for the drying and wetting curves is a result of the hysteresis effect. The adsorption and desorption isotherms do not show the same behavior. Due to capillary condensation, during desorption at a certain R_H value more water is retained on the clay surface than the amount of water the surface uptakes during adsorption at the same R_H. The reason of capillary condensation is that, in a system having nonuniform pore sizes, wetting process is determined by the smaller pores, whereas, drying process is controlled by the larger pores. The hysteresis effect becomes more significant as the bentonite content increases, since the amount of water adsorbed or desorbed also increases.

The other parameter of the Freundlich Equation, *m*, is related to the intensity of sorption. The value of *m* is generally close to 1 (Calvet 1989, Hamaker and Thompson 1972), which gives a linear equation. Figure 4b shows that the *m* value of the adsorption curve follows the literature trend, but the one for desorption ranges between 1.2 to 1.4 and increases with increasing bentonite content. This result is due to the stepwise shape of the desorption isotherm of bentonite. A logarithmic curve represents the stepwise shape better than a linear curve.

2.4.2.2 BET Equation

The two parameters of the BET equation, X_m and C, are plotted with respect to increasing bentonite content in Figure 5. As the bentonite fraction increases, the surface for the sorption of water molecules also increases, leading to an increase in monolayer coverage, X_m. As explained before, due to capillary condensation, at a certain R_H value the water content is greater on the desorption curve. Consequently, at a certain bentonite content value, the drying curve has greater monolayer coverage. The difference in X_m values between the wetting and drying curves increase as the bentonite content increases. This is interpreted to indicate that the effects of capillary condensation become more significant.

C, the energy constant, depends on the net heat of adsorption, which is the difference between the heat of adsorption of the first monolayer of water vapor (E_1) and the heat of liquefaction of water vapor (E_2). The second term (E_2) is constant for the constant laboratory conditions, and thus the only term that changes the C value is the heat of monolayer adsorption on the surface, which depends only on the type of the adsorbent. Figure 5b shows that, the BET C value stays relatively constant (~50). This is an expected result, since the E_1 value that is representative of the whole R_H range should be regarded as an average value of heat of adsorption for the less active part of the adsorbent (Brunauer *et al*. 1938). Also, the wetting curves give lower C values than the drying curves, suggesting that the heat of desorption of a specific soil is slightly higher than the heat of adsorption.

2.4.2.3 FHH Equation

Trends in the parameters of FHH equation, X_m, K, and s, with the increasing bentonite content are shown in Figure 6. Figure 6a shows that X_m, the monolayer coverage, increases with the increasing bentonite content, showing the same behavior as the X_m values calculated from the BET Equation. The trend in the energy parameter (K) of the FHH equation with the increasing bentonite content is shown in Figure 6b. The energy required both for adsorption and desorption increases as the bentonite content increases. This trend can be explained by the mineral structures of bentonite and kaolinite. Bentonite sorbs much more water than kaolinite in the interlayer space between the two subsequent 2:1 semi-basic units. However, kaolinite forms by stacking of 1:1 semi-basic units where the octahedral unit and the tetrahedral unit of the two subsequent 1:1 layers attract each other strongly, leaving no space for water molecules to enter. By adsorption, the water content of bentonite increases up to about 16% in the R_H range of 5% to 80% whereas, for kaolinite, the increase is only up to about 1.05% in the same R_H range. Since the work done is greater in the case of bentonite, the energy is also higher. The trend is the same for the drying cycle, but the value of K is greater than for adsorption. Due to the hysteresis effect, for the same R_H the drying path always has a higher water content value than the wetting path. As the amount of water increases, the work done increases, thus the energy required for desorption will be greater than the one for adsorption.

The s parameter (Figure 6c) stays almost constant as bentonite content increases. The drying curve values, on average, are about 15.5% greater than the wetting curve values. For the drying curve a slight increase (~12.5%) is observed as the bentonite fraction increases from 0% to 40%. In contrast, for the wetting curve, the value of s decreases about 10.4% as bentonite fraction increases from 0% to 20% and after 20% bentonite, stays almost constant around 1.5.

This nearly constant *s* value is reasonable considering all the different proposed physical meanings of the parameter. As mentioned before, *s* could indicate the interaction strength of the adsorbent and the adsorbate (Halsey 1948), the effects of micropore and mesopore filling (Carrot *et al*. 1982), or the amount of surface heterogeneity (Rudzinski and Everett 1992). The interaction strength is most likely to stay constant for all soil samples, since the adsorbate is always water vapor, and the adsorbent is a clay mineral. Kaolinite and bentonite are both formed of the same atoms, the only difference is how the sheets of atoms come together. The amount of water, and thus the total energy of the sorption, changes between the two minerals, but the interaction energy of these minerals with the water molecule most likely to be the same. The pores in the clay minerals are micropores, so there is no expected effect of the pore sizes. Comparing the amount of surface heterogeneity of kaolinite and bentonite is difficult. However, the effects of surface heterogeneity are higher for the wetting cycle than the drying cycle, since the soil surface is initially dry at the adsorption case (Mooney 1952). As the surface heterogeneity increases, the value of *s* decreases between the drying and wetting cycles.

2.4.2.4 GAB Equation

Trends in the parameters of the GAB Equation (X_m, c_1, and k_b) with increasing bentonite content are shown in Figure 7. The X_m parameter, which is an indicator of SSA, shows the expected trend, increases with increasing bentonite content.

The c_1 parameter of the GAB equation has the same physical meaning as the C parameter of the BET equation, but the values of the two parameters differ considerably from each other. As mentioned before, BET theory assumes that the energy of adsorption of the layers beyond a monolayer is equal to the energy of liquefaction. Because of this assumption, BET theory overestimates the energy parameter and, consequently, underestimates the monolayer coverage.

GAB model assumes that the energy of adsorption beyond a monolayer is less than the energy of liquefaction and has an additional parameter, k_b, in the equation to account for this difference. The c_1 parameter of the GAB equation is also similar to the K parameter of the FHH equation, since they both indicate the attraction between the adsorbate and the adsorbent. However, the important difference between the two is that although K is indicative of the energy of adsorption (Hill 1949), c_1 is related to the binding strength of water to the primary binding surfaces (Sabard *et al*. 2012). The primary binding surfaces for bentonite are interlayer cations. Researchers agree that at low R_H values water is first adsorbed around interlayer cations (*e.g.,* Kraehenbuehl *et al.* 1987, Cases *et al*. 1997, Chiou and Rutherford 1997, Prost *et al*. 1998). For kaolinite, since there is no interlayer space, the primary binding surfaces are the surface molecules. Figure 7b implies that the binding strength between the water molecules and the clay molecules is larger than the binding strength between the water molecules and the interlayer cations. Once the soil sample has some bentonite content, the c_1 value remains nearly constant because the type of the interlayer cations should be the same for the same bentonite regardless of its fraction.

Figure 7c shows the trend in the k_b parameter of the GAB equation with increasing bentonite content. k_b remains unchanged for the soils having bentonite regardless of the fraction, but the value nearly doubles when the soil is pure kaolinite. This result implies that the adsorbed water does not interact with the kaolinite surface as much as it interacts with the bentonite surface. The value of k_b both for the wetting and drying cycles is greater than 0.4, which shows that the adsorption is not limited to first and second monolayers (Anderson 1946). Wetting curves give a higher k_b value than drying curves. This shows that the soil surface-sorbed water molecules interactions are smaller during the wetting process than the interactions during the drying process. A similar conclusion was reached from the trend observed for the s parameter of the FHH Equation. The FHH *s* parameter, which shows the strength of interaction between the adsorbate and the adsorbent, has a higher value during desorption.

2.4.2.5 DLP Equation

The trends in the parameters of the DLP Equation with increasing bentonite content are shown in Figure 8. To understand the physical meaning of the equation parameters better, the derivation steps should be investigated.

The equation of the chi plot for a single adsorption plane was given by Equation 5. Chi plots are additive. For sorption of water vapor by soil surface, there are several surface planes with different energies and consequently, with different chi plots. For various surface planes, the equation of the chi plot (Equation 12) is the summation of the chi-plots derived for each plane (Condon 2006).

$$\frac{\delta X}{\delta \chi} = \sum_i \frac{SSA_i \cdot X_m}{f \cdot A_m} U(\chi - \chi_c) \tag{12}$$

For the whole surface, the equation of the chi plot then becomes the integral of Equation 12.

$$\frac{\delta X}{\delta \chi} = \int \frac{SSA \cdot X_m}{f \cdot A_m} U(\chi - \chi_c) \tag{13}$$

Taking the derivative of both sides to omit the Heaviside step function from the equation and using K instead of all the constants (*i.e.*, $K = \frac{SSA \cdot X_m}{f \cdot A_m}$),

$$\frac{\delta^2 X}{\delta \chi^2} = (\chi - \chi_c) \cdot K \tag{14}$$

Equation 14 is integrated twice to obtain X

$$\frac{\delta X}{\delta \chi} = \left(\frac{\chi^2}{2} - \chi_c \chi\right) K + b_1 \tag{15}$$

$$X = \left(\frac{\chi^3}{6} - \frac{\chi_c \chi^2}{2}\right) K + b_1 \chi + b_2 \tag{16}$$

where b_1 and b_2 are integration constants.

Equation 16 can be written in the form of a polynomial function by using four constants, c_1 to c_4, and using water content instead of the amount adsorbed (X) (Equation 6). Then, c_1 and c_2 become integration constants. The equation can be reduced to three parameters by equating c_1 to water content at 37% R_H (χ is equal to 0 at 37% R_H). The parameter c_2 is the initial rate of adsorption, and could be obtained by equating the first derivative of the isotherm equation to zero. c_3 is proportional to $K\chi_c$, and c_4 is proportional to K.

The parameter c_3 is related to the specific surface area of the adsorbent, monolayer coverage, and total energy of adsorption. c_3 increases as the bentonite content increases (Figure 8) since the amount of adsorption sites and the adsorbed molecules increases. The negative values during desorption only show the direction of sorption.

The parameter c_4 is related to the SSA of the adsorbent, and the monolayer coverage. c_4 increases with the increasing bentonite content since the adsorption sites increase. For the drying cycle, there is a drop at 80% bentonite content, which could be regarded as an outlier.

2.4.2.6 D-A Equation

The trends in the parameters of D-A Equation, X_m, E, and n, with increasing bentonite content are shown in Figure 9. Monolayer coverage, X_m, should be the lowest for pure kaolinite and is expected to increase with increasing bentonite content, since the interlayer space increases. Figure 9a shows that the X_m values for kaolinite obtained from D-A model are unrealistically too high. Although further investigation is required, the D-A model can be concluded to be non-representative for soils that do not have bentonite content (i.e., soils having low specific surface area). Also, X_m values obtained from the drying curve are expected to be higher than the values obtained from the wetting curve because, due to capillary effects, clay retains more water during desorption. However, the soils with bentonite content do not follow this expected trend.

The change in parameter E with increasing bentonite content is shown in Figure 9b. The behavior is expected to be similar to the C parameter of BET Equation and c_1 parameter of GAB equation since they all account for the characteristic sorption energy. Except for the kaolinite, the expected trend is observed, that is, a nearly constant E value with increasing bentonite content. Similar to the trend in X_m, the characteristic adsorption energy was also observed to be higher than the characteristic desorption energy.

The trend in the empirical constant n with increasing bentonite content is shown in Figure 9c. Except for the kaolinite, n values are constant that can be rounded to 1, the closest integer. This result contradicts the values proposed by Dubinin and Astakhov (1971). Their study on microporous carbon adsorbents and activated charcoals showed that, as micropore radii decreased, the n value increased. Bentonite is expected to have a micropore space smaller than 0.5 nm, the smallest value in the study of Dubinin and Astakhov (1971), even at 70% R_H (Likos and Lu 2006). Therefore, according to the previous study, n values would be expected to be at least 3.

Since the parameters of kaolinite found by R^2 maximization do not follow the expected trend, a target R^2 of 0.95 for drying and 0.98 for wetting was set, and the related parameters were calculated (squares in Figure 9). E and n parameters, in this case, have the same values as the soils with some bentonite content, yet X_m parameter is still too high and yields almost twice of the expected SSA value. It could be concluded, therefore, that D-A equation does not give realistic SSA values for low SSA soils.

2.4.3 Specific Surface Area (SSA) Comparison

SSA of the mixtures was calculated by using all the equations, except the Freundlich Equation. The SSA values calculated from the desorption branches of the water vapor sorption isotherms are shown in Figure 10. To compare the validity of the models, SSA_{EGME} values were used as the ‘true’ values. Although the D-A Model does not give realistic results for pure kaolinite, when there is bentonite content in the mixture, D-A Equation gives the most accurate results (*i.e.,* closest to the theoretical values). The commonly used BET Equation gives the lowest SSA values. The BET results were expected to be non-accurate since the R_H range that BET Theory is applicable is between 5% and 35%. Although the calculated SSA values do not exactly match with the theoretical SSA values, GAB, FHH, and BET theory gives consistent results among the bentonite-kaolinite mixtures. Therefore, any of the three equations could potentially be used to compare the SSAs of multiple clayey soils.

Usage of the whole R_H range for SSA computations will bring some practicality. The layer-by-layer sorption methods use the number of layers sorbed on clay surface. However, at a specific R_H value, it is not known if a layer is completed. Choosing a R_H value for a specific number of layers, which will be valid for all types of clays will also be challenging. Micropore filling sorption methods will also have the similar ambiguity if a R_H value is tried to be chosen to represent all types of clays.

2.5 IMPLICATIONS

2.5.1 Isotherm Estimation from SSA_{EGME}

Experimental approaches to obtain the water vapor sorption isotherm of clayey soils can be very tedious and time consuming if humidity control techniques are used (*e.g.*, non-contact filter paper methods, dew point methods), or can be expensive if a dynamic dew point method (*e.g.*, Vapor Sorption Analyzer®, Decagon Devices Inc., Pullman, WA) is used. Evaluation of several models for water vapor isotherms, and the above discussion of SSA brings up the question of whether or not it is possible to estimate the sorption isotherm from the SSA_{EGME} value, which is relatively easy and inexpensive to obtain. In this section of the study, the applicability of a computational approach by using the DLP Model to obtain the water vapor sorption isotherms of clayey soils with low to medium specific surface area (SSA) values (SSA < 450 m^2/g) is discussed.

First, SSA_{EGME} values of the mixtures were determined and plotted against SSA_{DLP} values (Figure 11). The relationship ($R^2 = 0.97$) between SSA_{EGME} and SSA_{DLP} is given by

$$SSA_{DLP} = 1.50 \cdot SSA_{EGME} + 44.42 \tag{17}$$

To obtain the isotherm of a natural soil, the surface area is calculated by the EGME Method. DLP surface area is determined from Figure 11. Bentonite content is obtained by using

$$SSA_{DLP} = \frac{809x + 21(100 - x)}{100} \tag{18}$$

where SSA_{DLP} is the DLP surface area of the natural soil obtained from Figure 11, 809 and 21 are the DLP surface area (m^2/g) of 100% bentonite and 100% kaolinite respectively, and x is the bentonite content (%).

Once the bentonite content is obtained, all the parameters of DLP equation can be obtained from Figure 8, and the isotherm can be plotted. The isotherms of 13 natural clays were determined from the SSA_{EGME} values and the recommended range of DLP model parameters. Table 2 shows the surface properties and the Atterberg limits of the natural clays. The best and the worst fit to the real sorption data was obtained with (a) Wcs Andrews (R^2 = 0.98) and (b) New Orleans soils (R^2 = 0.32) (Figure 12). The isotherms obtained from a single EGME measurement should not be expected to be exact, but they can provide easy and quick insight about the water vapor sorption behavior of clayey soils.

2.6 SUMMARY AND CONCLUSIONS

Performance of six existing models for sorption isotherms were evaluated for the specific behavior of water vapor sorption by clays. Assumptions underlying each equation were discussed. Bentonite-kaolinite mixtures were prepared in seven different proportions, and the equation parameters of the mixtures were found by least squares optimization both for adsorption (wetting) and desorption (drying) curves. Adsorption curves were found to give higher R^2 values than the desorption curves because of the more significant stepwise shape of the drying curve of bentonite. The most frequently used sorption models in geotechnical engineering, BET and FHH models, are the least representative models, in average, respectively having almost 6.1% and 2.0% lower R^2 values than the other models for the whole R_H range of sorption (i.e. 3% R_H to 80% R_H). Monolayer coverage (X_m) increases with increasing bentonite content and has a greater value for desorption curves. The trends in the energy parameters of the equations with increasing bentonite content show that the sorption capacity and the energy of sorption increases with increasing bentonite content, whereas characteristic adsorption energy, or the binding strength of water to the soil surface stays constant. Also, similar to the monolayer coverage, energy parameters of the drying curves have slightly greater values than the energy parameters of the wetting curves. The models with energy parameters that indicate the sorption capacity of the soil (Freundlich, FHH, and DLP) are expected to give more reliable comparisons for clay surface properties regardless of the clay mineralogy. SSA values were calculated from all of the models except the Freundlich model. The D-A Model was found to give the most realistic values (*i.e.*, closest to the theoretical values) if the soil has some bentonite content, whereas for pure kaolinite the model does not give realistic SSA values. Although the computed SSA values are lower than the theoretical SSA values, GAB, FHH, and BET models were found to give consistent SSA values for the mixtures. Therefore, either the GAB, FHH, or BET model is recommended to be used for comparing SSA values of multiple soils. The discussions in this study imply that the physical meanings of the equation parameters should be considered to choose the most applicable isotherm model for a specific goal. The water vapor sorption isotherm of clays could roughly be estimated by using the SSA_{EGME} and the recommended range of model parameters.

2.7 REFERENCES

Anderson, R.B., 1946, “Modifications of the Brunauer, Emmett and Teller Equation,” *Journal of American Chemical Society*, 68(4): 686-691.

Bain, D., Costanzo, P.M. and Guggenheim, S., (eds.), (2001). *Clays and Clay Minerals*, 49: 371-453.

Bishop, A.W., 1959, “The principle of effective stress,” *Tek. Ukeblad*, 106(39): 859-863.

Brunauer, S., Emmett, P.H. and Teller, E., 1938, “Adsorption of gases in multimolecular layers,” *Journal of American Chemical Society*, Vol. 60, pp. 309-319.

Calvet, R., 1989, “Adsorption of organic chemicals in soils,” *Environmental Health Perspectives*, Vol. 83, pp. 145-177.

Campbell, G.S., Smith, D.M. and Teare, B.L., 2007, “Application of a dew point method to obtain the soil water characteristic,” Experimental Unsaturated Soil Mechanics, T. Schanz (Ed.), Springer, pp. 71-77.

Carrott, P.J., Mcleod, A.I. and Sing, K.S.W., 1982, “Application of the Frenkel-Halsey-Hill equation to multilayer isotherms of nitrogen on oxides at 77K,” *Adsorption at the Gas-Solid and Liquid-Solid Interface*, pp. 403-410.

Cases, J.M., Berend, I., Francois, M., Uriot, J.P., Michot, L.J. and Thomas, F., 1997, ”Mechanism of adsorption and desorption of water vapor by homoionic montmorillonite: 3. the Mg2+, Ca2+, Sr2+, and Ba2+-exchanged forms,” *Clays and Clay Minerals*, 45(1): 8-22.

Cerato, A.B. and Lutenegger, A.J., 2004, “Determining intrinsic compressibility of fine-grained soils,” *Journal of Geotechnical and Geoenvironmental Engineering*, 130(8): 872-877.

Chiou, C.T., and Rutherford, D.W., 1997, “Effects of exchanged cation and layer charge on the sorption of water and EGME on montmorillonite clays,” *Clays and Clay Minerals*, 45: 867-880.

Condon, J.B., 2006, *Surface Area and Porosity Determinations by Physisorption: Measurements and Theory,* Elsevier Science, Amsterdam.

de Boer, J.H., 1953, *The Dynamical Character of Adsorption*, Oxford University Press, Oxford.

de Boer, J.H., Lippens, B.C., Linsen, B.G., Broekhoff, J.C., van den Heuvel, A. and Osinga, T.J., 1966, “The t curve of molecular N2 adsorption,” *Journal of Colloid and Interface Science,* 21: 405-414.

Dubinin, M.M. and Astakhov, V.A., 1971, “Development of the concepts of volume filling of micropores in the adsorption of gases and vapors by microporous adsorbents,” *Bulletin of the Academy of Sciences of the USSR, Division of Chemical Science*, 20(1): 3-7.

Dutcher, C.S., Ge, X., Wexler, A.S. and Clegg, S.L., 2011, “Statistical Mechanics of Multilayer Sorption: Extension of the Brunauer-Emmett-Teller (BET) and Guggenheim-Anderson-de Boer (GAB) Adsorption Isotherms,” *The Journal of Physical Chemistry*, 115, 16474-16487.

Fowler, R.H. and Guggenheim, E.A., 1939, *Statistical Thermodynamics*, Cambridge University Press, Teddington.

Fredlund, D.G. and Morgenstern, N.R., 1977, “Stress state variables for unsaturated soils,” *J. Geotech. Eng. Dic., Am. Soc. Civ. Eng.*, 103(5): 447-466.

Frenkel, J., 1955, *Kinetic Theory of Liquids,* Dover Publications Inc., New York.

Freundlich, H., 1926, *Colloid and Capillary Chemistry,* Methuen and Co. Ltd, London.

Freundlich, H., 1932, “Of the adsorption of gases. Section II. Kinetics and energetics of gas adsorption. Introductory paper to section II,” *Transactions of the Faraday Society,* 28: 195-201.

Fuller Jr, E.L. and Condon, J.B., 1989, “Statistical Mechanical Evaluation of Surface Area from Physical Adsorption of Gases,” *Colloids and Surfaces*, pp. 171-181.

Gallipoli, D., Gens, A., Sharma, R. and Vaunat, J., 2003, “An elasto-plastic model for unsaturated soil incorporating the effects of suction and degree of saturation on mechanical behavior,” *Geotechnique*, 53(1): 123-135.

Ginns, J.W., 1902, *Elementary Principles in Statistical Mechanics: Developed with Especial Reference to the Rational Foundations of Thermodynamics,* Charles Scribner’s Sons, New York.

Gregg, S.J. and Sing, K.S.W, 1982, *Adsorption, Surface Area and Porosity,* 2nd Edition, Academic Press Inc., New York.

Guggenheim, E.A., 1966, *Applications of Statistical Mechanics*, Oxford University Press, London.

Halsey, D.H., 1952, “The role of surface heterogeneity in adsorption,” *Advances in Catalysis*, Vol. 4, pp. 259-271.

Halsey, G., 1948, “Physical adsorption on non-uniform surfaces,” *The Journal of Chemical Physics*, 16(10): 931-937.

Hamaker, J.W. and M, T.J., 1972, “Adsorption,” In A.I. Goring, & J. W. Hamaker, *Organic Chemicals in the Soil Environment* (Vol. 1, pp. 49-143), Marcel Dekker Inc., New York.

Hill, T.L., 1946, “Localized and mobile adsorption and absorption,” *The Journal of Chemical Physics,* Vol. 14, pp. 441.

Hill, T.L., 1949, “Statistical mechanics of adsorption. V. thermodynamics and heat of adsorption,” *The Journal of Chemical Physics*, 17(6): 520-535.

Hill, T.L., 1952, "Theory of Physical Adsorption," *Advances in Catalysis*, Vol. 4, pp. 211-258.

Kiselev, A.V., 1958, "Vapor adsorption in the formation of adsorbate molecule complexes on the surface," *Kolloid Zhur*, Vol. 20, pp. 338-348.

Kraehenbuehl, F., Stoeckli, H.F., Brunner, F., Kahr, G. and Muller-Vonmoos, M., 1987, "Study of the water-bentonite system by vapour adsorption, immersion calorimetry and x-ray techniques: 1. micropore volumes and internal surface areas, following Dubinin's theory," *Clay Minerals*, Vol. 22, pp. 1-9.

Langmuir, I., 1918, "The adsorption of gases on plane surfaces of glass, mica and platinum," *Journal of American Chemical Society*, 40(9): 1361-1403.

Leong, E.C., Tripathy, S. and Rahardjo, H., 2003, "Total suction measurement of unsaturated soils with a device using the chilled-mirror dew-point technique," Géotechnique, 53(2): 173-182.

Likos, W.J. and Lu, N., 2006, "Pore scale analysis of bulk volume change from crystalline swelling in Na^+- and Ca^{2+}-smectite," *Clays and Clay Minerals*, 54(4): 516 – 529.

Likos, W.J. and Lu, N., 2012, March 25-29, "Characterizing physical properties of clay by water vapor sorption," *Geotechnical Special Publication No. 225*. Oakland, California, USA: ASCE.

Lu, N. and Likos, W.J., 2006, "Suction stress characteristic curve for unsaturated soil," *Journal of Geotechnical and Geoenvironmental Engineering*, 132(2): 131-142.

Likos, W.J., Lu, N., and Wenszel, W., 2011, “Performance of a dynamic dew point method for moisture isotherms of clays,” Geotechnical Testing Journal, 34(4), DOI: 10.1520/GTJ102901.

McMillan, W.G., & Teller, E., 1951, “The role of surface tension in multilayer gas adsorption,” *The Journal of Chemical Physics*, 19(1): 25-32.

Mooney, R.W, Keenan, A.G., and Wood, L.A., 1952, “Adsorption of water vapor by montmorillonite. II. Effect of exchangeable ions and lattice swelling as measured by X-ray diffraction,” *Journal of American Chemical Society*, 74, 1371-1374.

Newman, A.C.D., 1987, “The interaction of water with clay mineral surfaces,” In A. C. Newman, *Chemistry of Clays and Clay Minerals* (pp. 237-274), Mineralogical Society.

Orchiston, H.D., 1953, “Adsorption of water vapor: 1. Soils at 25°C,” *Soil Science*, 76(6): 453-466.

Pagano, A.M. and Mascheroni, R.H., 2005, “Sorption isotherms for amaranth grains,” *Journal of Food Engineering*, Vol. 67, pp. 441-450.

Petersen, L.W., Moldrup, P., Jacobsen, O.H. and Rolston, D.E., 1996, “Relationships between specific surface area and soil physical and chemical properties,” *Soil Science*, 161(1): 9-21.

Ponec, V., Knor, Z., & Cerny, S., 1974, *Adsorption on Solids*, Butterworth & Co (Publishers) Ltd, London.

Prost, R., Benchara, A. and Huard, E., 1998, “State and location of water adsorbed on clay minerals: consequences of the hydration and swelling-shrinkage phenomena,” *Clays and Clay Minerals*, 46(2): 117-131.

Rudzinski, W. and Everett, D.H., 1992, *Adsorption of Gases on Heterogeneous Surfaces*, Academic Press, New York.

Sabard, M., Gouanve, F., Espuche, E., Fulchiron, R., Seytre, G., Fillot, L.A., and Trouillet-Fonti, L., 2012, “Influence of film processing conditions on themorphology of polyamide 6: Consequences on water and ethanol sorption properties,” *Journal of Membrane Science*, pp. 670-680.

Sing, K.S.W, Everett, D.H., Haul, R.A., Moscou, L., Pierotti, R.A., Rouquerol, J., *et al*., 1985, “Reporting Physisorption Data for Gas/Solid Systems with Special Reference to the Determination of Surface Area and Porosity,” *Pure & Appl. Chem*., 57(4): 603-619.

Stoeckli, F. and Jakubov, T., 1994, “Water Adsorption in Active Carbons described by the Dubinin-Astakhov Equation,” *J. Chem. Soc. Faraday Trans*., 90(5): 783-786.

Temkin, M.I., 1941, “Adsorption equilibrium and the kinetics of processes on nonhomogeneous surfaces and in the interaction between adsorbed molecules,” *The Journal of Chemical Physics*, 15: 296-332.

Yamanaka, S., Malla, P.B. and Komarneni, S., 1990, “Water Adsorption Properties of Alumina Pillared Clay,” *Journal of Colloid and Interface Science*, 134(1): 51-58.

2.8 TABLES

Table 1.

Equation	**Basis**	**Parameters**			
F	Empirical	***K*** Related to the relative adsorption capacity of the adsorbent	***m*** • related to the intensity of adsorption • 1/m ≈ 1 (often)		
BET	statistical thermodynamics	X_m Amount adsorbed in a monolayer	***C*** Constant related to heat of adsorption		
FHH	Semi-empirical	Θ Fractional coverage	***K*** In principle a parameter related to the energy of adsorption in the first layer, but empirical in practice		***s*** parameter depends on the surface structure of the adsorbent Different meanings • indicates the strength of interaction btw the adsorbate and the adsorbent • represents the effects of micropore and mesopore filling • represents the surface heterogeneity
GAB	Statistical thermodynamics	X_m Amount adsorbed in a monolayer	c_1 measures the binding strength of water and the primary binding surface		k_b • measures the difference between the standard chemical potential of the adsorbed molecule in the second and higher layers, and the potential of the adsorbate in the liquid phase. • < 1
DLP	Quantum mechanics	c_1 residual water content	c_2 initial rate of adsorption	c_3 energy parameter	c_4 indicative of SSA
D-A	Micropore filling, thermodynamic equilibrium	X_m Amount adsorbed in a monolayer	***E*** Characteristic adsorption energy Indicates the average micropore width		***n*** • empirical constant • 2 for most of the adsorbents • 3 for adsorbents having very fine micropores

Table 2.

		Atterberg limits			**Surface Properties**		
soil ID	**USCS**	**LL**	**PL**	**PI**	**CEC (meq/ 100 g)**	**SSA-water (m^2/g)**	**SSA-EGME (m^2/g)**
Denver**	CH	49	23	26	23.0	107	151
New Orleans**	CL sandy	30	12	18	8.0	27	51
Sacramento	n.d.	39	22	17	27.8	138	191
Atlanta, Georgia	MH	50	36	14	13.2	50	72
KF1	CL	42	23	19	35.6	157	258
KF2	n.d.	41	15	26	23.4	102	151
Alb1	CL	28	17	11	8.5	38	51
Alb2	CL	36	14	22	8.1	29	51
Albany red	SC	30	16	14	7.6*	32	43
Houston brown	CH	41*	16*	25*	32.2*	90	145
Mon 2	CL	31	17	14	15.2	69	84
Kamm clay	CL	49	21	28	26.3*	84	145
WCS Andrews	CH	50	18	32	17.6*	71	118

2.9 FIGURES

Figure 1.

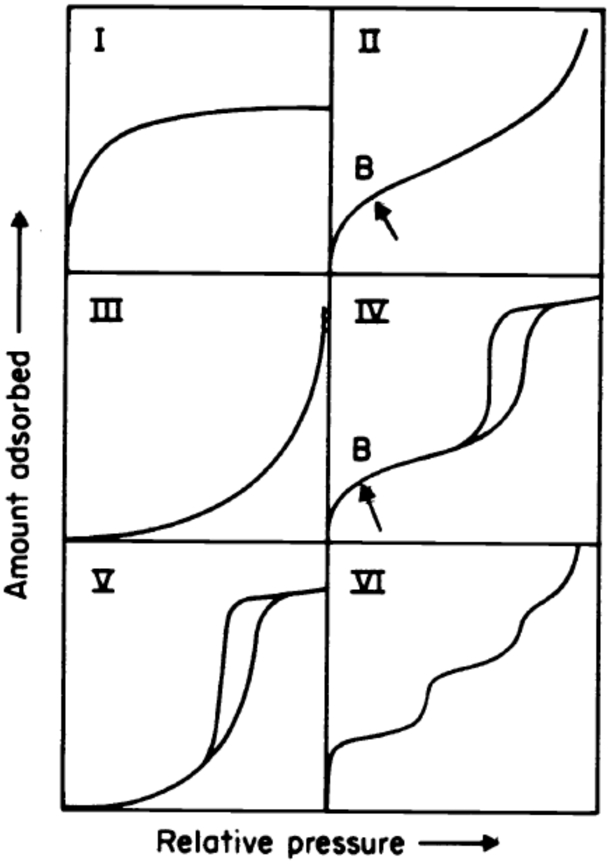

Figure 2.

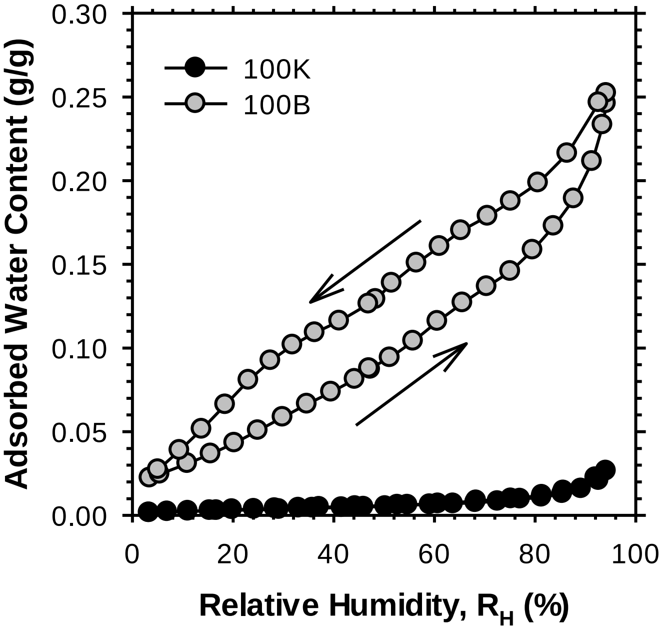

0.30
0.25
0.20
0.15
0.10
0.05
0.00
Adsorbed Water Content (g/g)
100K
100B
0
20
40
60
80
100
Relative Humidity, R_H (%)

(a)

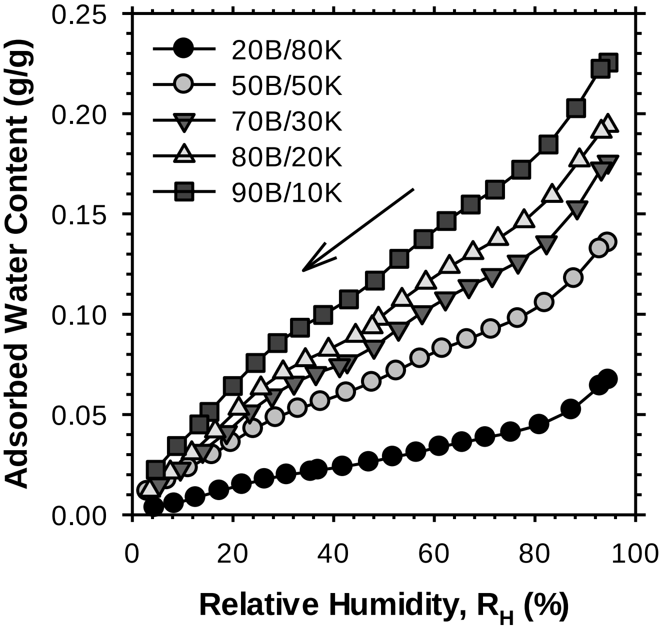

0.25
0.20
0.15
0.10
0.05
0.00
Adsorbed Water Content (g/g)
20B/80K
50B/50K
70B/30K
80B/20K
90B/10K
0
20
40
60
80
100
Relative Humidity, R_H (%)

(b)

Figure 3.

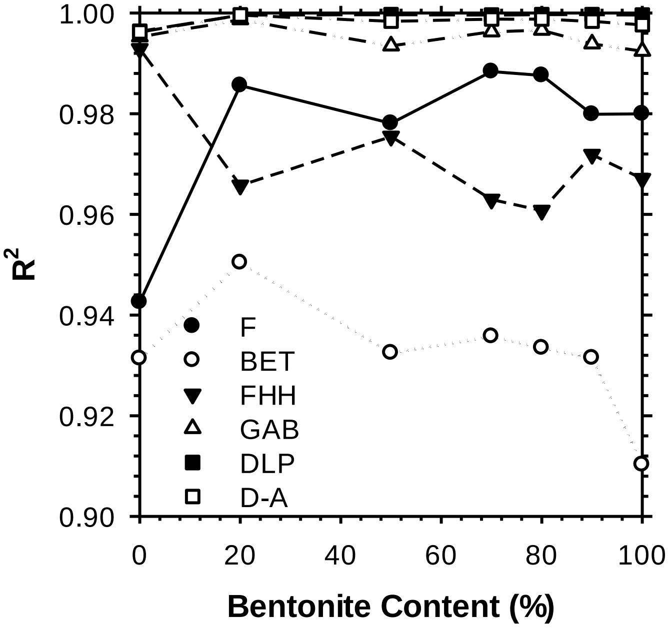
1.00
0.98
0.96
0.94
0.92
0.90
R²
0
20
40
60
80
100
Bentonite Content (%)
F
BET
FHH
GAB
DLP
D-A

(a)

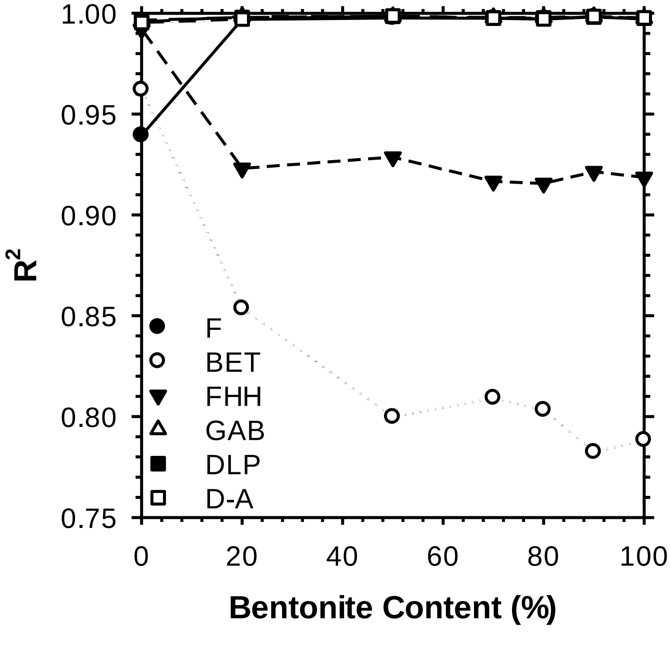
1.00
0.95
0.90
0.85
0.80
0.75
R²
0
20
40
60
80
100
Bentonite Content (%)
F
BET
FHH
GAB
DLP
D-A

(b)

Figure 4.

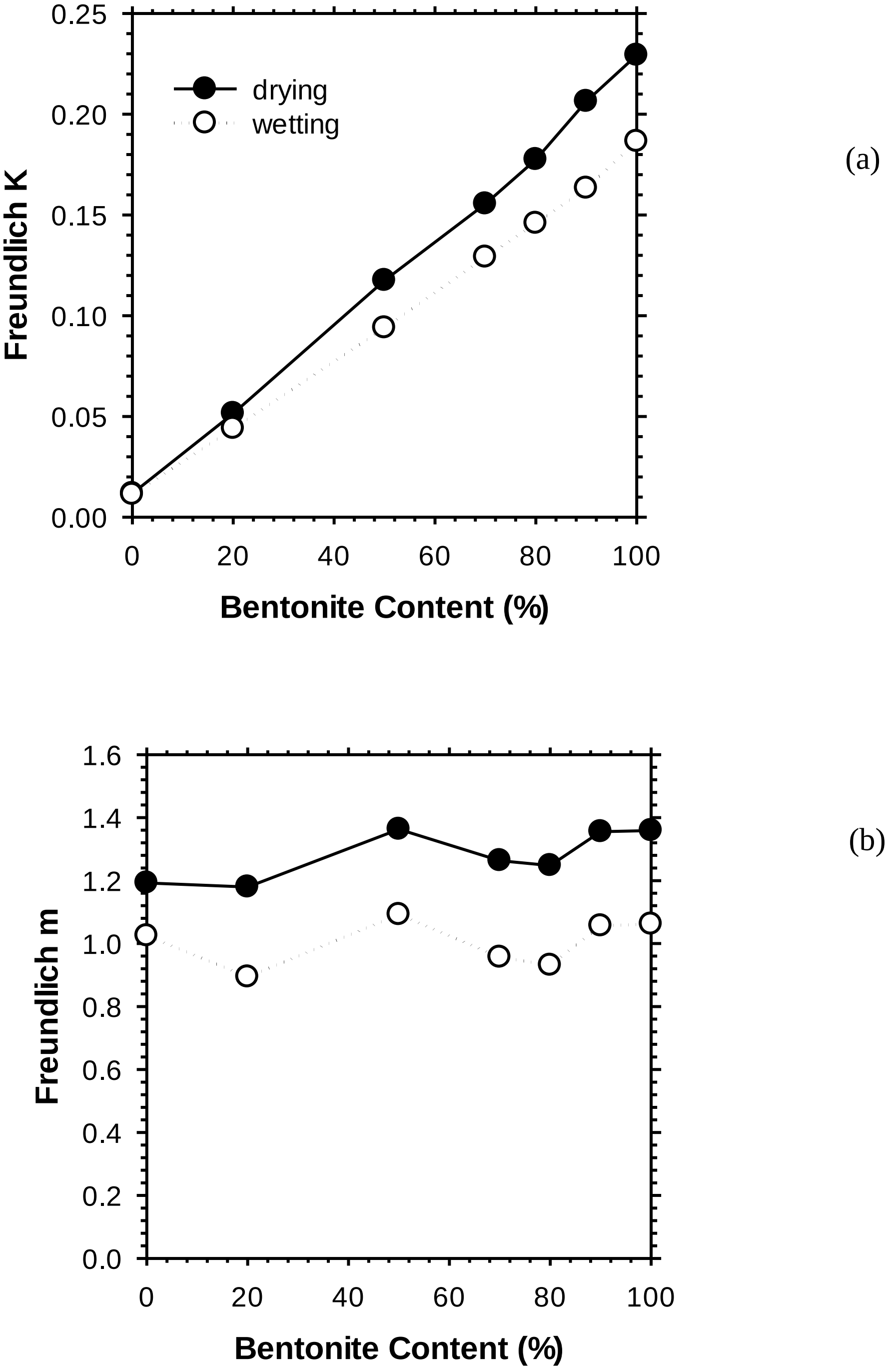
Freundlich K
0.25
0.20
0.15
0.10
0.05
0.00
0
20
40
60
80
100
Bentonite Content (%)
drying
wetting
(a)
Freundlich m
1.6
1.4
1.2
1.0
0.8
0.6
0.4
0.2
0.0
0
20
40
60
80
100
Bentonite Content (%)
(b)

Figure 5.

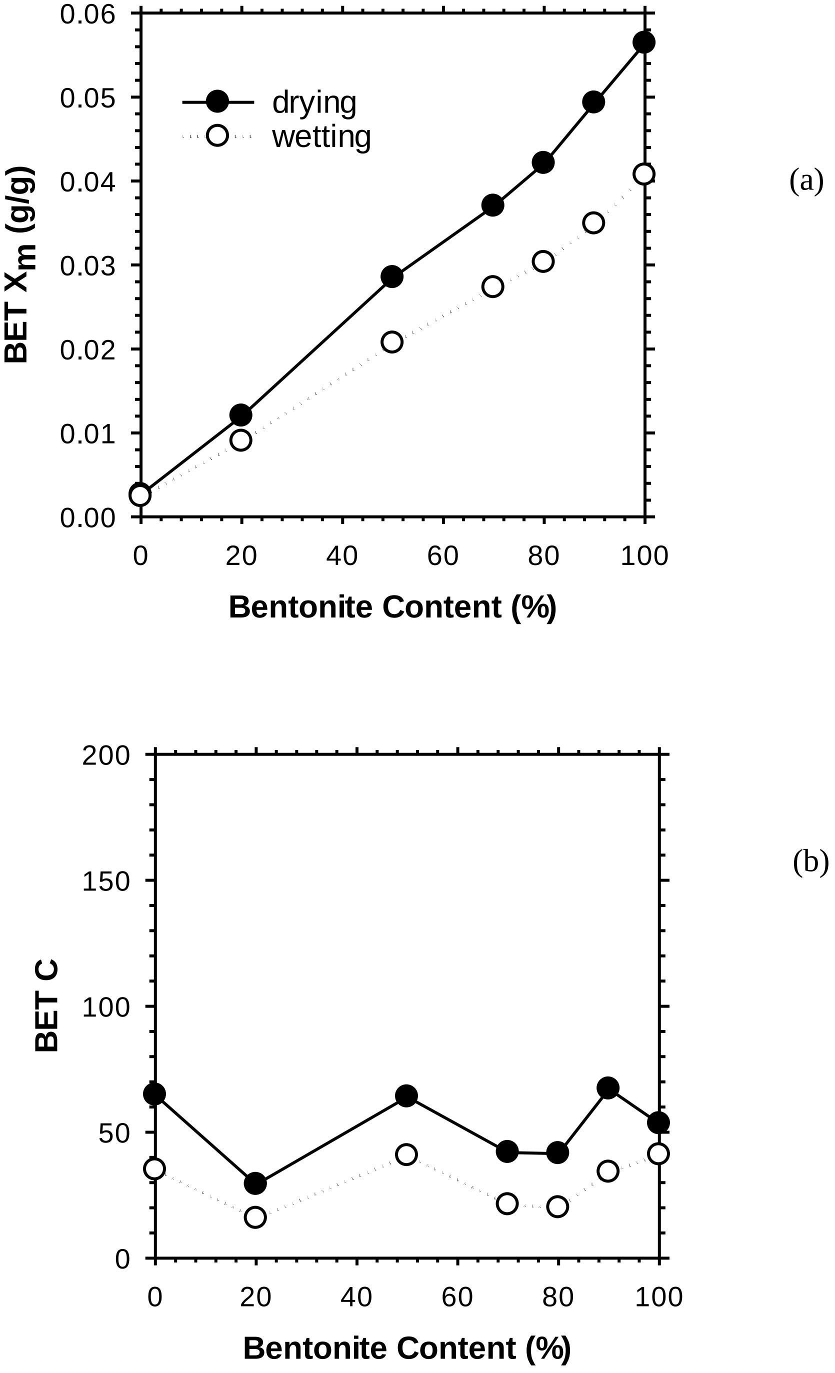
0.06
0.05
0.04
0.03
0.02
0.01
0.00
BET X_m (g/g)
drying
wetting
0
20
40
60
80
100
Bentonite Content (%)
(a)
200
150
100
50
0
BET C
0
20
40
60
80
100
Bentonite Content (%)
(b)

Figure 6.

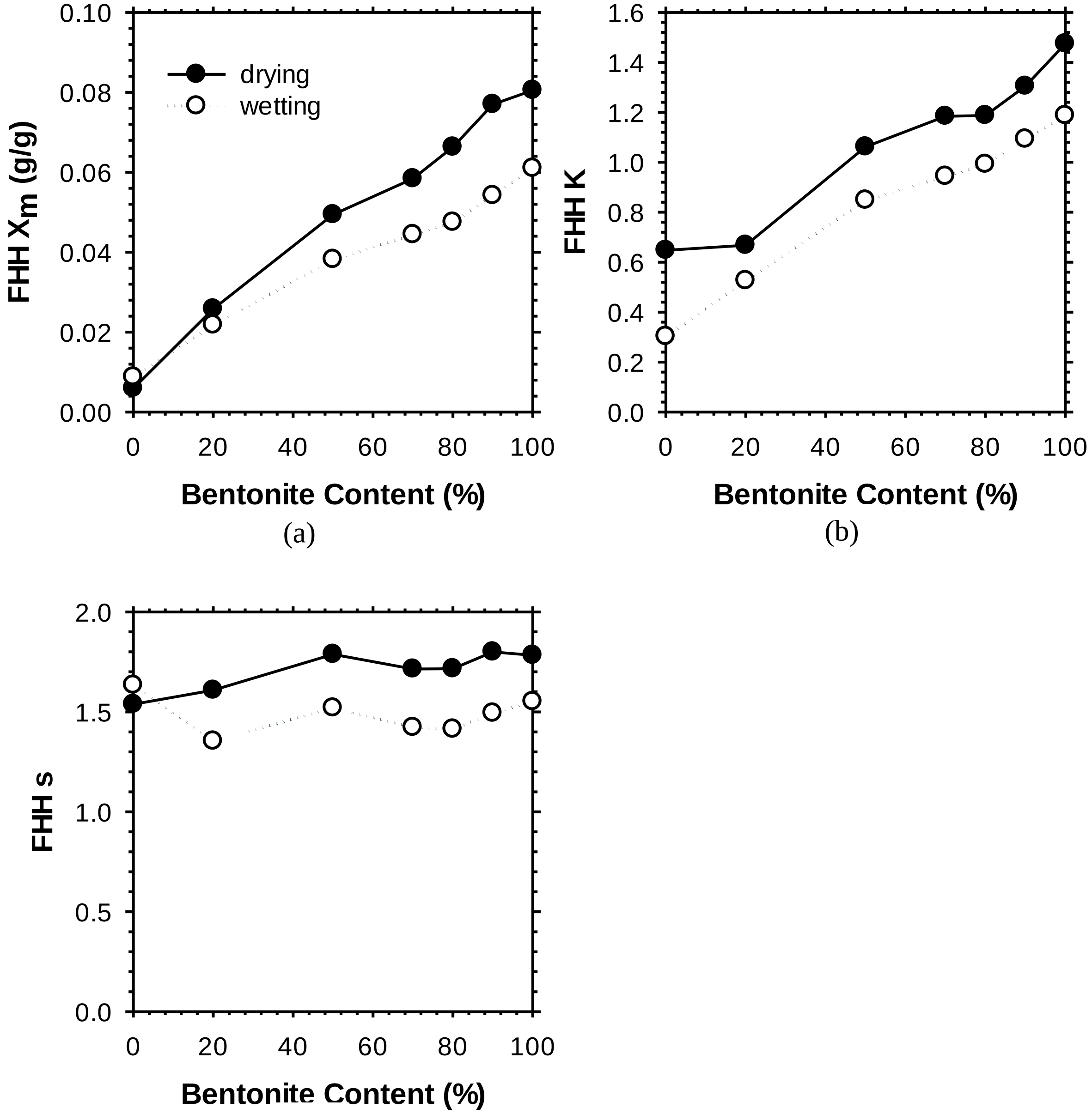
0.10
0.08
0.06
0.04
0.02
0.00
FHH X_m (g/g)
drying
wetting
0
20
40
60
80
100
Bentonite Content (%)
1.6
1.4
1.2
1.0
0.8
0.6
0.4
0.2
0.0
FHH K
0
20
40
60
80
100
Bentonite Content (%)
2.0
1.5
1.0
0.5
0.0
FHH s
0
20
40
60
80
100
Bentonite Content (%)

(a)

(b)

(c)

Figure 7.

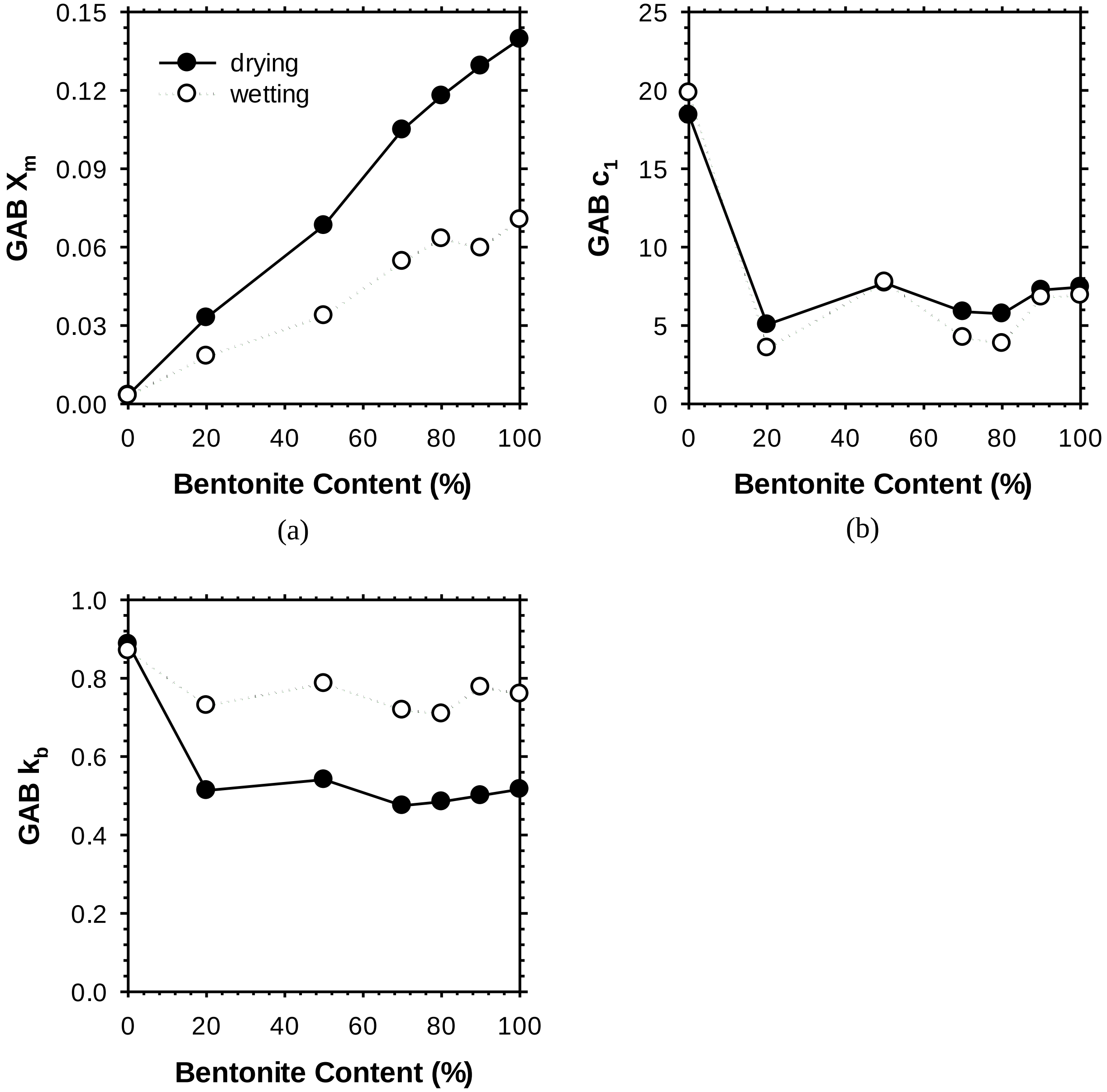

GAB X_m
0.15
0.12
0.09
0.06
0.03
0.00
drying
wetting
0
20
40
60
80
100
Bentonite Content (%)
GAB c_1
25
20
15
10
5
0
0
20
40
60
80
100
Bentonite Content (%)
GAB k_b
1.0
0.8
0.6
0.4
0.2
0.0
0
20
40
60
80
100
Bentonite Content (%)

(a)

(b)

(c)

Figure 8.

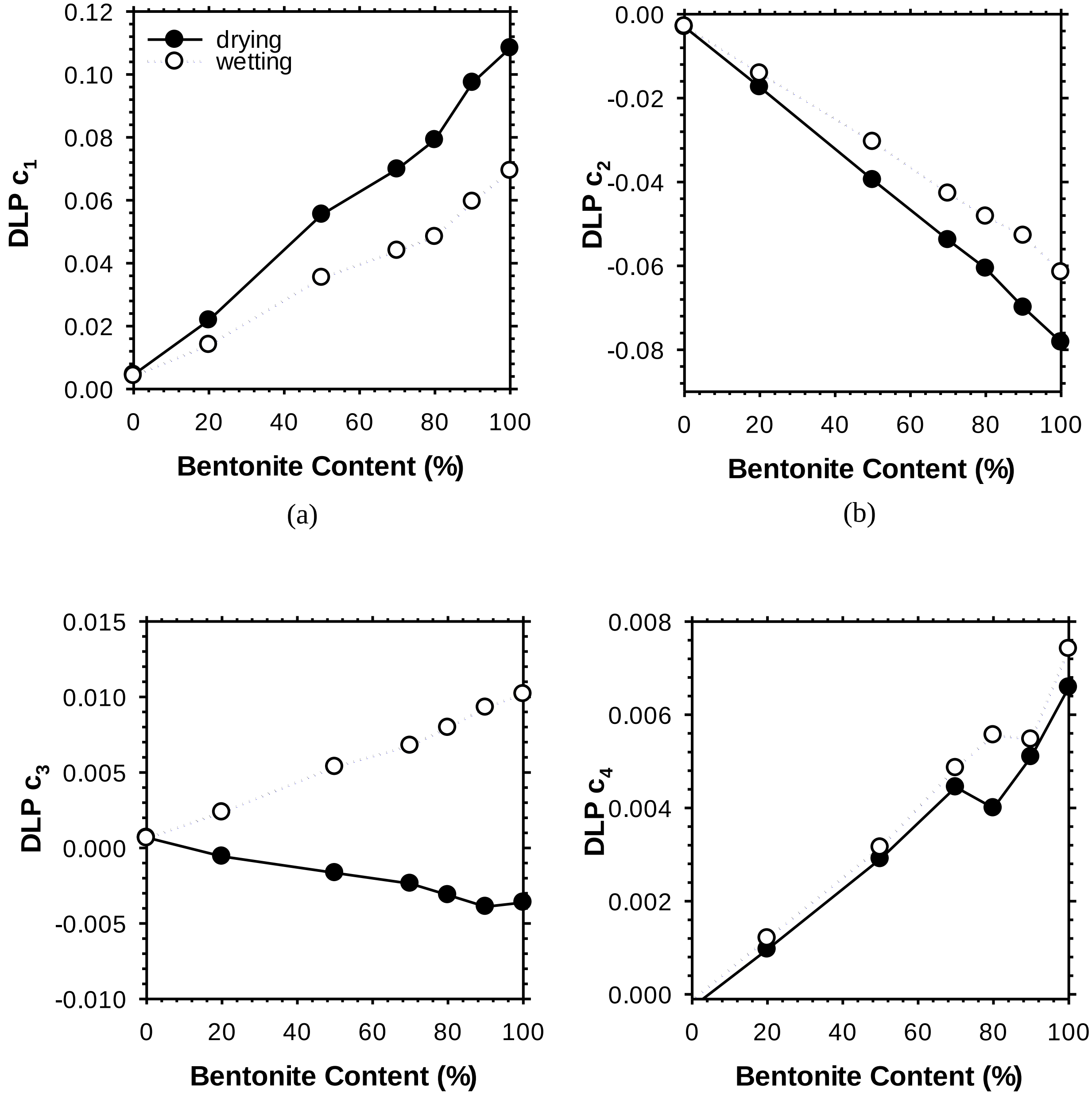

(a) (b)

(c) (d)

Figure 9.

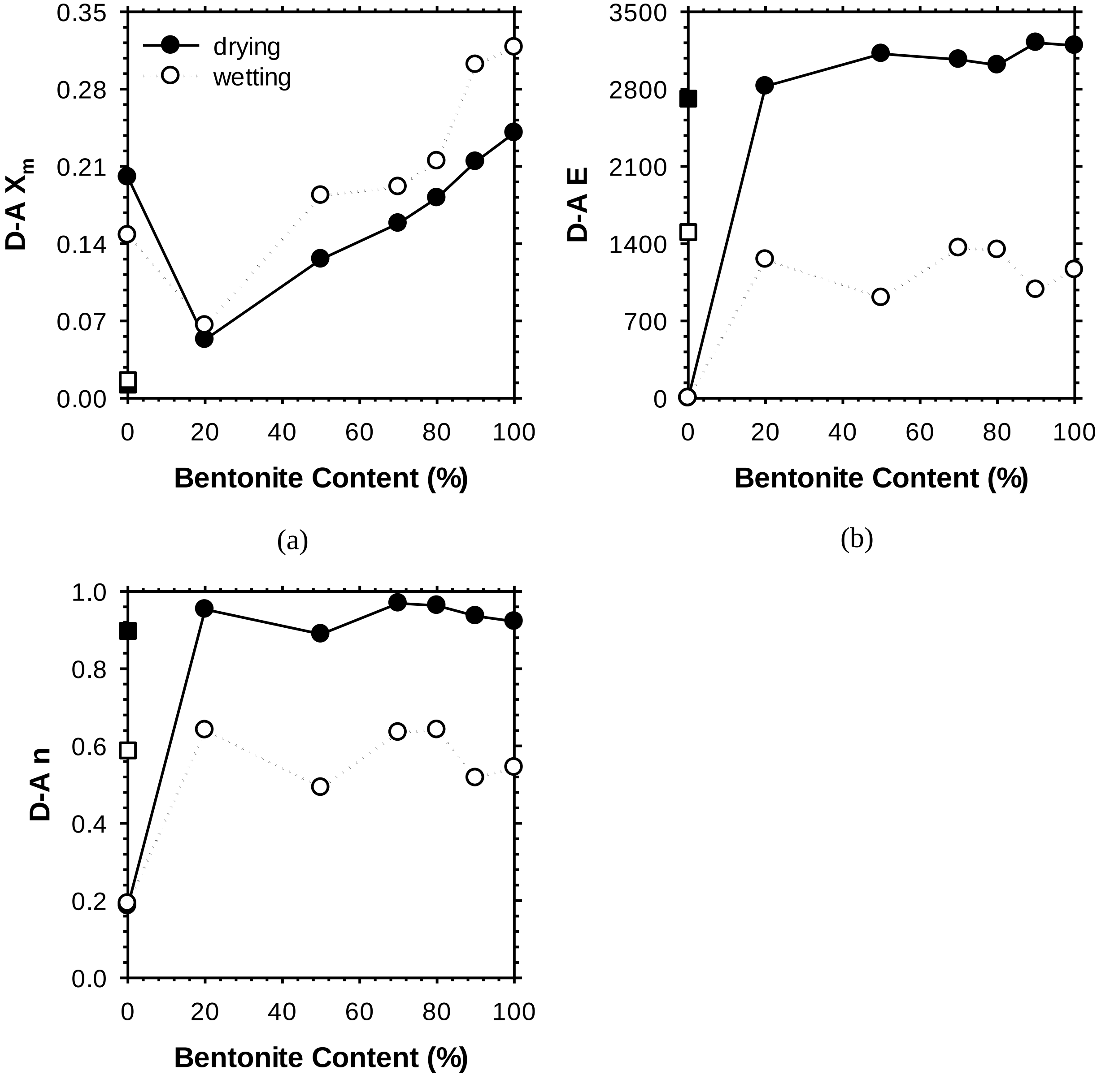
0.35
0.28
0.21
0.14
0.07
0.00
D-A X_m
drying
wetting
0
20
40
60
80
100
Bentonite Content (%)
3500
2800
2100
1400
700
0
D-A E
Bentonite Content (%)
1.0
0.8
0.6
0.4
0.2
0.0
D-A n
Bentonite Content (%)

(a)

(b)

(c)

Figure 10.

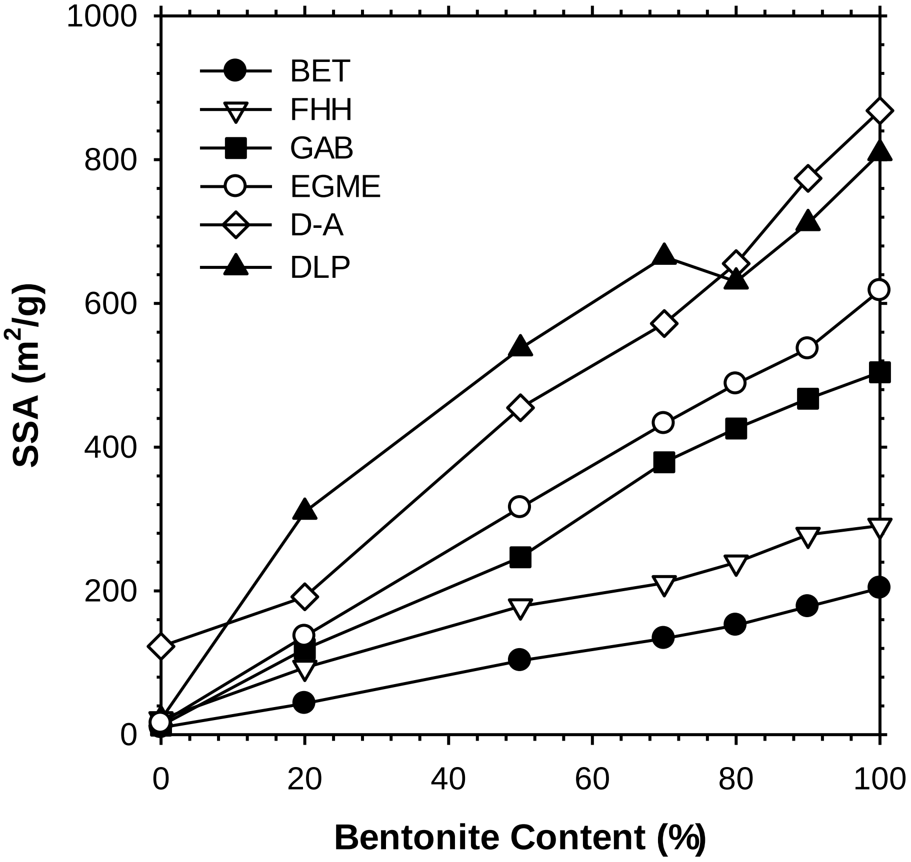

BET
FHH
GAB
EGME
D-A
DLP
SSA (m^2/g)
Bentonite Content (%)
0
200
400
600
800
1000
0
20
40
60
80
100

Figure 11.

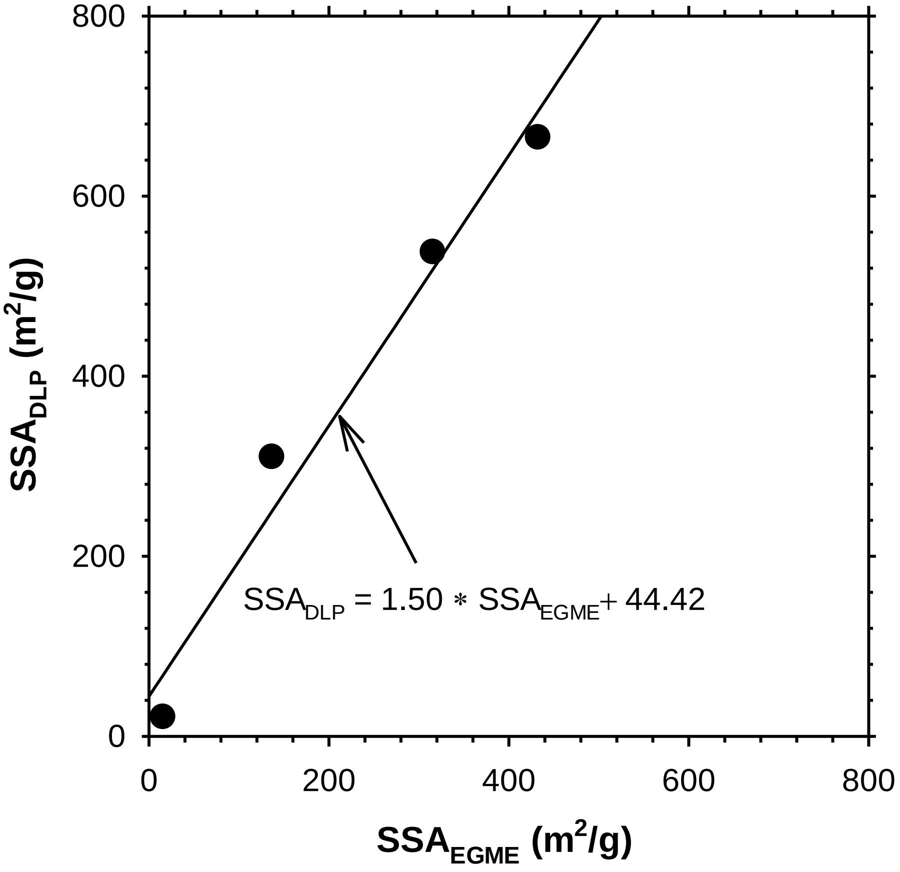
800
600
400
200
0
0
200
400
600
800
SSA_{DLP} (m^2/g)
SSA_{EGME} (m^2/g)
$SSA_{DLP} = 1.50 * SSA_{EGME} + 44.42$

Figure 12.

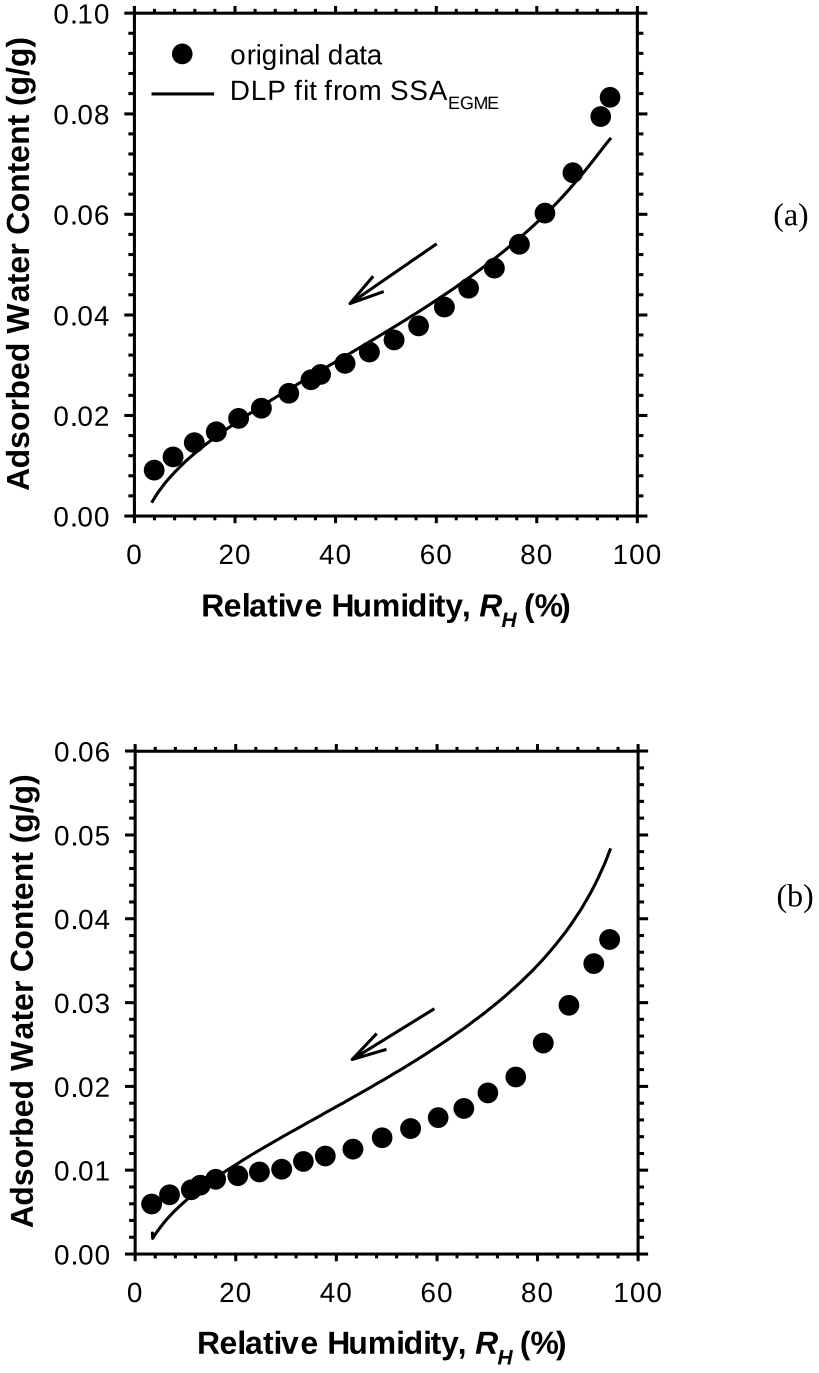
0.10
0.08
0.06
0.04
0.02
0.00
0
20
40
60
80
100
Adsorbed Water Content (g/g)
Relative Humidity, R_H (%)
original data
DLP fit from SSA_{EGME}
(a)
0.06
0.05
0.04
0.03
0.02
0.01
0.00
0
20
40
60
80
100
Adsorbed Water Content (g/g)
Relative Humidity, R_H (%)
(b)

CHAPTER 3

CATION EXCHANGE CAPACITY OF CLAYS FROM WATER VAPOR SORPTION ISOTHERM

3.1 INTRODUCTION

Cation exchange capacity (CEC) is typically expressed in miliequivalents per 100 g of dry clay (meq/100g) and is a measure of exchangeable mineral charge. Larger CEC values reflect a greater layer charge and corresponding surface activity. CEC is thus an indirect measure of the interaction forces between the clay surface and surrounding molecules. Since these interaction forces can appreciably influence the clay behavior, CEC, together with specific surface area (SSA), is gaining recognition as a fundamental property to characterize fine-grained soil behavior (*e.g.*, Sposito 1981, Iwata *et al*. 1995). Numerous studies have shown that CEC is closely related to clay mineralogy and SSA (*e.g.*, Cerato 2001, Chittoori and Puppala 2011). Consequently, relationships have been proposed between CEC and Atterberg limits (Farrar and Coleman 1967, Churchman and Burke 1991, Muhunthan 1991), and dispersion and frost-heave susceptibility (Anderson and Tice 1972, Reike *et al*. 1983, Nixon 1991). A related property, surface charge density (σ), is defined as CEC divided by SSA, which accounts for the charge of 100 m^2 of surface.

CEC measurement methods are typically based on replacing the cations in the natural exchange complex with a known cation species, most commonly using the ammonium displacement method. Alternative methods include methylene blue (MB) titration (Cokca and Birand 1993), and surface tension methods (Burrafato and Miano 1993). However, all of these methods are time consuming, expensive, and require specialized expertise or equipment not typically available to practicing geotechnical engineers.

This study investigates an alternative method to determine the CEC of clayey soils directly from water vapor sorption isotherms by using an empirically determined master curve. Performance of the proposed method is evaluated by comparing results with CEC values determined by the conventional ammonium displacement method.

3.2 BACKGROUND

3.2.1 Ammonium Displacement Method

The ammonium displacement method, described in detail by ASTM D7503, is the most commonly used method in geotechnical engineering practice for CEC determination (*e.g.,* Farrar and Coleman 1967, Borden and Giese 2001, Likos and Wayllace 2010, Chittoori and Puppala 2011). The basis of the approach is to replace the cations in the natural exchange complex with a known cation species. First, the soil is mixed with 1 M NH_4OAc (ammonium acetate), and hydrated for 24 h. Then the soil is washed by 1 M NH_4OAc by applying vacuum filtration. At the end of this stage, the natural complex is completely exchanged by ammonium. The soil is then rinsed with isopropanol by vacuum filtration to remove the remaining excess cations, if any. Then, the soil is washed by 1 M KCl to extract the ammonium in the exchange complex. The KCl extract is analyzed using a spectrophotometer to measure the nitrogen concentration and corresponding CEC.

Determination of the concentration of soluble and bound cations and to report these values together with the CEC is also typically recommended. To determine the soluble cations, soil is washed with deionized water and the extract is analyzed using inductively coupled plasma spectrometry or atomic absorption. To determine the bound cations, the NH_4OAc extract is analyzed using inductively couple plasma spectrometry or atomic absorption. Typically, the concentration of the major cations Na^+, Ca^{2+}, Mg^{2+}, and K^+ are determined. Then, CEC is determined by subtracting the concentration of soluble cations from the concentration of bound cations.

3.2.2 Methylene Blue (MB) Titration Method

Determination of CEC by MB absorption methods has been used by many researchers (*eg.*, Fairbairn and Robertson 1957, Hang and Brindley 1970, Kahr and Madsen 1995). Here, the MB titration method of Cokca and Birand (1993) will be described, which has the same basic rationale as the previously used MB procedures, and depends on the adsorption of MB by clay minerals. As the adsorption process is controlled by CEC and SSA together, this method can be used for determination of both the SSA and the CEC of clayey soils.

To determine the CEC by MB titration methodology, the soil is first mixed with deionized water until a homogeneous slurry is obtained. Then, a known concentration of MB is added to the slurry. The mixture is then agitated after taking a drop on a filter paper. The color change of the slurry on the filter paper is observed. When the adsorption stops, the color of the drop on the filter paper changes remarkably, and the test is stopped (Figure 1). The CEC of the soil determines the amount of adsorption. Therefore, the CEC can be determined by using the amount and concentration of the MB added to the slurry until the remarkable color change is obtained.

3.2.3 Surface Tension Methods

The surface tension method proposed by Burrafato and Miano (1993) is not common in geotechnical engineering practice. Still, there are some applications in other areas of science like the colloid sciences (*e.g.*, Yamaguchi and Hoffmann 1997), where the method has received attention.

The surface tension method to determine the CEC requires clay suspension in deionized water, and then titrating the mixture with a known concentration of hexadecylpyridinum chloride (CPC) solution, a cationic surface-active agent or surfactant. Then, the surface tension of the mixture is measured, typically with a tensiometer. Tensiometers directly measure the negative pore water pressure at the gas-liquid interface of the pores of a saturated high-air-entry (HAE) material. The HAE materials are typically made of ceramic and have uniform-sized micropores (Lu and Likos 2004). Soil with adsorbed CPC has a high and constant surface tension value until the clay surface reaches saturation. After saturation, if adsorption continues, the surface tension drops suddenly. The amount of CPC added until the drop occurs is related to the CEC value.

3.2.4 Relationship between SSA and CEC

A number of studies have shown a direct linear relationship between CEC and SSA. The linear relationship between CEC and SSA is generally attributed to the cation exchange that occurs on the clay surface. CEC is, therefore, expected to increase with the increasing SSA as there will be more surface for the exchange.

Figure 2 shows the linear relationship between SSA and CEC for a range of results available in the literature. Figure 2a shows the relation between CEC and SSA determined by water vapor sorption (SSA_{water}), whereas Figure 2b shows the relation between CEC and SSA determined by EGME sorption (SSA_{EGME}). SSA_{water} values for Cases *et al*. (1997, 1992), Yamanaka *et al*. (1990), Kraehenbuehl *et al*. (1990), and Branson and Newman (1983) were calculated from water vapor sorption isotherms by BET theory. CEC of the soils from Arthur *et al*. (2013) were obtained from Olesen *et al*. (1999). SSA_{EGME} values for the soils from Tiller and Smith (1990) were calculated from the EGME retention values. The data from the current study was also included (see Chapter 1). The approaches followed by the researchers were not the same for the EGME and water vapor sorption methods and also for CEC determination methods. The data were grouped only based on the type of the sorbed molecule used to determine the SSA.

The relation between SSA_{water} and CEC for the 77 data points in Figure 2a is captured by the following equation ($R^2 = 0.87$)

$$CEC\ (meq/100g) = 0.13 \cdot SSA_{water} + 14.43 \tag{1}$$

The results of Srodon and McCarty (2008) show a different trend than the results of the other studies. The main reason is that, Srodon and McCarty heated the soil samples to 200 °C prior to obtaining water vapor sorption isotherms. As more amount of water was removed before the test, the determined monolayer coverage values became higher than the other methods. The linear relation between SSA_{water} and CEC for 65 data points, excluding the results of Srodon and McCarty, is captured by the following equation ($R^2 = 0.94$)

$$CEC\ (meq/100g) = 0.22 \cdot SSA_{water} + 5.71 \tag{2}$$

More data was available in the literature for the EGME method (146 data points). The relation between SSA_{EGME} and CEC in Figure 2b is best fit ($R^2 = 0.91$) by the linear equation

$$CEC\ (meq/100g) = 0.13 \cdot SSA_{water} + 4.51 \tag{3}$$

3.2.5 Normalization of Water Vapor Sorption Isotherms with CEC

Results from Woodruff and Revil (2011) suggest that the water vapor sorption isotherms of clays may converge to a master curve when normalized with CEC and scaled with empirically-determined parameters that account for different cation types. They suggest an equation for this master curve, which originates from BET theory. By using the master curve equation, the isotherm of clayey soils may be estimated.

Figure 3 shows the CEC-normalized desorption curves for four homoionic bentonites produced from a natural Na^+/Ca^{2+}-bentonite by treating the clay two times with pure chloride solutions of Mg^{2+}, Ca^{2+}, Na^+, and Li^+. To accomplish the full cation exchange, clay was treated two times with a 1 M solution of the chloride of monovalent cations or a 0.1 M solution of the chloride of divalent cations, followed by repeated washing with deionized water and a check for excess chloride using $AgNO_3$. To account for different cation types, scaling parameters suggested by Woodruff and Revil (2011) were used, which are 0.6, 0.8, 0.5, and 0.4, respectively, for Mg^{2+}, Ca^{2+}, Na^+, and Li^+. The CEC of the homoionic bentonites was assumed to be the same and equal to the CEC of the natural Na^+/Ca^{2+} bentonite; *i.e.,* 77 meq/100 g.

Figure 3 shows that the isotherms of the homoionic bentonites do not exactly merge to a single curve. Ca^{2+}-, and Na^+-exchanged bentonites seem to show the same behavior at low R_H values (R_H < 40%) but start to deviate from each other as R_H gets higher. Mg^{2+}-exchanged bentonite has a similar behavior with the Ca^{2+}-, and Na^+-exchanged bentonites, but Li^+-exchanged bentonite has significantly different behavior. The difference in the normalized isotherms might be occured because a single CEC value was assumed for all the bentonites. However, even though the CEC values were to be different such that the isotherms collapse when normalized, they still could not form a single master curve because the shapes of the curves are also different.

Even if the difference in the shapes of the curves is disregarded, the Woodruff and Revil (2011) method is still not practical for natural soils because, to be able to apply this method, the mineralogy of the clay must be known to choose the appropriate scaling parameter. Figure 4 shows the CEC-normalized isotherms of fifteen natural clayey soils without using any scaling parameters. The figure indicates that without applying any scaling parameters, the CEC-normalized sorption curves to dot merge into a single master curve.

3.3 MATERIALS

Tests described herein were conducted using fifteen samples of natural clayey soils, a suite of artificially prepared bentonite-kaolinite (B-K) mixtures, a natural Na^+/Ca^{2+}-bentonite, and an additional sodium bentonite that is frequently used in geosynthetic clay liners (GCLs). The natural clays were selected from the University of Wisconsin-Madison (UW) soil bank, which contains clayey soil samples having a wide range of properties and geological histories, including glacial tills and glacio-fluvial clays from the midwest and northeastern regions of the United States, residual soils from the southeast, marine clays from the gulf coast, alluvial clays from the intermountain range and west coast, and eolian clayey soils from the northwest (Benson 2014). Samples range from non-plastic to highly plastic and have both narrow and broad particle size distributions.

Bentonite-kaolinite mixtures were prepared in seven mass-controlled ratios denoted by their respective bentonite (B) and kaolinite (K) content (100K, 20B/80K, 50B/50K, 70B/30K, 80B/20K, 90B/10K, 100B). End member bentonite and kaolinite for these mixtures was obtained from the Source Clay Repository of the Clay Minerals Society (Bain *et al.* 2001). This included

SWy-2, which is a Na^+-rich montmorillonite from Crook County, Wyoming, and KGa-1b, which is a low-defect kaolinite from Washington County, Georgia. Combined, the suite of test soils represents a wide range of natural and artificial clays having a broad spectrum of mineralogy, surface area, and corresponding cation exchange capacity. The surface properties of test soils are given in Table 1.

For the validation of the proposed method, a set of soils with a wide range of CEC and SSA is obtained from Colorado School of Mines and they will be referred here as Colorado soils. CEC and SSA of the soils were measured respectively with ammonium displacement and water vapor sorption methods. Table 2 shows the surface properties of the Colorado soils.

3.4 METHODS

3.4.1 Water Vapor Sorption Isotherms

Sorption isotherms for the current study were obtained using a commercially available vapor sorption analyzer (VSA) operating in dynamic dewpoint isotherm (DDI) mode (Decagon Devices, Pullman WA). Unlike similar systems for measuring water vapor sorption isotherms from the equilibrium mass of adsorbed water, the DDI approach involves concurrent measurement of sample water content and R_H in a dynamically changing vapor pressure environment. As described by Likos *et al*. (2011), samples are placed into an environmental chamber and continuously wetted or dried by circulating either a vapor saturated or desiccated air stream through the chamber. Changing R_H is periodically measured using a chilled-mirror dew point sensor (Leong *et al*. 2003, Campbell *et al*. 2007) while concurrently tracking changes in sample mass.

Hysteretic sorption isotherms were obtained along an initial drying path from ambient conditions down to 3% R_H to dry the sample from its initial air-dry water content, immediately followed by a wetting cycle up to 95% R_H and then a second drying cycle back down to 3% R_H. All isotherms were obtained at a set point temperature of 25 ± 0.2˚C automatically maintained by the VSA system. Initial air-dry mass of the samples passing #40 sieve was 1.90 ± 0.08 grams. Complete adsorption-desorption loops typically contained as many as 170 to 225 discrete measurements and were obtained in 24 to 72 hours.

3.4.2 Specific Surface Area (SSA)

The mass of water required to form a monomolecular layer, heat of adsorption, and SSA were estimated from the measured H_2O sorption isotherms using Brunauer-Emmett-Teller (BET) theory (Brunauer *et al.* 1938). BET Theory was applied on the desorption curves between P/P_0 ranging from 0.1 to 0.3.

According to BET theory, physical sorption involves the formation of many molecular layers of adsorbate on the adsorbent surface. Sorption is modeled by the following linear equation

$$\frac{P}{X(P_0-P)} = \frac{1}{X_m C} + \frac{C-1}{X_m C} \cdot \frac{P}{P_0} \tag{4}$$

where X is the mass of adsorbate at vapor pressure P and temperature T, P_0 is the corresponding saturated vapor pressure, and X_m is the quantity adsorbed (g/g) at monolayer coverage. The BET constant C is an energetic term defined as

$$C = \frac{exp(E_1-E_L)}{RT} \tag{5}$$

where E_1 is the heat of adsorption of the first molecular layer of adsorbate, E_L is the heat of condensation, R is the molar gas constant (8.314 J $mol^{-1}K^{-1}$) and T is absolute temperature (K).

The difference ($E_1 - E_L$) is a measure of the energy of interaction (J/mol) between the first monolayer of adsorbed molecules and the surface. Large values of ($E_1 - E_L$) indicate large forces of hydration between the surface and the monolayer.

If the cross-sectional area of the adsorbate molecule is known, SSA_{BET} may be approximated from monolayer coverage X_m according to

$$SSA_{BET} = \frac{X_m}{M_w} \cdot N \cdot A \tag{6}$$

where, for H_2O sorption on clay, M_w is the molecular mass of water ($M_w = 0.018$ kg mol^{-1}), N is Avogadro's number ($6.023 \cdot 10^{23}$ mol^{-1}), and A is the area covered by one H_2O molecule ($A = 0.108$ nm^2). Values of X_m and C can thus be obtained from a plot of experimental sorption data to back-calculate the mass of H_2O at monolayer coverage, heat of adsorption, and SSA. The linear range of applicability for water vapor sorption on clay surfaces is generally less than about P/P_0 from 0.4.

3.4.3 Cation Exchange Capacity (CEC)

CEC values were determined by the ammonium displacement method following ASTM D7503. First, the soluble (deionized water extract) and bound cations (1 M NH_4OAc extract) were determined by analyzing the respective extracts with inductively couple plasma spectrometry. Calibration curves were created by using High Purity Standards of the major cations Na^+, K^+, Ca^{2+}, and Mg^{2+}. Then, the 1 M KCl extract was analyzed via the salicylate method (EPA method 350.1) using high-range nitrogen NH_3 "Test 'N Tube" vials (Hach Company: Method 10031) by using a spectrophotometer. The two methods give very close results. The percent difference between the two methods averages 10.7% for 7 of the soils. The CEC values used further in this study refer to the CEC determined by the salicylate method.

3.4.4 Determination of Freundlich K Parameter

The Freundlich isotherm equation (Equation 7) is used to represent sorption on heterogeneous surfaces (Freundlich 1932). The equation implies that as surface coverage increases, heat of adsorption decreases logarithmically due to surface heterogeneities. Specifically, the Freundlich equation relates the surface concentration of the adsorbent to the equilibrium solution concentration. For adsorption of water vapor on soil, the surface concentration may be quantified by gravimetric water content (w) as a function of relative humidity (R_H), in the form of

$$w = K{R_H}^{\frac{1}{m}} \tag{7}$$

where K is a constant related to the relative sorption capacity of the adsorbent, and m is a constant related to the intensity of sorption.

The parameters of the equation parameters were determined by using least-squares regression and maximizing Equation (8).

$$R^2 = 1 - \frac{\sum_{i=1}(w_i - \dot{w}_i)^2}{\sum_{i=1}(\bar{w} - w_i)^2} \tag{8}$$

where w_i represents the measured water content at each increment, $\dot{w}_i$ is the water content calculated from the isotherm equation, and $\bar{w}$ is the mean of the measured w values. The equations were fit to the original desorption data without applying constraints in the R_H range of 3% to 80%, where the surface forces dominate the sorption behavior.

3.4.5 Obtaining the Surface Charge-Normalized Sorption Curve

The surface charge-normalized sorption curve is the linear plot of the water content at 80% R_H (w_{80}) normalized with surface charge versus the Freundlich K parameter. By using the surface charge-normalized sorption curve, determination of the CEC from water vapor sorption isotherm could be possible.

Water uptake at lower R_H (up to 80%) is dominated by short-ranged sorption mechanisms dependent on cation type and mineral surfaces, but at higher R_H, is dominated by longer-ranged capillary mechanisms that are dependent on pore structure. Therefore, w_{80} represents the total amount of water bound to the clay surface by short-ranged sorption mechanisms.

CEC and SSA are material properties that have a combined effect in sorption behavior as well as in adsorption capacity. To account for this combined effect, a related property, surface charge density, is defined as CEC divided by SSA. Surface charge density represents the charge of a soil, if the soil were to have a surface of 100 m^2. Dividing w_{80} by the surface charge density gives the total amount of sorbed water per charge on 100 m^2 surface. By making the surface a constant, only the effect of the charge on the sorption is accounted for; thus, it becomes possible to compare the sorption behavior of soils with different surface properties.

The plot of normalized sorbed water with the Freundlich K parameter gives a linear correlation as expected (Figure 5) because both parameters account for the adsorption capacity of the soil. The equation of the surface charge-normalized sorption curve ($R^2 = 0.93$) is

$$\frac{w_{80}}{\sigma} = 3.64 \cdot K + 0.02 \qquad (9)$$

3.4.6 Determination of CEC from Water Vapor Sorption Isotherm

CEC can be estimated from the water vapor sorption isotherm of clays in three steps. First, the Freundlich K parameter is obtained from the desorption curve by least squares optimization. Then, by using the Freundlich K parameter, the total amount of sorbed water per surface charge ($S = w_{80}$ / (CEC / SSA)) is determined empirically from Figure 5. Finally, w_{80} is obtained directly from the desorption curve of the isotherm, SSA is obtained by BET theory and substituted in S to determine the CEC.

3.5 VALIDATION OF THE METHOD AND DISCUSSIONS

The applicability of the proposed empirical method to determine the CEC of clayey soils from the water vapor sorption data was analyzed using the Colorado soils and soils data from the literature (Figure 6). The percent difference between $CEC_{measured}$ and $CEC_{calculated}$ averages 26.9% for 21 soils. Although the proposed method estimates slightly lower CEC values than the ammonium displacement method, there is a consistently linear trend that can be captured by the equation ($R^2 = 0.94$)

$$CEC_{calculated} = 1.09 \cdot CEC_{measured} - 7.69 \tag{10}$$

The data found from the literature is not expected to show a perfect fit to the results of the current study because the approaches followed to obtain the water sorption isotherms and the CEC are different from each other. In most of the cases, no information could be found about the testing approaches. The data was selected only based on the molecule used to obtain the sorption isotherms (*i.e.*, water vapor sorption isotherms).

The consistent results show that the proposed method is potentially a practical alternative to estimate the CEC of clayey soils. The approach gave reliable comparisons between the CEC of number of soils tested. Although the approach depends on an empirical correlation, it is easy to apply, not user dependent, and gives consistent results. Moreover, it is environmentally friendly, since the only molecule used is DI water. Table 3 shows the chemicals used in ammonium displacement method (salicylate method). Material safety data sheets (MSDS) of the chemicals indicate that all of the chemicals listed for ammonium displacement method could have potential harm to human health and to the environment.

3.6 SUMMARY AND CONCLUSIONS

To determine the cation exchange capacity (CEC) of clays, an alternative method based on water vapor sorption isotherms is proposed. An empirical master curve was created by normalizing water content at 80% R_H (w_{80}) with surface charge (CEC/SSA) and plotting the results for 24 soils against their Freundlich K parameters. The suite of 24 test soils included fifteen samples of natural clayey soils, a natural Na^+/Ca^{2+}-bentonite, a suite of artificially prepared bentonite-kaolinite mixtures in seven different proportions, and an additional Na^+-bentonite typically used in geosynthetic clay liners. The master curve, called the surface charge-normalized sorption curve, showed that the amount of water bound to the surface by short-range sorption mechanisms is linearly related to the relative sorption capacity of the soil surface. For validation of the proposed method, twelve different soil samples with a wide range of surface properties were obtained from Colorado School of Mines. Results were supported with the addition of nine data points found from literature review. CEC of the validation soils were determined by the proposed method using the surface charge-normalized sorption curve and compared with the values determined by the ammonium displacement method. The results indicate that although the proposed method estimates lower CEC values than the ammonium displacement method, it gives consistent estimations. The proposed water vapor sorption method is practical considering that the method is easy and fully-automated; therefore, the user effect is minimum and sustainable as only DI water is employed. Especially for the studies where the comparison of CEC values among the soils are the primary concern rather than the exact value of the CEC, using the proposed method would be more efficient.

3.7 REFERENCES

Anderson, D.M. and Tice, A.R., 1972, "Predicting unfrozen water contents in frozen soils from surface area measurements," *Highway Research Record No. 393*, pp. 12-18.

Arthur, E., Tuller, M., Moldrup, P., Resurreccion, A. C., Meding, M. S., Kawamoto, K. and de Jonge, L. W., 2013, "Soil specific surface area and non-singularity of soil-water retention at low saturations," *Soil Science Society of America Journal*, 77(1), 43-53.

ASTM D7503 (2010). "Standard Test Method for Measuring Exchange Complex and Cation Exchange Capacity of Inorganic Fine-Grained Soils", *Annual Book of ASTM Standards* DOI: 10.1520/D7503-10

Bain, D., Costanzo, P.M. and Guggenheim, S., (eds.), 2001, *Clays and Clay Minerals,* 49:371-453.

Benson, C.H., 2014, personal communication.

Borden, D. and Giese, R.F., 2001, "Baseline studies of the clay mineral society source clays: cation exchange capacity measurements by the ammonia-electrode method," *Clays and Clay Minerals,* 49(5): 444-445.

Branson, K. and Newman, A.C.D., 1983, "Water sorption on Ca-saturated clays: I. Multilayer sorptionand microporosimetry in some illites," *Clay Minerals,* Vol. 18, pp. 277-287.

Brunauer, S., Emmett, P.H. and Teller, E., 1938, "Adsorption of gases in multi-molecular layers," *Journal of the American Chemical Society*, 60, 309-319.

Burrafato, G. and Miano, F., 1993, "Determination of the cation exchange capacity of clays by surface tension measurements," *Clay Minerals*, 28: 475-481.

Campbell, G.S., Smith, D.M. and Teare, B.L., 2007, “Application of a dew point method to obtain the soil water characteristic,” *Experimental Unsaturated Soil Mechanics*, T. Schanz (Ed.), Springer, pp. 71-77.

Cases, J.M., Berend, I., Besson, G., Francois, M., Uriot, J.P., Thomas, F. and Poirier, J.E., 1992, “Mechanism of adsorption and desorption of water vapor by homoionic montmorillonite. I. The sodium exchanged form.” *Langmuir*, Vol. 8, pp. 2730-2739.

Cases, J.M., Berend, I., Francois, M., Uriot, J.P., Michot, L.J. and Thomas, F., 1997, ”Mechanism of adsorption and desorption of water vapor by homoionic montmorillonite: 3. the Mg2+, Ca2+, Sr2+, and Ba2+-exchanged forms,” *Clays and Clay Minerals*, 45(1): 8-22.

Cerato, A.B., 2001, *Influence of Specific Surface Area on Geotechnical Characteristics of Fine-Grained Soils,* MS Thesis, University of Massachusetts-Amherst, Dept. Civil and Environmental Engineering, 298 pp.

Chittoori, B. and Puppala, A.J., 2011, “Quantitative estimation of clay mineralogy in fine-grained soils,” *Journal of Geotechnical and Geoenvironmental Engineering*, 137(11): 997-1008.

Churchman, G.J. and Burke, C.M., 1991, “Properties of subsoils in relation to various measures of surface area and water content,” *Journal of Soil Science,* 42: 463-478.

Cokca, E. and Birand, A., 1993, “Determination of cation exchange capacity of clayey soils by the methylene blue test,” *Geotechnical Testing Journal,* 16(4): 518-524.

Fairbairn, P.E. and Robertson, R.H.S., 1957, “Liquid limit and dye adsorption,” *Clay Minerals Bulletin,* 3, 129-136.

Farrar, D. and Coleman, J., 1967, "The correlation of surface area with other properties of nineteen British clay soils," *Journal of Soil Science*, Vol. 18, pp. 118-124.

Freundlich, H., 1932, "Of the adsorption of gases. Section II. Kinetics and energetics of gas adsorption. Introductory paper to section II," *Transactions of the Faraday Society,* 28: 195-201.

Hach Company: Method 10031 (2013). Method 10031: "Salicylate Method, Test 'N Tube™ Vials, HR, 0 to 50 mg/L NH_3-N." Retrieved April 23, 2014 from Web site: https://www.hach.com/fmmimghach?/CODE%3ANITROGENAMM_TNT_HIGH2071%7C1

Hang, P.T. and Brindley, G.W, 1970, "Methylene blue absorption by clay minerals," Determination of surface areas and cation exchange capacities (Clay-organic studies XVIII). *Clays and Clay Minerals,* 18: 203-212.

Iwata, S., Tabuchi, T. and Warkentin, B.P., 1995, *Soil-Water Interactions: Mechanisms and Applications,* 2nd Edition, Marcel Dekker Inc., New York.

Kahr, G., and Madsen, F.T., 1995, "Determination of the cation exchange capacity and the surface area of bentonite, illite and kaolinite by methylene blue adsorption," *Applied Clay Science,* 9(5): 327-336.

Kraehenbuehl, F., Stoeckli, H.F., Brunner, F., Kahr, G. and Muller-Vonmoos, M., 1987, "Study of the water-bentonite system by vapour adsorption, immersion calorimetry and x-ray techniques: 1. micropore volumes and internal surface areas, following Dubinin's theory," *Clay Minerals*, Vol. 22, pp. 1-9.

Leong, E.C., Tripathy, S. and Rahardjo, H., 2003, "Total suction measurement of unsaturated soils with a device using the chilled-mirror dew-point technique," *Géotechnique,* 53(2): 173-182.

Likos, W.J., Lu, N. and Wenszel, W., 2011, "Performance of a dynamic dew point method for moisture isotherms of clays," *Geotechnical Testing Journal,* 34(4), DOI: 10.1520/GTJ102901.

Likos, W.J. and Wayllace, A., 2010, "Porosity evolution of free and confined bentonites during interlayer hydration," *Clays and Clay Minerals,* 58(3): 399-414.

Lu, N. and Likos, W.J., 2004, *Unsaturated Soil Mechanics.* John Wiley & Sons Inc., New Jersey.

Muhunthan, B., 1991, "Liquid limit and surface area of clays," *Géotechnique,* 41(1): 135-138.

Nixon, J.F., 1991, "Discrete ice lens theory for frost heave in soils," *Canadian Geotechnical Journal,* Vol. 28, pp. 843-859.

Olesen, T., Moldrup, P. and Gamst, J., 1999, "Solute diffusion and adsorption in six soils along a soil texture gradient," *Soil Sci. Soc. Am. J.,* Vol. 63, pp. 519-524.

Reike, R.D., Vinson, T.S. and Mageau, D.W., 1983, "The role of specific surface area and related index properties in the frost heave susceptibility of soils," *Proceeding of the 4th International Permafrost Conference,* pp. 1066-1071.

Sposito, G., 1981, *The Thermodynamics of Soil Solutions,* Oxford Clarendon Press, London.

Tiller, K.G. and Smith, L.H., 1990, "Limitations of EGME retention to estimate the surface area of soils," *Australian Journal of Soil Research,* 28(1): 1-26.

Woodruff, W. F. and A. Revil (2011), “CEC-normalized clay-water sorption isotherm,” *Water Resour. Res.*, 47, W11502, doi:10.1029/2011WR010919.

Yamaguchi, Y. and Hoffmann, H., 1997, “Interaction between saponite and cationic, zwitterionic and nonionic surfactants,” *Colloids and Surfaces A: Physicochemical and Engineering Aspects*, 121(1): 67-80.

Yamanaka, S., Malla, P.B. and Komarneni, S., 1990, “Water Adsorption Properties of Alumina Pillared Clay,” *Journal of Colloid and Interface Science*, 134(1): 51-58.

3.8 TABLES

Table 1.

soil ID	CEC (meq/ 100 g)	SSA_{water} (m^2/g)
Denver	23.0	107
New Orleans	8.0	27
Sacramento	27.8	138
Atlanta, Georgia	13.2	50
KF1	35.6	157
KF2	23.4	102
Alb1	8.5	38
Alb2	8.1	29
Albany red	7.6*	32
Houston brown	32.2*	90
Mon 2	15.2	69
Kamm clay	26.3*	84
WCS Andrews	17.6*	71
K1	5.5	23
I1	72.0	294
SWy-2	76.0	376
KGa-1b	2	13
Na^+/Ca^{2+}-bentonite	77.0	269

Table 2.

soil	**CEC (meq/100g)**	**SSA (m^2/g)**
1	70.6	269
2	19.3	29
3	101.8	425
4	31.8	82
5	8.1	18
6	23.3	52
7	17.8	51
8	19.3	64
9	19.7	61
10	21.0	63
11	22.8	72
12	3.6	19

Table 3.

Ammonium Displacement	**Water Vapor Sorption**
NH_4OAc	DI water
Isopropanol	
KCl	
NH_4OH	
Ammonium Salicylate	
Ammonium Cyanurate	
Hach Test vial solution	
DI water	

3.9 FIGURES

Figure 1.

Light blue coloration (at full saturation)

All dye adsorbed (still not saturated)

Figure 2.

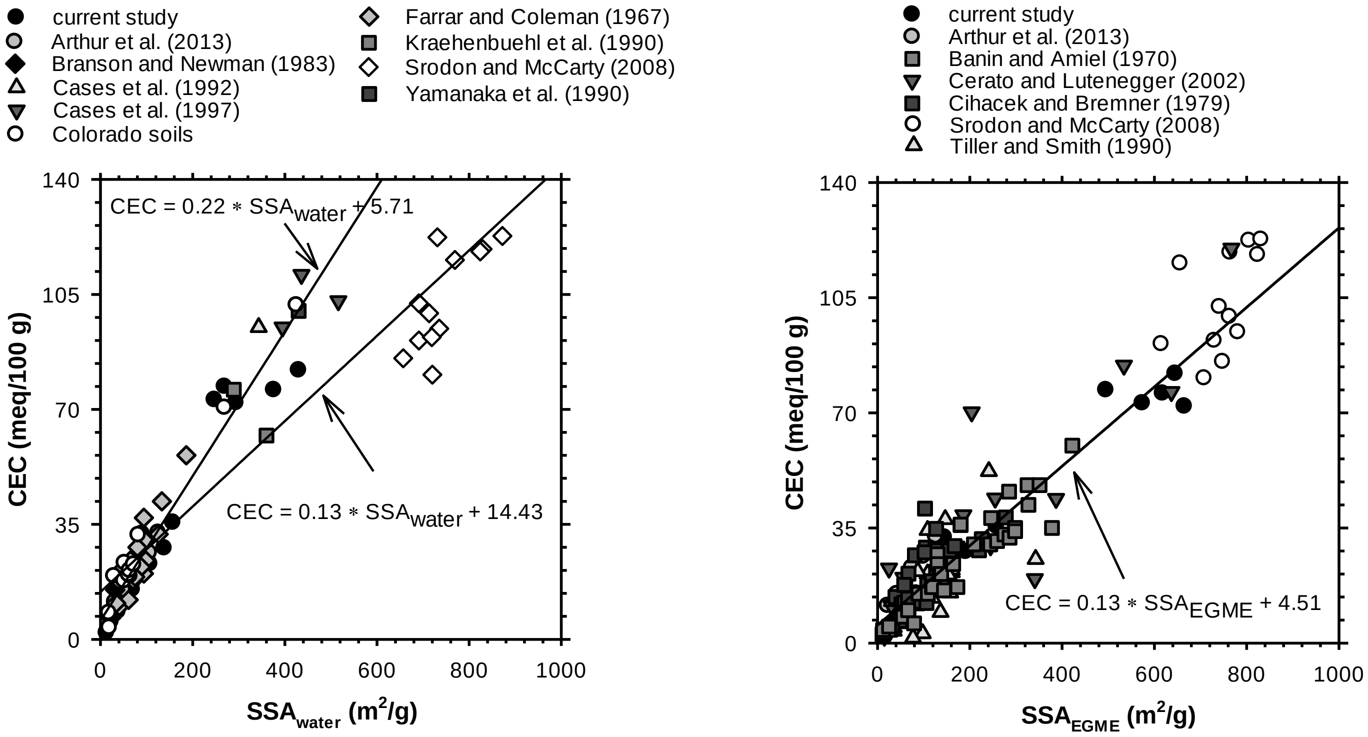
current study
Arthur et al. (2013)
Branson and Newman (1983)
Cases et al. (1992)
Cases et al. (1997)
Colorado soils
Farrar and Coleman (1967)
Kraehenbuehl et al. (1990)
Srodon and McCarty (2008)
Yamanaka et al. (1990)
CEC = 0.22 * SSA_water + 5.71
CEC = 0.13 * SSA_water + 14.43
CEC (meq/100 g)
SSA_water (m²/g)
0
35
70
105
140
0
200
400
600
800
1000
current study
Arthur et al. (2013)
Banin and Amiel (1970)
Cerato and Lutenegger (2002)
Cihacek and Bremner (1979)
Srodon and McCarty (2008)
Tiller and Smith (1990)
CEC = 0.13 * SSA_EGME + 4.51
CEC (meq/100 g)
SSA_EGME (m²/g)
0
35
70
105
140
0
200
400
600
800
1000

(a)

(b)

Figure 3.

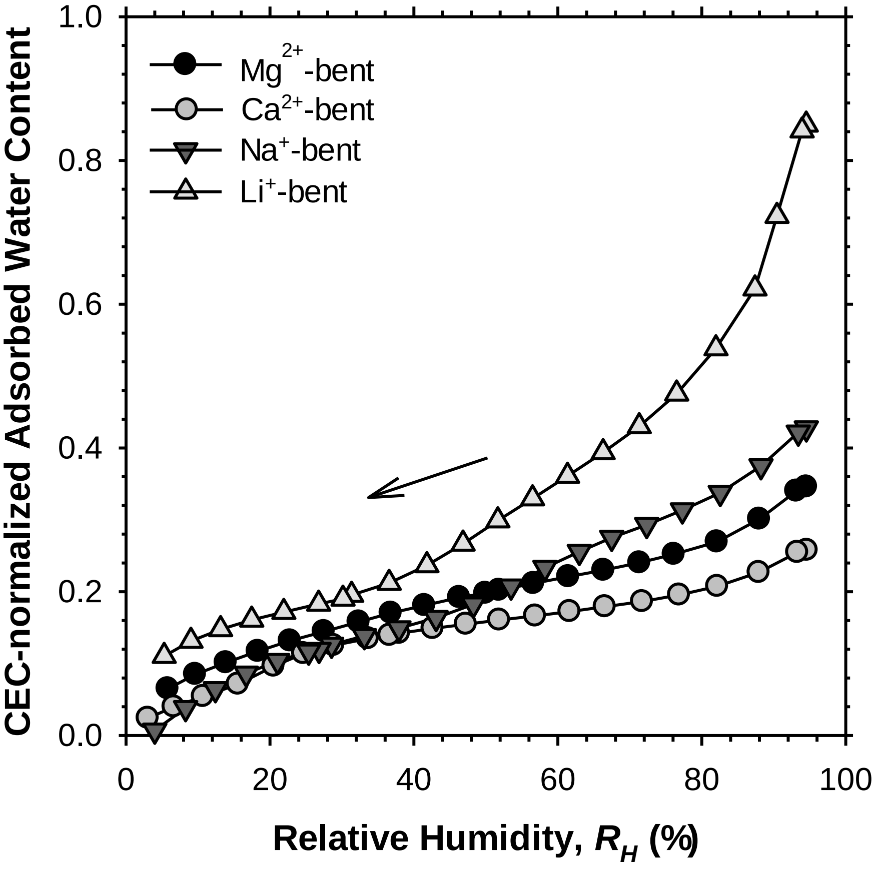
1.0
0.8
0.6
0.4
0.2
0.0
0
20
40
60
80
100
CEC-normalized Adsorbed Water Content
Relative Humidity, R_H (%)
Mg^{2+}-bent
Ca^{2+}-bent
Na^{+}-bent
Li^{+}-bent

Figure 4.

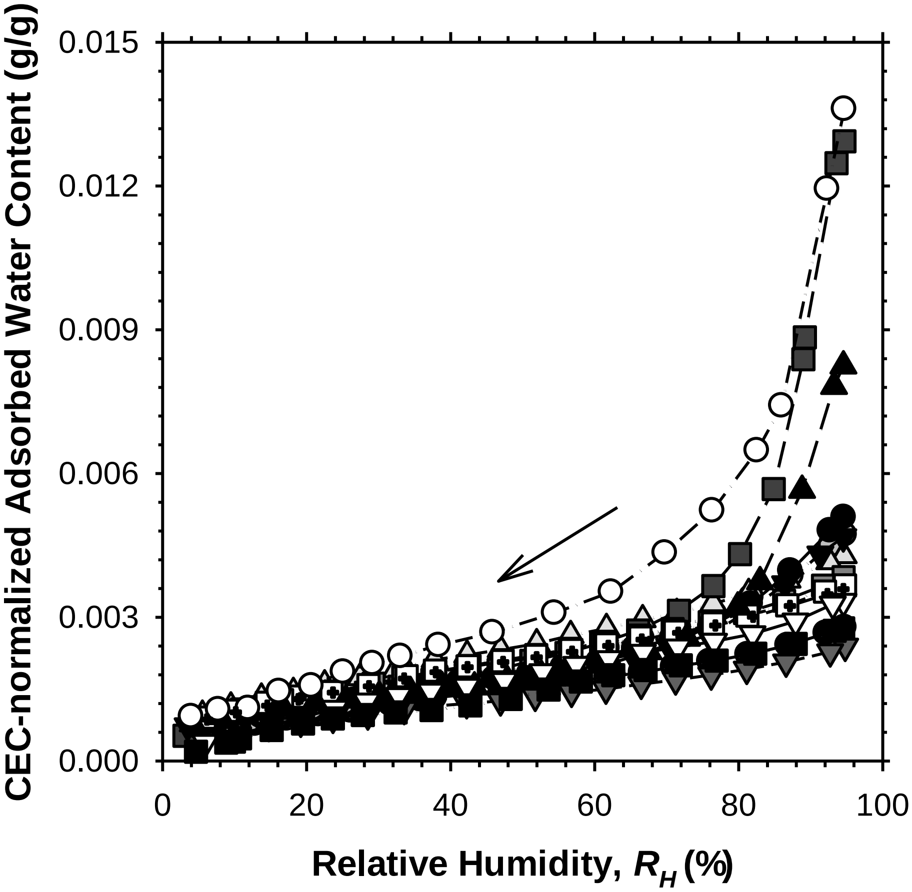
CEC-normalized Adsorbed Water Content (g/g)
0.015
0.012
0.009
0.006
0.003
0.000
0
20
40
60
80
100
Relative Humidity, R_H (%)

Figure 5.

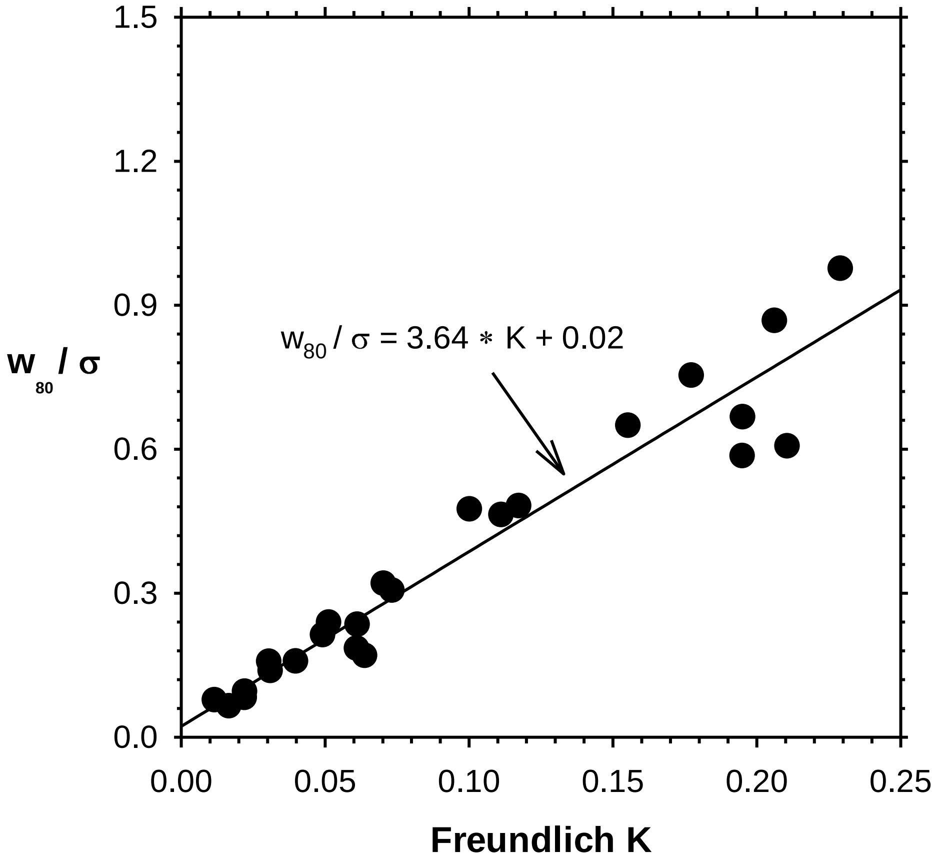
1.5
1.2
0.9
0.6
0.3
0.0
0.00
0.05
0.10
0.15
0.20
0.25
w_{80} / σ
Freundlich K
$w_{80} / \sigma = 3.64 * K + 0.02$

Figure 6.

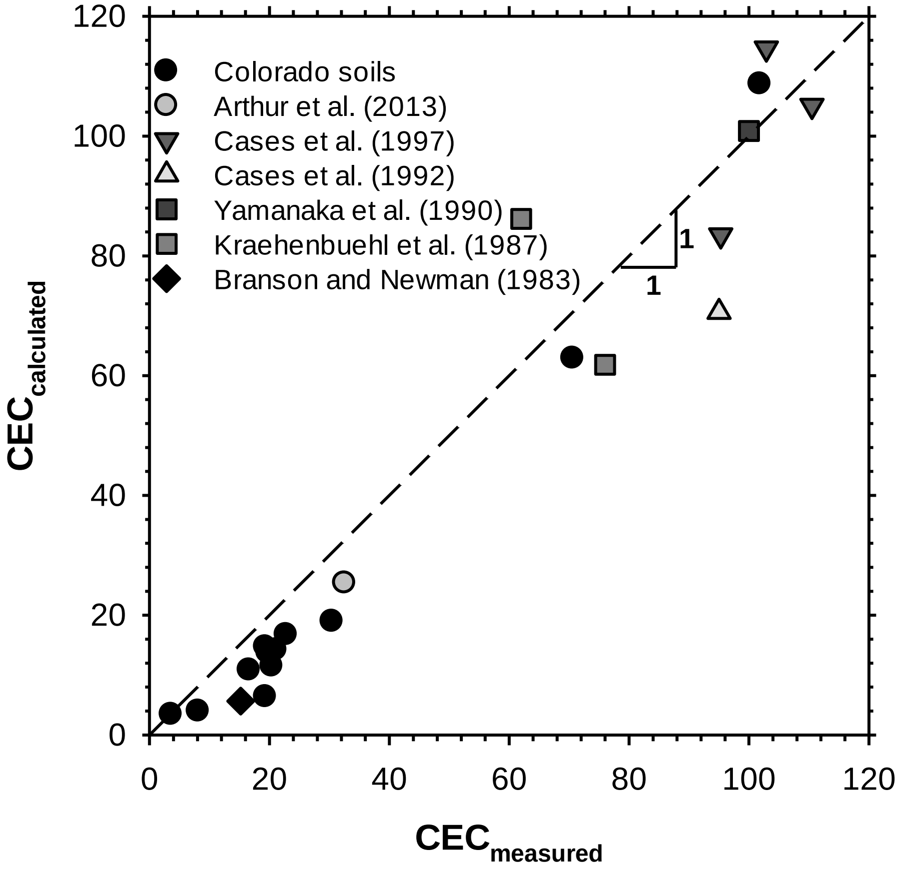

● Colorado soils
○ Arthur et al. (2013)
▽ Cases et al. (1997)
△ Cases et al. (1992)
■ Yamanaka et al. (1990)
■ Kraehenbuehl et al. (1987)
◆ Branson and Newman (1983)
1
1
CEC$_{calculated}$
CEC$_{measured}$
0
20
40
60
80
100
120
0
20
40
60
80
100
120

EXECUTIVE SUMMARY

The goal of this study was to develop an alternative, modernized, and fully automated way to determine clay surface properties based on water vapor sorption measurements. Clay surface properties including specific surface area (SSA) and cation exchange capacity (CEC) are of interest because the engineering behavior of clays is fundamentally determined by their surface properties. Swelling behavior is in particular the motivation of this research. The long-term goal is to be able to characterize expansive soils based on their surface properties determined by water vapor sorption measurements.

The most commonly used method to determine SSA is the EGME method. The first chapter of this thesis compared SSA values determined by the conventional EGME method (SSA_{EGME}) with values determined by a water vapor sorption method using BET Theory (SSA_{BET}). A linear relationship was obtained between the two methods; however, SSA_{BET} values were found to be about 0.58 times the SSA_{EGME} values. The main reason for this underestimation was attributed to the assumptions made in deriving the BET theory, as well as the effect of cation type and the difference in γv_m (surface tension multiplied by partial molar volume) values for EGME and H_2O molecules. There is a need to better understand the derivations of the isotherm equations, the physical meaning of the model parameters, and to identify how the parameters of the isotherm equations differ among different soils.

The second chapter examines six different isotherm equations including the Freundlich (F), Brunauer-Emmett-Teller (BET), Frenkel-Halsey-Hill (FHH), Guggenheim-Anderson-de Boer (GAB), Double Log Polynomial (DLP), and Dubinin-Astakhov (D-A) models. These models have primarily been developed by chemists or physicists and are widely used in chemical engineering, physical chemistry, colloid sciences, and food science, but are very rarely used in geotechnical engineering. In the field of geotechnical engineering, researchers most commonly use the BET equation or the FHH equation. Trends in equation parameters with increasing bentonite content were observed for a suite of bentonite-kaolinite mixtures. Possible ranges of the parameters for water vapor sorption by clay surfaces were proposed. SSA values were determined using the equations and compared. The D-A Model was found to give the most realistic SSA values if the soil has some bentonite content; whereas, for pure kaolinite, the model does not give realistic SSA values. For SSA from water vapor sorption method, as long as the model is consistent, the isotherm equation that is chosen is not very important. The equations all have their own assumptions, causing a wide variation in SSA values. However, all equations tend to give linearly increasing SSA values with increasing bentonite content, particularly the GAB, FHH, and BET models. To determine the energy parameter, though, the equations should be investigated carefully because the energy parameters of different equations could have different meanings. The energy parameters of the equations F, FHH, and DLP indicate the sorption capacity of the soil, whereas the energy parameters of the BET, GAB, and D-A equations indicate the characteristic adsorption energy, or the binding strength of water to the soil surface.

In the third chapter, an alternative empirical method was proposed to determine the CEC of clayey soils by water vapor sorption measurements. A surface charge-normalized sorption curve was created as a master curve by normalizing the water content at 80% R_H (w_{80}) with the surface charge density (CEC/SSA) and plotting this value against the Freundlich K parameter. The method was validated with twelve samples of natural clayey soils and nine sorption isotherms found from the literature. A consistent linear relationship ($R^2 = 0.94$) was found between the CEC values determined by the proposed water vapor sorption method and the ammonium displacement method. The proposed method estimates slightly lower CEC values.

Collectively, both SSA and CEC may be obtained from a single water vapor sorption measurement. Since only the desorption curve is required, the SSA and CEC of a soil can be determined in less than 24 h, regardless of the soil mineralogy. The method is fast, consistent, user independent, fully automated, and sustainable. It should be noted that SSA and CEC are mostly used as comparison parameters. Therefore, to compare the behavior of different soils the chosen model does not have to give the true values, but consistent results should be obtained from the model. In such cases, water vapor sorption methods could effectively be used to estimate the surface properties of clayey soils. Moreover, since it is very difficult to measure the exact value of surface properties, even the most commonly used standard methods rely on some assumptions and approximations, and the results obtained from these standard methods do not always match with the theoretical, or the ‘true’, values. The water vapor sorption method proposed in this study is an alternative modernized way to determine surface properties.